symmetry

MDPI

Article

On the Vibrations of a Rigid Solid Hung by Kinematic Chains

Alin-Florentin Stan [1,2], Nicolae Pandrea [2], Nicolae-Doru Stănescu [2,*], Ligia Munteanu [1] and Veturia Chiroiu [1]

[1] Department of Deformable Media & Ultrasonics, Institute of Solid Mechanics of the Romanian Academy, 010141 Bucharest, Romania; alin.stan@upit.ro (A.-F.S.); ligia.munteanu@imsar.ro (L.M.); veturia.chiroiu@imsar.ro (V.C.)

[2] Department of Manufacturing and Industrial Management, Faculty of Mechanics and Technology, University of Pitești, 110040 Pitești, Romania; nicolae.pandrea@upit.ro

* Correspondence: doru.stanescu@upit.ro

Abstract: In this paper we consider two situations. In the first, all kinematic chains are elastic, while the second situation is characterized by one rigid kinematic chain, with the rest of them being elastic. In addition, the kinematic joints are considered to be rigid. The calculations are performed using the screw coordinates. For the free vibrations of the rigid solid we determined the rigidity matrix and the eigenpulsations in both cases. It was proved that the results in the second case cannot be considered as limits for the results of the first situation, putting infinite values for the elements of the rigidity matrix of one kinematic chain. We also developed the theory for the forced vibrations of the system. A numerical application is considered and a great variety of cases are developed and discussed. The results obtained for the forced vibrations are presented and discussed. The paper combines elastic and rigid kinematic chains, as well as general configurations of the kinematic chains. The method presented here may be used for any number of kinematic chains, no matter if the structure is symmetrical or asymmetrical.

Keywords: rigidity matrix; screw coordinates; free and forced vibrations; elastic kinematic chains; rigid kinematic chain

Citation: Stan, A.-F.; Pandrea, N.; Stănescu, N.-D.; Munteanu, L.; Chiroiu, V. On the Vibrations of a Rigid Solid Hung by Kinematic Chains. *Symmetry* **2022**, *14*, 770. https://doi.org/10.3390/sym14040770

Academic Editors: Polidor Bratu, Gilbert-Rainer Gillich and Doru-Nicolae Stanescu

Received: 9 March 2022
Accepted: 1 April 2022
Published: 7 April 2022

1. Introduction

In practice, there exist very different structures where spatial kinematic chains support a rigid platform. The paper proposes a general approach toward the dynamic modelling of such systems. The main focus is on the vibrational analysis of a Gough–Stewart type of platform.

This platform has several applications and can be purchased and adapted to many applications as made distinct by the payloads. The possibility of a dynamic model, such as the one herein developed, allows the establishment of a mobile payload, supporting the kinematic chains' stiffness and driving laws consistent with the accuracy requirements.

The problems concerning the platforms are very different. Usually the platforms are studied from the kinematic or dynamic point of view. The references can be divided into two categories: papers in which the rigid solid (platform) is hung by rigid elements, and papers in which one or more of the elements are elastic.

Paper [1] considers a general platform for which the authors perform an analysis of the mobility, describe its finite kinematics and realize the direct and inverse analysis of the displacements. The approach is based on the theory of screw coordinates. Different types of parallel manipulators are studied in [2–4], the authors realizing the analysis of the displacements, infinitesimal kinematics, and determination of the singular positions, with the calculations being performed with the use of the screw coordinates. Yi and Kim [5] consider combinations of parallel mechanisms having a common platform and study their synthesis in the same coordinates. In reference [6] the authors discuss the study of the mobility of the parallel manipulators using the intersection of the screw manifolds, while Nazari et al. [7] treat the problem of the mobility and the kinematic analysis of a particular manipulator of type 3-CRRR (where C stands for cylindrical, and R for rotational kinematic joint). Bu et al. [8] analyze a series–parallel manipulator with a platform of type 2 (SP+SPR+SPU) (where S means spherical, P means prismatic, R stands for rotational, while U means universal kinematic joint) from the point of view of the rigidity and elastic deformations of different elements. The case of a platform attached to a manipulator for ophthalmology, taking into account the inertia, is discussed in [9]. A general case of a manipulator with parallel kinematics can be found in [10].

Zhao et al. [11] use the principle of the invariance of the terminal constraints that resulted from the theory of screw coordinates for kinematic chains with zero, one, two, three, four, or five terminal constraints and apply the obtained results to a Stewart platform for which the terminal constraints are of the following types: spherical joint, cylindrical joint, or universal joint (Hook). A more complex approach in which one considers the rotations of the legs about their own axis is presented in [12]. A robust solution obtained on the basis of the kinematic analysis is presented in reference [13], while the singularities of the working space are discussed in [14]. The properties that resulted from the symmetry of the platform are studied in [15]. The dynamics of a platform acted on by a pneumatic actuator, considering the inertia of the actuators, is studied in [16], while the dynamics of the platform acted on by linear actuators is described in [17,18]. The dynamics of the Stewart platform are studied with the aid of the principle of virtual work [19], or with the aid of the equations of classical mechanics considering a certain delay for the answer [20]. Reference [21] considers a Stewart platform for which a combination of methods are presented for the mathematical representation of its direct kinematics as well as algorithms of optimization. Reference [22] considers a Stewart platform for which the jerk of the mobile platform is studied, as well as the possibilities for reducing this jerk. Bai et al. [23] obtain the automatic generation of the equations of motion and the concept of adaptive control for the dynamic analysis of the platform. The dynamic of the platform for an asymmetric load is studied with the Lagrange equations [24]; the singularities of the platform and their analysis are described in [25], while the control using Lyapunov-type methods is studied in [26]. The equations of motion can be obtained with the aid of the principle of superposition [27,28]. Lazard and Merlet [29] proved that a Stewart platform can have a maximum of 12 configurations and constructed such a platform. The control of the trajectory such that the positioning error tends to zero is described in [30]. The control of the trajectory using some approximate inverse dynamics is presented in [31].

A comparative kinematic study between the original Gough platform and the Stewart platform was performed by Gallardo-Alvarado [32]. The determination of forces and moments is described in [33]. The parametric vibrations of a symmetric Stewart platform are studied in [34], and their damping in [35]. The study of some defects for a Stewart platform is discussed in [36], the solution being given with the aid of a control. The theory of graphs is also used in the study of the behavior [37] and dynamic analysis [38] of a Stewart platform. Optimization problems for the Stewart platforms are solved in [39–46].

The analysis of the rigidity of the kinematic chains is presented in [47], and the calculation of the rigidity matrix of a robot is presented in [48]. Other situations of Stewart platforms are studied in [49] by considering the flexibility of the upper shell, and in [50] by considering that some kinematic joints are flexible, while others are rigid, the dynamics of which are presented in [51]. Other different situations of platforms with elastic elements are described in [52–58]. The approaches are based on the Kane's equations, principle of virtual work, linearization of the equations of motion, introduction of certain redundant actuators, or finite elements method [59]. An excellent state of the art example can be found in [60]. The stochastic control of structures influenced by random excitations (earthquakes) using the Monte Carlo method and a new proposed algorithm is discussed in [61], with the authors considering that the loads and stiffness are variable parameters. The numerical results proved that the mass is the most important parameter that influences the control response.

One says that the rigid solid is hung when it is linked to the base (the fixed rigid solid), in the most general case, by kinematic chains. The kinematic chains are linked to the rigid solid and to the base either by kinematic linkages or by clamping. In particular, the kinematic chain may be reduced to a single element. Moreover, the intermediary kinematic chains may contain either rigid or elastic elements (bars).

Generally speaking, the references consider that the kinematic chains are identical or symmetric chains. Moreover, the payload is symmetric. The situation in which the kinematic chains are unsymmetrical [60] is not a common one and the calculations are performed only in particular cases. The combination of rigid and elastic kinematic chains is new and has not been studied before. If the payload is unsymmetrical, then the forces in the elements and the reactions in the kinematic joints are different; consequently, the structure may be unsymmetrical. Our goal is to discuss the most general case of a rigid solid hung by several kinematic chains (not necessary identical or having a symmetrical distribution), one of these kinematic chains having rigid elements. The calculation is performed using screw coordinates.

2. Vibrations of the Rigid Solid Hung by Several Elastic Kinematic Chains and One Kinematic Chain with Rigid Elements

2.1. Generalities

The mobile structures with rigid elements are the so-called Stewart platforms, which are used as components of the industrial robots. The most general schema is captured in Figure 1 where, at the points $A_1, A_2, \ldots, A_6$, one has spherical kinematic linkages with the finger (kinematic linkages of the fourth class), and at the points $B_1, B_2, \ldots, B_6$, one has kinematic linkages of the fifth class (usually hydraulic actuators), while at the points D_1, $D_2, \ldots, D_6$, one has spherical joints.

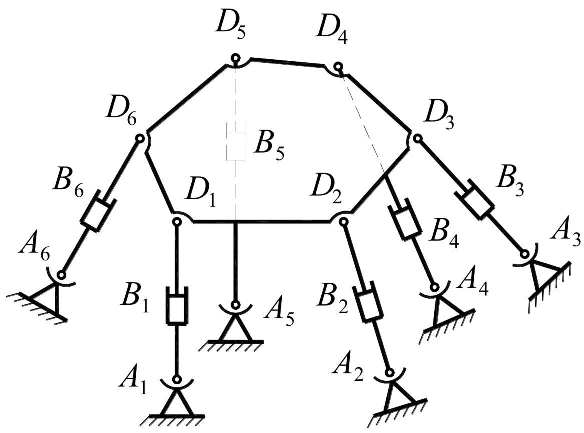

Figure 1. The most general schema of a Stewart platform.

The mobility M is given by the relation

$$M = 6n - 5c_5 - 4c_4 - 3c_3 \tag{1}$$

where n is the number of elements, c_5 is the number of kinematic linkages of the fifth class, c_4 is the number of kinematic linkages of the fourth class, while c_3 is the number of kinematic linkages of the third class; since $n = 13$, $c_5 = 6$, $c_4 = 6$, and $c_3 = 6$, one deduces $M = 6$; hence, the mobility is equal to the number of the driving elements.

A similar construction is that of the following mechanism of the satellites captured in Figure 2; it has two degrees of mobility, the mechanism being actuated by the rotational motors M_1 and M_2. Moreover, in this case $n = 8$, $c_5 = 6$, $c_4 = 1$, $c_3 = 4$, and $M = 2$.

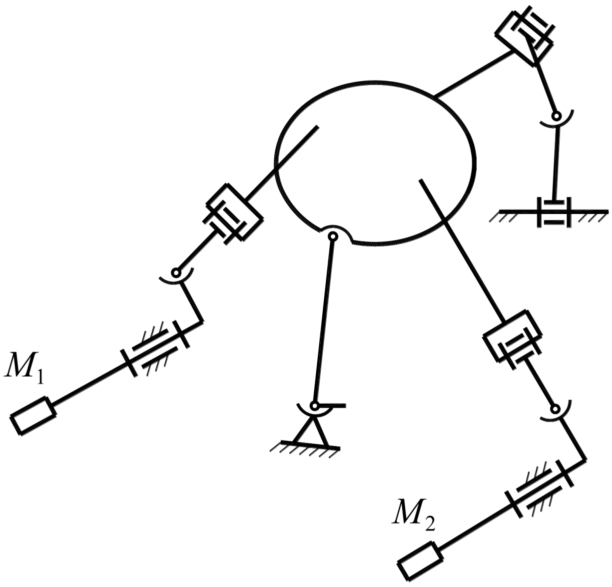

Figure 2. Following mechanism of a satellite.

The structures of the parallel robots and of the follower antennas have been well studied as kinematics, dynamics, and automation in numerous papers.

The structures of the type that are a rigid solid hung by kinematic chains with the mobility $M \leq 0$ are called fixed, while if the elements of their kinematic chains are elastic, then they become vibratory structures.

The mobile structures in which the driving elements are blocked also become vibratory structures; in this case the mobility equals zero ($M = 0$).

We consider the system in Figure 3, with mobility $M \leq 0$, and consisting of a rigid solid hung by one kinematic chain with rigid elements (denoted by $ABCD$), and by several kinematic chains with elastic elements (in Figure 3 we presented only one denoted by $EFGH$). Moreover, all the kinematic linkages are represented by small circles, no matter their conventional representations.

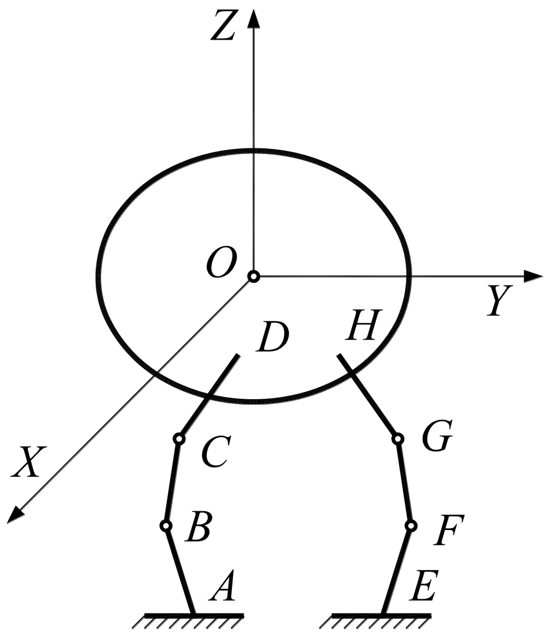

Figure 3. General system.

2.2. Notations

We use the following notations:

- $Bxyz$ (Figure 4)—the local reference system for the rigid bar BC;
- $Exyz$, $Fxyz$, $Gxyz$, … (Figure 5)—local reference systems of the elastic bars, where the axes Ex, Fx, Gx, … are along the bars, and the axes Ey, Ez, Fy, Fz, Gy, Gz, … are the inertial axes of the cross-sections, which pass through the points E, F, G, …

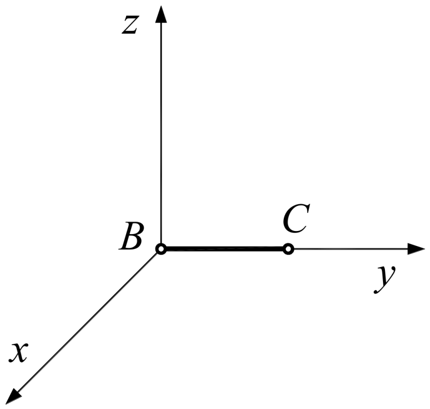

Figure 4. Local reference system of a rigid bar.

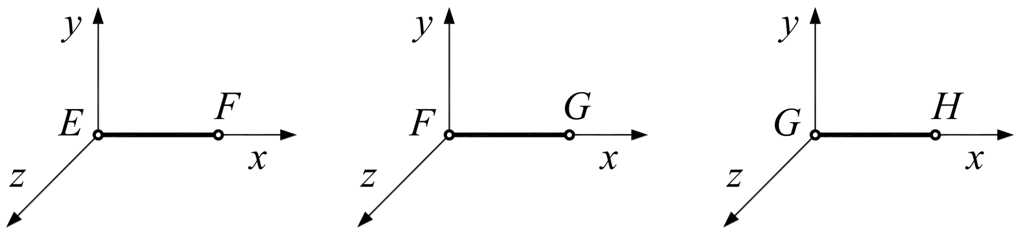

Figure 5. Local reference systems of the elastic bars.

The rest of the notations are given in the nomenclature.

2.3. Small Displacements

The total displacement in the kinematic joint B reads

$$[\mathbf{U}_B]\{\boldsymbol{\xi}_B\} \tag{2}$$

Similar relations may be written for the point C.

If we denote

$$[\mathbf{U}_{BC}] = \begin{bmatrix} [\mathbf{U}_B] & [\mathbf{U}_C] \end{bmatrix} \tag{3}$$

$$\{\boldsymbol{\xi}_{BC}\} = \begin{bmatrix} \{\boldsymbol{\xi}_B\} \\ \{\boldsymbol{\xi}_C\} \end{bmatrix} \tag{4}$$

then one may write the matrix relation

$$\{\boldsymbol{\Delta}\} = \begin{bmatrix} [\mathbf{U}_B] & [\mathbf{U}_C] \end{bmatrix}\{\boldsymbol{\xi}_{BC}\} \tag{5}$$

2.4. The Rigidity Matrix

The rigidity matrix $[\mathbf{k}]$ of the bar relative to the local reference system reads (see Appendix A)

$$[\mathbf{k}] = \begin{bmatrix} 0 & 0 & 0 & \frac{EA}{l} & 0 & 0 \\ 0 & 0 & \frac{6EI_z}{l^2} & 0 & \frac{12EI_z}{l^3} & 0 \\ 0 & -\frac{6EI_y}{l^2} & 0 & 0 & 0 & \frac{12EI_y}{l^3} \\ \frac{GI_x}{l} & 0 & 0 & 0 & 0 & 0 \\ 0 & \frac{4EI_y}{l} & 0 & 0 & 0 & -\frac{6EI_y}{l^2} \\ 0 & 0 & \frac{4EI_z}{l} & 0 & \frac{6EI_z}{l^2} & 0 \end{bmatrix} \tag{6}$$

while the flexibility matrix $[\mathbf{h}] = [\mathbf{k}]^{-1}$ is

$$[\mathbf{h}] = \begin{bmatrix} 0 & 0 & 0 & \frac{l}{GI_x} & 0 & 0 \\ 0 & 0 & \frac{l^3}{2EI_y} & 0 & \frac{l}{EI_y} & 0 \\ 0 & -\frac{l^2}{2EI_z} & 0 & 0 & 0 & \frac{l}{EI_z} \\ \frac{l}{EA} & 0 & 0 & 0 & 0 & 0 \\ 0 & \frac{l^3}{3EI_z} & 0 & 0 & 0 & -\frac{l^2}{2EI_z} \\ 0 & 0 & \frac{l^3}{3EI_y} & 0 & \frac{l^2}{2EI_y} & 0 \end{bmatrix} \tag{7}$$

In the general reference system, this results in

$$[\mathbf{K}] = [\mathbf{T}][\mathbf{k}][\mathbf{T}]^{-1} \tag{8}$$

$$[\mathbf{K}]^{-1} = [\mathbf{T}][\mathbf{k}]^{-1}[\mathbf{T}]^{-1} = [\mathbf{T}][\mathbf{h}][\mathbf{T}]^{-1} \tag{9}$$

The matrix of rigidity of the kinematic chain $EFGH$, considered as a rigid bent bar, is

$$\left[\tilde{\mathbf{K}}_{EH}\right] = \left[[\mathbf{K}_{EF}]^{-1} + [\mathbf{K}_{FG}]^{-1} + [\mathbf{K}_{GH}]^{-1}\right]^{-1} \tag{10}$$

Denoting $[\mathbf{U}_{FG}]$ for the matrix

$$[\mathbf{U}_{FG}] = \begin{bmatrix} [\mathbf{U}_F] & [\mathbf{U}_G] \end{bmatrix} \tag{11}$$

one obtains the rigidity matrix $[\mathbf{K}_{EH}]$ of the elastic kinematic chain $EFGH$

$$[\mathbf{K}_{EH}] = \left[\tilde{\mathbf{K}}_{EH}\right] - \left[\tilde{\mathbf{K}}_{EH}\right][\mathbf{U}_{FG}]\left[[\mathbf{U}_{FG}]^{\mathrm{T}}[\boldsymbol{\eta}]\left[\tilde{\mathbf{K}}_{EH}\right][\mathbf{U}_{FG}]\right]^{-1}[\mathbf{U}_{FG}]^{\mathrm{T}}[\boldsymbol{\eta}]\left[\tilde{\mathbf{K}}_{EH}\right] \tag{12}$$

3. Calculation of the Displacement

Let us consider that the rigid solid is acted on by the force $\{\mathbf{F}\}$ and one asks for the determination of the displacement $\{\boldsymbol{\Delta}\}$.

The force that acts upon the kinematic chain at the point H is given by

$$\{\mathbf{F}_H\} = [\mathbf{K}_{EH}]\{\boldsymbol{\Delta}\} \tag{13}$$

Isolating the rigid solid, one obtains the equality

$$\{\mathbf{F}_D\} + \sum [\mathbf{K}_{EH}]\{\boldsymbol{\Delta}\} = \{\mathbf{F}\} \tag{14}$$

using the notation

$$[\mathbf{K}] = \sum [\mathbf{K}_{EH}] \tag{15}$$

it results in the relation

$$\{\mathbf{F}_D\} + [\mathbf{K}]\{\boldsymbol{\Delta}\} = \{\mathbf{F}\} \tag{16}$$

Assuming that the weights of the bars are negligible, one obtains

$$\{\mathbf{F}_D\} = \{\mathbf{F}_C\} = \{\mathbf{F}_B\} \tag{17}$$

and

$$[\mathbf{U}_{BC}]^{\mathrm{T}}[\boldsymbol{\eta}]\{\mathbf{F}_D\} = \{0\} \tag{18}$$

Thus, we obtain the equality

$$[\mathbf{U}_{BC}]^{\mathrm{T}}[\boldsymbol{\eta}]\{\mathbf{F}_D\} = \{0\} \tag{19}$$

or, equivalently

$$[\mathbf{U}_{BC}]^{\mathrm{T}}[\boldsymbol{\eta}][\mathbf{K}][\mathbf{U}_{BC}]\{\boldsymbol{\xi}_{BC}\} = [\mathbf{U}_{BC}]^{\mathrm{T}}[\boldsymbol{\eta}]\{\mathbf{F}\} \tag{20}$$

wherefrom

$$\{\boldsymbol{\xi}_{BC}\} = \left[[\mathbf{U}_{BC}]^{\mathrm{T}}[\boldsymbol{\eta}][\mathbf{K}][\mathbf{U}_{BC}]\right]^{-1}[\mathbf{U}_{Bc}][\boldsymbol{\eta}]\{\mathbf{F}\} \tag{21}$$

with

$$\{\boldsymbol{\Delta}\} = [\mathbf{U}_{BC}]\{\boldsymbol{\xi}_{BC}\} \tag{22}$$

Other approaches that use the screw coordinates are described in [1–4,19,22,32]. The formulae presented above are equivalent to those reported in the references mentioned above.

4. The Equation of the Free Vibrations

Knowing that the matrix of the screw (plückerian) coordinates of the inertial force is given by $-[\mathbf{M}]\left\{\ddot{\boldsymbol{\Delta}}\right\}$, then from Equation (19) one obtains the matrix differential equation

$$[\mathbf{U}_{BC}]^{\mathrm{T}}[\boldsymbol{\eta}][\mathbf{M}][\mathbf{U}_{BC}]\left[\ddot{\boldsymbol{\xi}}_{BC}\right] + [\mathbf{U}_{BC}]^{\mathrm{T}}[\boldsymbol{\eta}][\mathbf{K}][\mathbf{U}_{BC}]\{\boldsymbol{\xi}_{BC}\} = \{0\} \tag{23}$$

From the last equation one determines $\{\boldsymbol{\xi}_{BC}\}$, and from Equation (22) one obtains the displacement $\{\boldsymbol{\Delta}\}$.

Moreover, the displacements in the kinematic linkages F and G are given by

$$\{\boldsymbol{\xi}_{FG}\} = \left[[\mathbf{U}_{FG}]^{\mathrm{T}}[\boldsymbol{\eta}]\left[\tilde{\mathbf{K}}_{EH}\right][\mathbf{U}_{FG}]\right]^{-1}[\mathbf{U}_{FG}]^{\mathrm{T}}[\boldsymbol{\eta}]\left[\tilde{\mathbf{K}}_{EH}\right]\{\boldsymbol{\Delta}\} \tag{24}$$

5. The Equation of the Forced Vibrations

In this case we have to correct the right-hand term in Equation (23) resulting in

$$[\mathbf{U}_{BC}]^{\mathrm{T}}[\boldsymbol{\eta}][\mathbf{M}][\mathbf{U}_{BC}]\left[\ddot{\boldsymbol{\xi}}_{BC}\right] + [\mathbf{U}_{BC}]^{\mathrm{T}}[\boldsymbol{\eta}][\mathbf{K}][\mathbf{U}_{BC}]\{\boldsymbol{\xi}_{BC}\} = [\mathbf{U}_{BC}]^{\mathrm{T}}[\boldsymbol{\eta}]\{\mathbf{F}\} \tag{25}$$

where $\{\mathbf{F}\}$ is the matrix of the screw coordinates of the forces that act upon the rigid solid. Relative to the system $OXYZ$, considering that the resultant force is $\mathbf{F} = F_X\mathbf{i} + F_Y\mathbf{j} + F_Z\mathbf{k}$, while the resultant moment reads $\mathbf{M}_O = M_{OX}\mathbf{i} + M_{OY}\mathbf{j} + M_{OZ}\mathbf{k}$, then the matrix $\{\mathbf{F}\}$ takes the form

$$\{\mathbf{F}\} = \begin{bmatrix} F_X & F_Y & F_Z & M_{OX} & M_{OY} & M_{OZ} \end{bmatrix}^{\mathrm{T}} \tag{26}$$

Different formulae for certain particular cases are presented in [34,44,48,51]. The Equations (23) and (25) represent the most general case.

6. Example

We consider the Stewart platform captured in Figure 6. The triangles $A_1A_2A_3$ and $C_1C_2C_3$ are equilateral with edges equal to $\frac{l\sqrt{3}}{2}$ and $l\sqrt{3}$, respectively. The origin O is the center of the weight of the shell $A_1A_2A_3$. The common length of the bars A_iB_i, $i = \overline{1,\ 3}$, is

$2l$, and the common length of the bars B_iC_i, $i = \overline{1, 3}$, is l. The bars A_iB_i, $i = \overline{1, 3}$, form an angle of 30° with the normal to the plane $A_1A_2A_3$, while the bars B_iC_i, $i = \overline{1, 3}$, form an angle of 30° with the normal to the plane $C_1C_2C_3$. Both planes $A_1A_2A_3$ and $C_1C_2C_3$ are considered to be horizontal. Consequently, the measures of the angles $A_iB_iC_i$ are all equal to 90°. At the points A_i, $i = \overline{1, 3}$, there exist spherical joints, while at the points B_i, $i = \overline{1, 3}$, there exist prismatic joints.

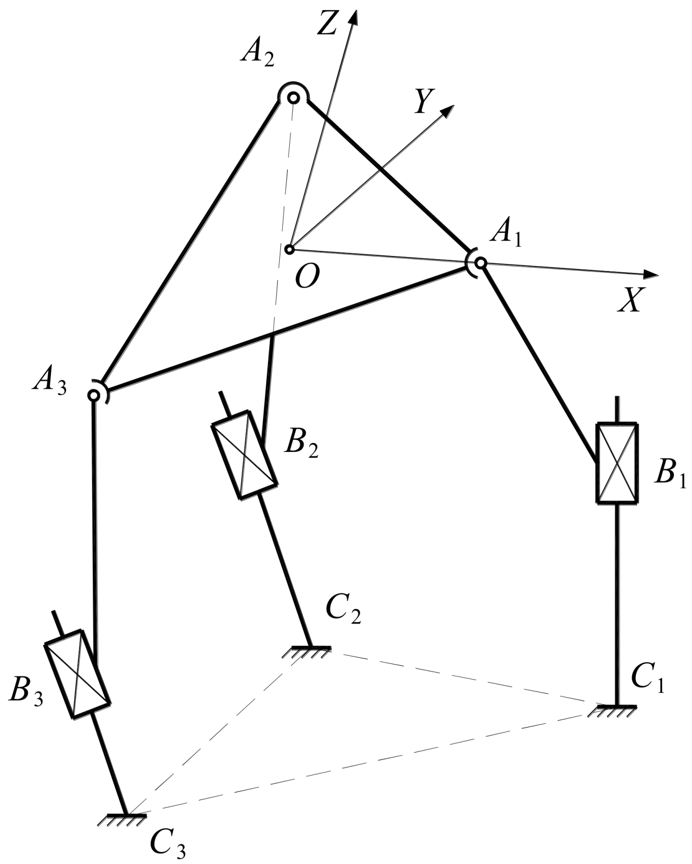

Figure 6. Numerical application.

The numerical values are, $E = 2.1 \times 10^{11}$ N/m^2 and $G = 8 \times 10^{10}$ N/m^2; the mass of the shell $A_1A_2A_3$, $m = 10$ kg.

For the case of free vibrations, we will consider a few cases:

(i) $l = 0.2$ m, $d_1 = d_2 = d_3 = 0.01$ m (the diameters of the bars for each kinematic chain, d_1 corresponds to the bars of the kinematic chain $A_1B_1C_1$ etc.);
(ii) $l = 0.5$ m, $d_1 = d_2 = d_3 = 0.01$ m;
(iii) $l = 0.2$ m, $d_1 = 0.03$ m, $d_2 = 0.01$ m, $d_3 = 0.01$ m;
(iv) $l = 0.2$ m, $d_1 = 0.03$ m, $d_2 = 0.01$ m, $d_3 = 0.02$ m.

For each case we will discuss the following situations: (a) all the kinematic chains $A_iB_iC_i$, $i = \overline{1, 3}$, consisting of elastic elements, and (b) the kinematic chain $A_1B_1C_1$ is compounded by rigid elements, while the kinematic chains $A_2B_2C_2$ and $A_3B_3C_3$ are formed by elastic bars.

The complete calculations are presented only for the first case in Appendix B.

The matrix differential systems in each case are presented in Appendix C.

6.1. Case (i)

(a) If we consider that all the kinematic chains contain only elastic elements, then the eigenpulsations are $p_1 \approx 25.36$ s^{-1}, $p_2 \approx 8.87$ s^{-1} (for θ_x and δ_y), $p_3 \approx 25.36$ s^{-1},

$p_4 \approx 8.87\ \mathrm{s}^{-1}$ (for θ_y and δ_x), $p_5 \approx 30.27\ \mathrm{s}^{-1}$ (for θ_z), and $p_6 \approx 10.51\ \mathrm{s}^{-1}$ (for δ_z); they form two pairs of doubly degenerate ones (p_1, p_3, and p_2, p_4, respectively), and a pair of singly degenerate one s(p_5, p_6).

(b) If the kinematic chain $A_1B_1C_1$ consists of rigid elements, then the corresponding eigenvalues are $p_1 \approx 25.83\ \mathrm{s}^{-1}$, $p_2 \approx 13.49\ \mathrm{s}^{-1}$, (for θ_x and θ_z), $p_3 \approx 12.54\ \mathrm{s}^{-1}$, and $p_4 \approx 8.96\ \mathrm{s}^{-1}$ (for θ_y and δ_X).

(c) The correspondences mentioned above between the eigenpulsations and the kinematic parameters (at points (*a*) and (*b*)) also hold true for the rest of the cases.

6.2. Case (ii)

Proceeding in a similar way, one obtains the following values:

(a) if all kinematic chains consist of elastic elements, then the eigenpulsations are given by $p_1 \approx 6.42\ \mathrm{s}^{-1}$, $p_2 \approx 2.24\ \mathrm{s}^{-1}$, (for θ_x and δ_y), $p_3 \approx 6.42\ \mathrm{s}^{-1}$, $p_4 \approx 2.24\ \mathrm{s}^{-1}$ (for θ_y and δ_x), $p_5 \approx 7.66\ \mathrm{s}^{-1}$ (for θ_z), and $p_6 \approx 2.66\ \mathrm{s}^{-1}$ (for δ_z).

Again, the eigenpulsations form two pairs of doubly degenerate ones (p_1, p_3, and p_2, p_4, respectively), and a pair of singly degenerate ones (p_5, and p_6). Denoting by $p_i^{(\text{case } i)}$, and $p_i^{(\text{case } ii)}$, $i = \overline{1, 6}$, the corresponding eigenpulsations in the first and the second case, respectively, we have that $\frac{p_i^{(\text{case } i)}}{p_i^{(\text{case } ii)}} = \text{constant}$, that is, one may determine the eigenpulsations in the case of when all kinematic chains are elastic ones knowing only a set of eigenpulsations for a certain length l.

(b) if the kinematic chain $A_1B_1C_1$ consists of rigid elements, then it results in the eigenpulsations: $p_1 \approx 3.41\ \mathrm{s}^{-1}$, $p_2 \approx 6.53\ \mathrm{s}^{-1}$ (for θ_x and θ_z), and $p_3 \approx 2.26\ \mathrm{s}^{-1}$, and $p_4 \approx 3.17\ \mathrm{s}^{-1}$ (for θ_y and δ_x). Again, denoting $p_i^{(\text{case } i)}$, and $p_i^{(\text{case } ii)}$, $i = \overline{1, 4}$, for the corresponding eigenpulsations in the first and the second case, respectively, we have that $\frac{p_i^{(\text{case } i)}}{p_i^{(\text{case } ii)}} = \text{constant}$; that is, one may determine the eigenpulsations in the case of when a kinematic chain consists of rigid elements knowing only a set of eigenpulsations for a certain length l. Moreover, the constant that gives the ration in the case when all kinematic chains are elastic ones is equal to the constant value of the ratio in the case when one kinematic chain consists of rigid elements.

We may conclude that by changing the length l, the structures of the systems that give the eigenpulsations remain the same; that is, the symmetry cannot be destroyed.

6.3. Case (iii)

The results are as follows:

(a) if all kinematic chains consist of elastic elements, then the eigenpulsations read now $p_1 \approx 177.01\ \mathrm{s}^{-1}$, $p_2 \approx 25.83\ \mathrm{s}^{-1}$, $p_3 \approx 13.42\ \mathrm{s}^{-1}$ (for θ_x, θ_z, and δ_y), and $p_4 \approx 189.55\ \mathrm{s}^{-1}$, $p_5 \approx 12.49\ \mathrm{s}^{-1}$, and $p_6 \approx 8.94\ \mathrm{s}^{-1}$ (for θ_y, δ_x, and δ_z);

(b) if the kinematic chain $A_1B_1C_1$ consists of rigid elements, then one obtains the eigenpulsations $p_1 \approx 25.83\ \mathrm{s}^{-1}$, $p_2 \approx 13.49\ \mathrm{s}^{-1}$ (for θ_x and θ_z), and $p_3 \approx 12.54\ \mathrm{s}^{-1}$, and $p_4 \approx 8.96\ \mathrm{s}^{-1}$ (for θ_y and δ_x).

6.4. Case (iv)

The numerical results are:

(a) if all kinematic chains consist of elastic elements, then one obtains the eigenpulsations $p_1 \approx 194.39\ \mathrm{s}^{-1}$, $p_2 \approx 184.60\ \mathrm{s}^{-1}$, $p_3 \approx 80.14\ \mathrm{s}^{-1}$, $p_4 \approx 45.66\ \mathrm{s}^{-1}$, $p_5 \approx 14.66\ \mathrm{s}^{-1}$, and $p_6 \approx 10.82\ \mathrm{s}^{-1}$;

(b) if the kinematic chain $A_1B_1C_1$ consists of rigid elements, then one obtains the eigenpulsations $p_1 \approx 80.86\ \mathrm{s}^{-1}$, $p_2 \approx 48.64\ \mathrm{s}^{-1}$, $p_3 \approx 14.69\ \mathrm{s}^{-1}$, and $p_4 = 10.86\ \mathrm{s}^{-1}$.

One may easily observe that there exists no obvious mathematical expression that connects the values of the eigenpulsations obtained, considering that all kinematic chains consist of elastic elements to the values of the eigenpulsations obtained in the case in which one kinematic chain consists of rigid elements. Moreover, the corresponding values of the eigenvalues are very different from case to case.

Determination of the eigenvalues is also considered in [51] for a particular mechanical system. The authors calculated only the first three eigenpulsations.

It is interesting to see the variations in the eigenpulsations in the functions of different geometrical and mechanical parameters. The standard values of the parameters are those presented above. Further on, the values of the parameters are the standard ones, excepting those parameters for which we specify other values.

The authors are not aware of the existence of a similar study in the references.

6.5. Dependency on the Diameters of Bars

First of all, we consider that all bars (no matter if they are elastic of rigid) have the same diameter. Four cases are considered. In the first case the diameters are equal, that is, $d_1 = d_2 = d_3$; in the second case the relation between the diameter d_1 and the diameters d_2 and d_3 is given by $d_2 = d_3 = \frac{d_1}{2}$; the third case is similar to the second one, but $d_2 = d_3 = \frac{d_1}{4}$; finally, the fourth situation is characterized by $d_2 = \frac{d_1}{5}$, and $d_3 = \frac{d_1}{10}$.

In all diagrams the subscript index e means that the eigenvalues are calculated considering that all kinematic chains consist of elastic elements, while the subscript index r means that the eigenvalues are calculated considering that one kinematic chain consists of rigid elements.

The variations in the eigenpulsations in the function of the diameter d_1 are given in Figure 7. The diameter varies between 0.001 m and 0.05 m. The eigenpulsations decrease in order; that is, the eigenpulsation p_1 is the greatest, while the eigenpulsation p_6 (when all kinematic chains are elastic), or the eigenpulsation p_4 (when one kinematic chain is rigid) is the smallest. The codification of colors is as follows: blue means the first eigenpulsation, green means the second, red means the third, cyan stands for the fourth eigenpulsation, magenta for the fifth, while yellow stands for the sixth.

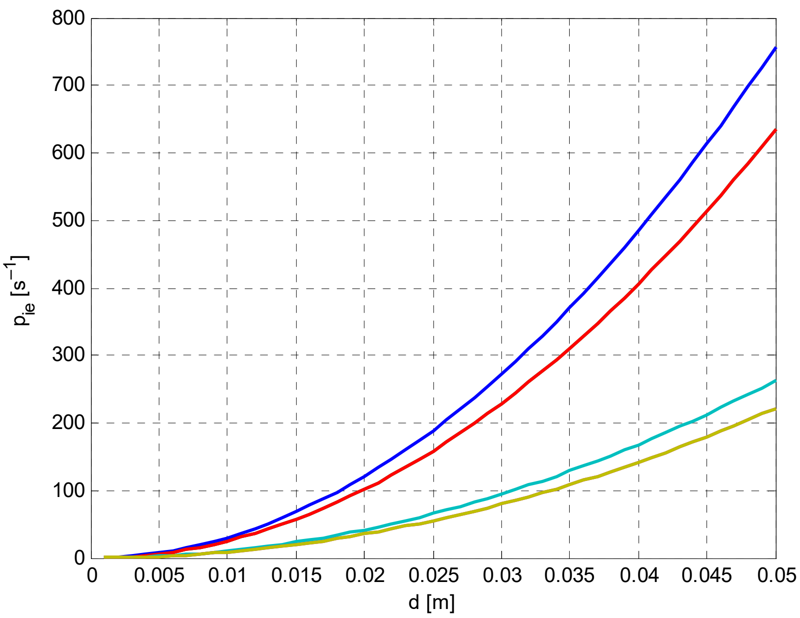

(a1)

Figure 7. *Cont.*

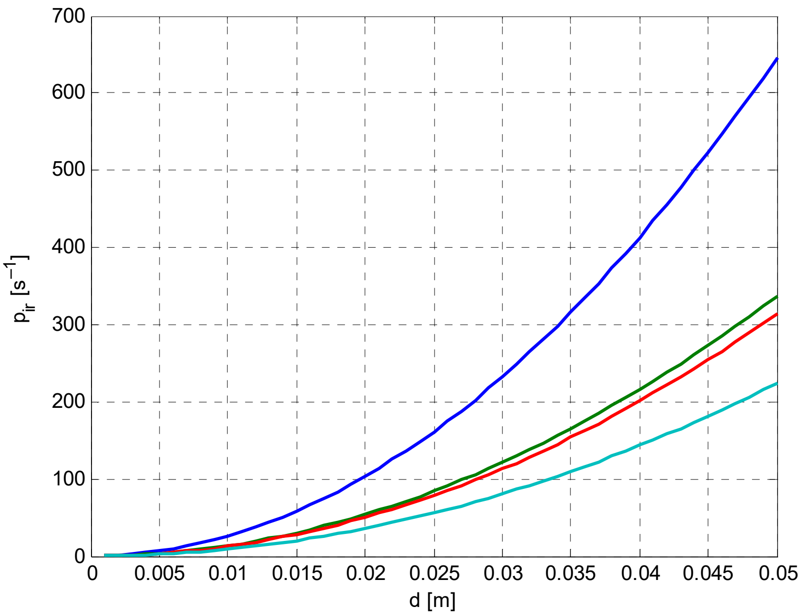

(**a2**)

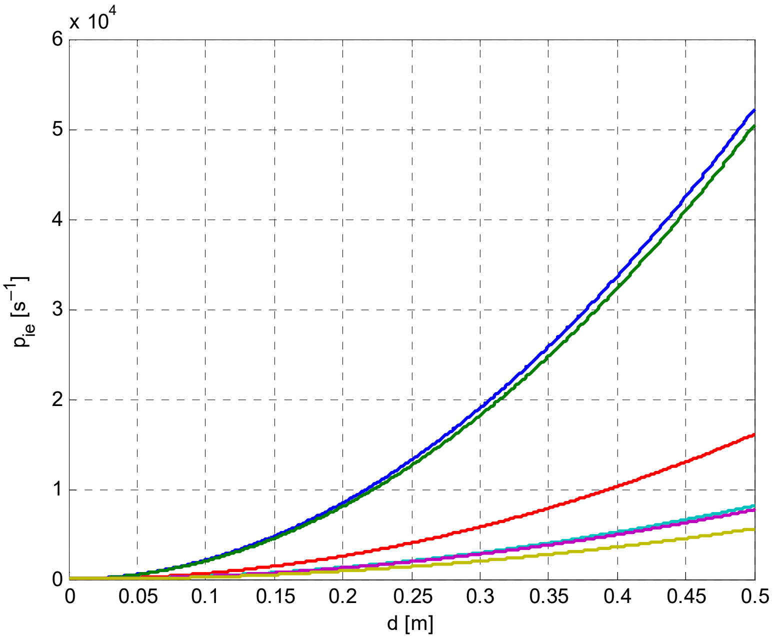

(**b1**)

Figure 7. *Cont.*

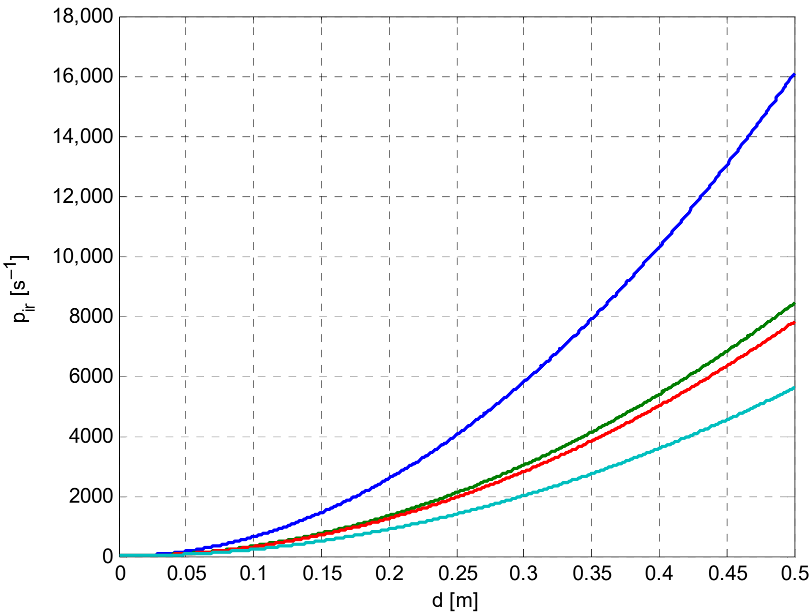

(**b2**)

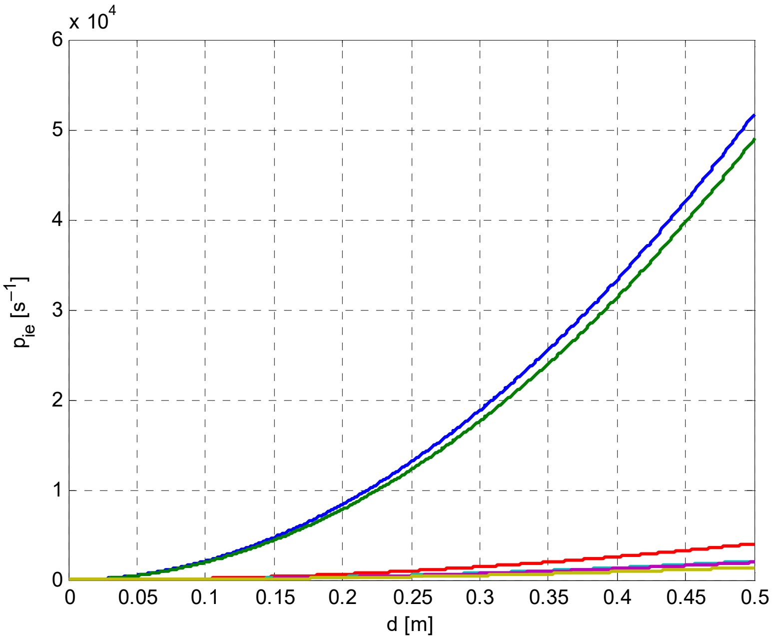

(**c1**)

Figure 7. *Cont.*

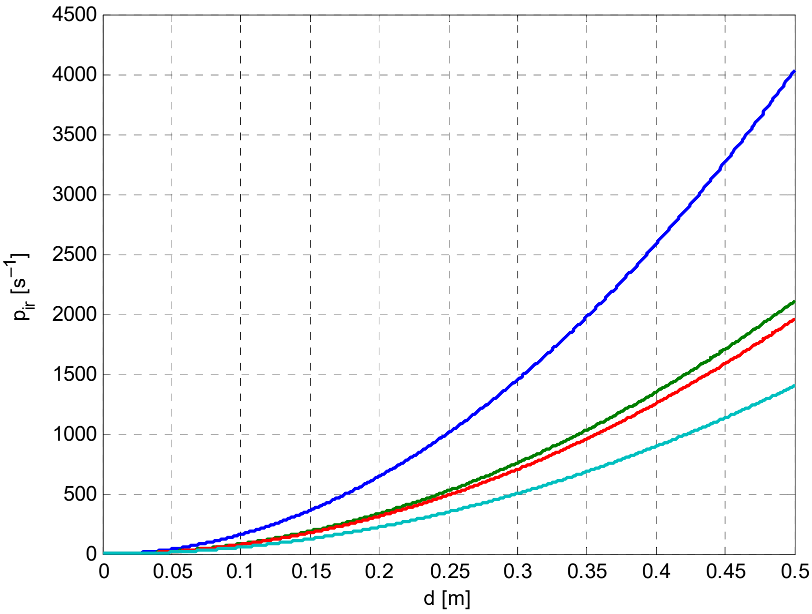

(**c2**)

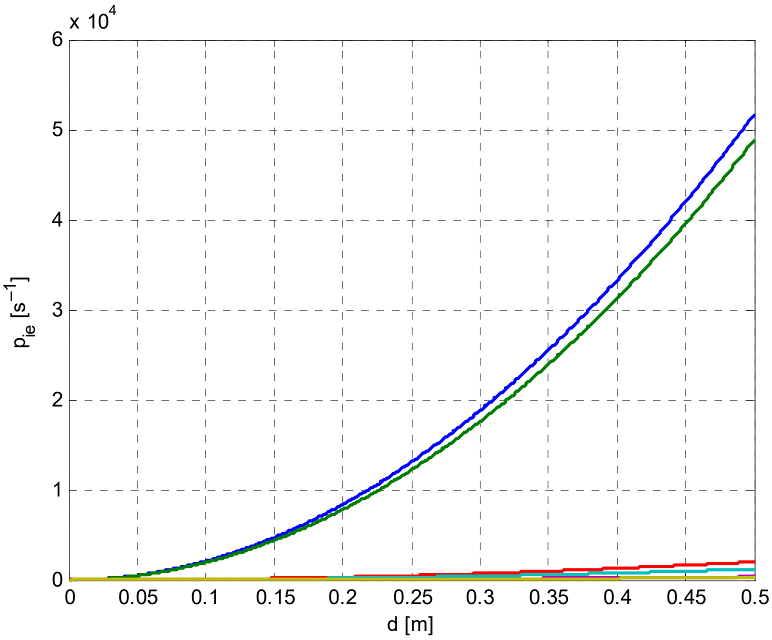

(**d1**)

Figure 7. *Cont.*

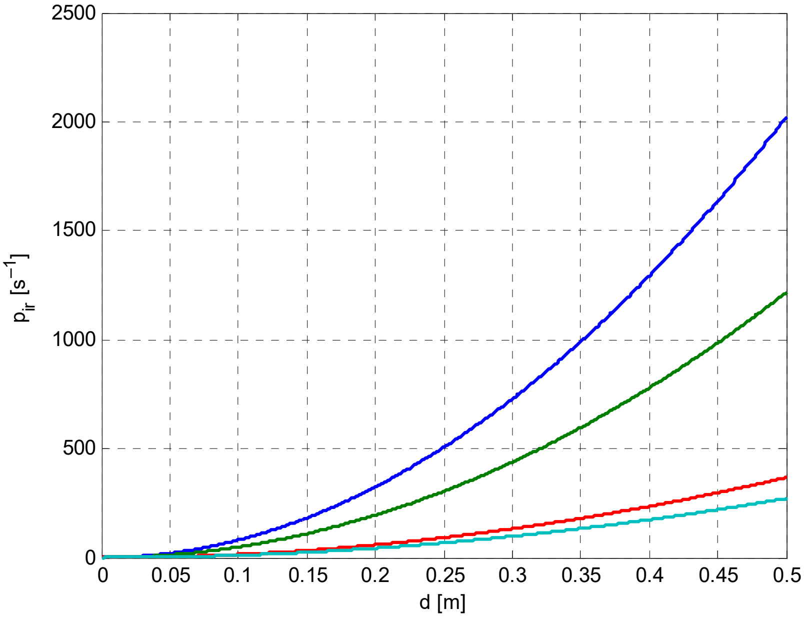

(**d2**)

Figure 7. Diagrams of variations $p_i = p_i(d)$: (**a**) first case, (**b**) second case, (**c**) third case, and (**d**) fourth case; subscript index e means that all kinematic chains are elastic ones, while subscript index r signifies that one kinematic chain consists of rigid elements. In (**a1**) only four eigenpulsations are distinct: p_1, $p_2 = p_3$, p_4, and $p5 = p_6$; in (**b1**,**c1**) only five eigenpulsations are distinct: p_1, p_2, p_3, $p_4 = p_5$, and p_6, while in (**d1**) all six eigenpulsations are distinct. The first three considered cases are cases of degeneracy (the first is of double degeneracy, while the second and the third are of simple degeneracy). The last case is a regular one. The degeneracy does not imply a diminishing of the number of eigenvalues in the situation of a kinematic chain with rigid elements (see (**a2**,**b2**,**c2**,**d2**)).

Recalling the results from the previous paragraphs, we have to observe that in the degeneracy cases, some eigenpulsations have equal values; that is, in a few of the next diagrams one may observe a smaller number of curves.

For instance, referring to the first case when all kinematic chains are elastic ones (see Section 6.1), then the actual eigenpulsation p_1 corresponds to the eigenpulsation p_5 in Section 6.1, the actual eigenpulsations $p_2 = p_3$ correspond to the eigenpulsations $p_1 = p_3$ in Section 6.1, the actual eigenpulsation p_4 corresponds to the eigenpulsation p_6 in Section 6.1, while the actual eigenpulsations $p_5 = p_6$ correspond to the eigenpulsations $p_2 = p_4$ in Section 6.1. When one kinematic chain consists of rigid elements, then the correspondence is as follows: the actual eigenpulsations p_1, p_2, p_3, and p_4 correspond to the eigenpulsations p_1, p_3, p_4, and p_2, respectively, in Section 6.1.

Similar correspondences may be stated for the rest of the cases.

All eigenpulsations present a parabolic variation increasing on the entire interval of the diameter. One cannot determine a mathematical formula to link the eigenvalues obtained when all the kinematic chains are elastic to the eigenvalues obtained when one kinematic chain has rigid elements.

The eigenpulsations do not depend on the diameters of the bars forming the rigid kinematic chain.

6.6. Dependency on the Length of Bars

In this situation we will also consider four cases: the first case is the standard one; the second case is defined by $d_1 = 0.02$ m, and $d_2 = d_3 = 0.01$ m; the third case is characterized by $d_1 = 0.03$ m, and $d_2 = d_3 = 0.02$ m, while for the fourth case, the values are $d_1 = 0.03$ m, $d_2 = 0.01$ m, and $d_3 = 0.02$ m.

Again the codifications for the subscript indices *e* and *r* hold true.

The diagrams of variation are captured in Figure 8. The common length of the bars varies between 0.01 m and 1 m. The codification of colors remains the same.

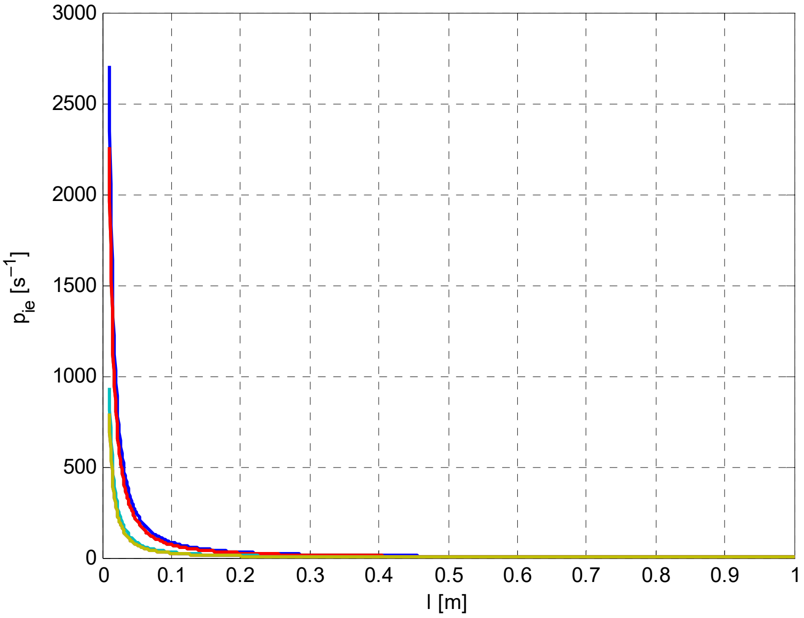

(**a1**)

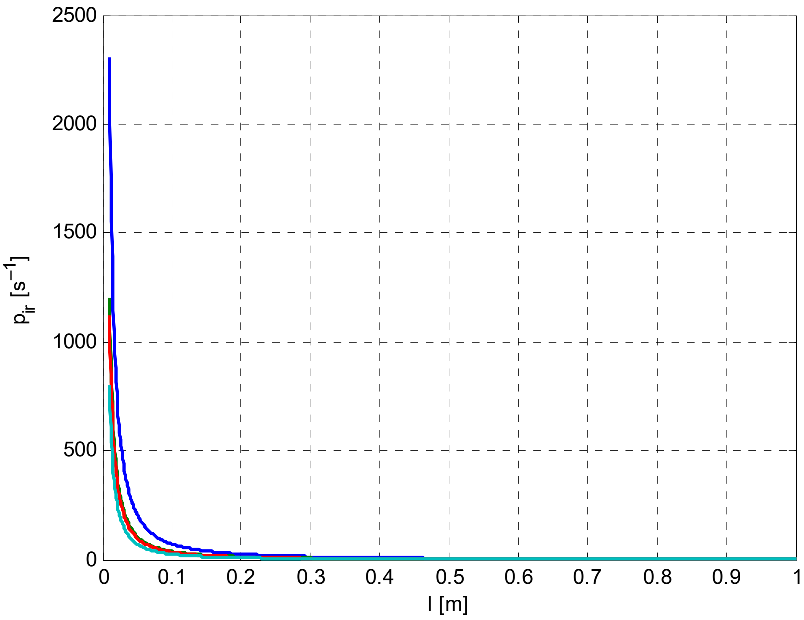

(**a2**)

Figure 8. *Cont*.

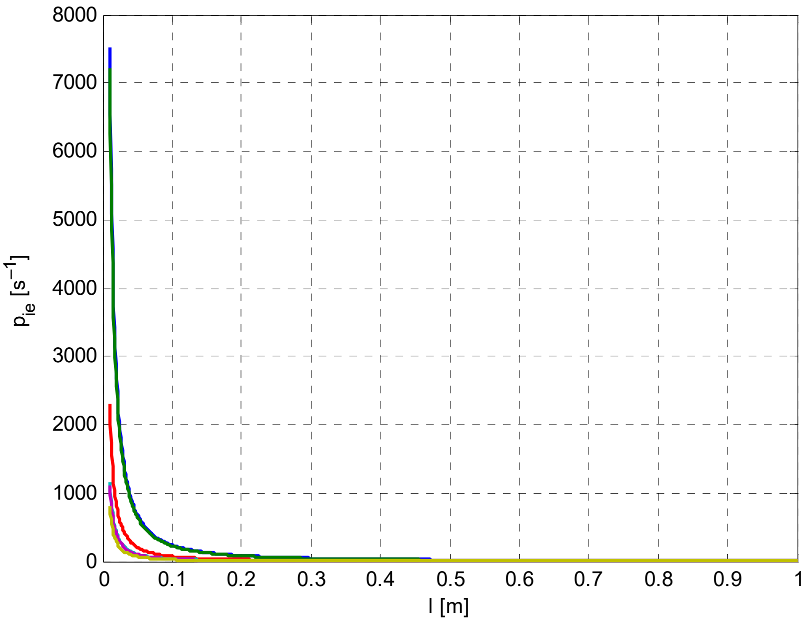

(**b1**)

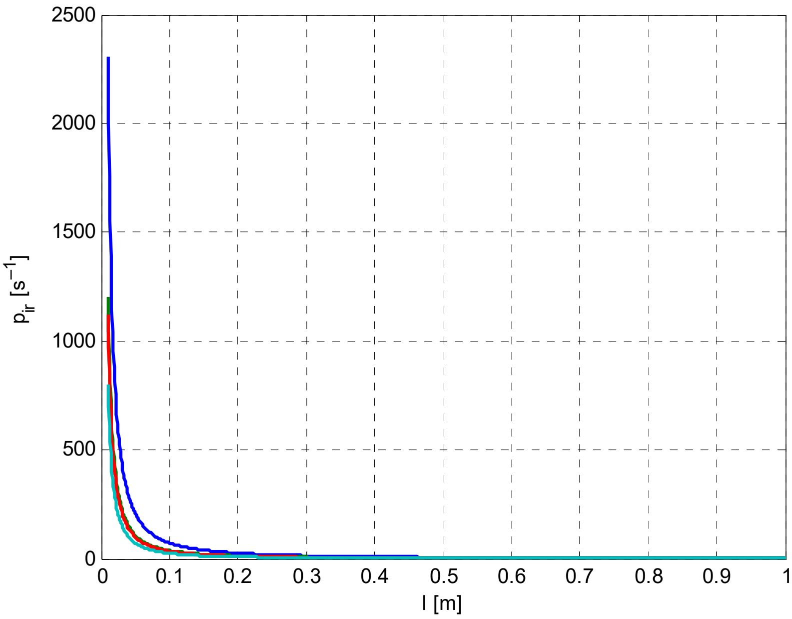

(**b2**)

Figure 8. *Cont.*

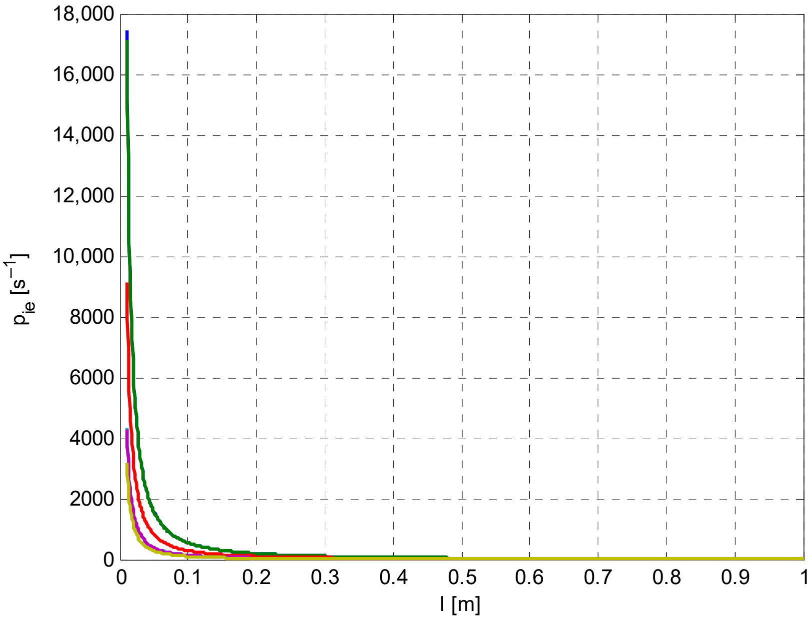

(**c1**)

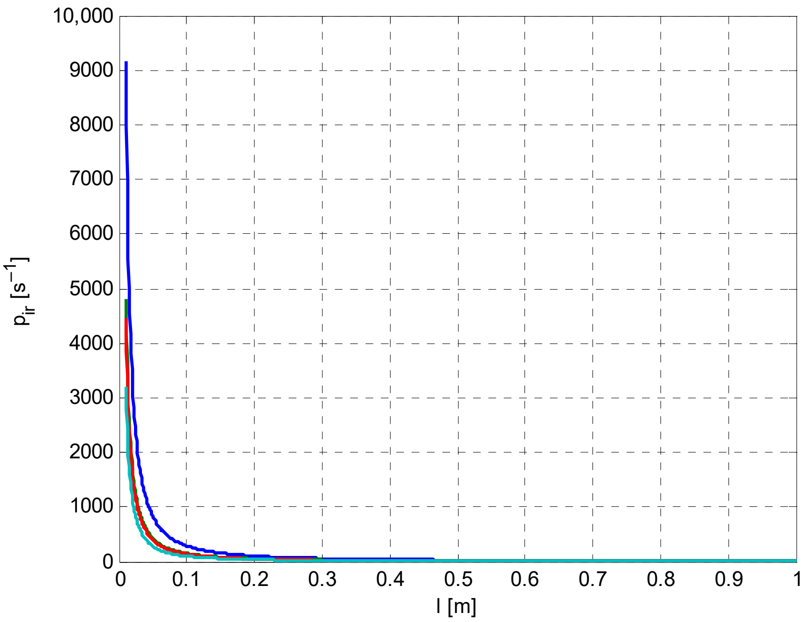

(**c2**)

Figure 8. *Cont*.

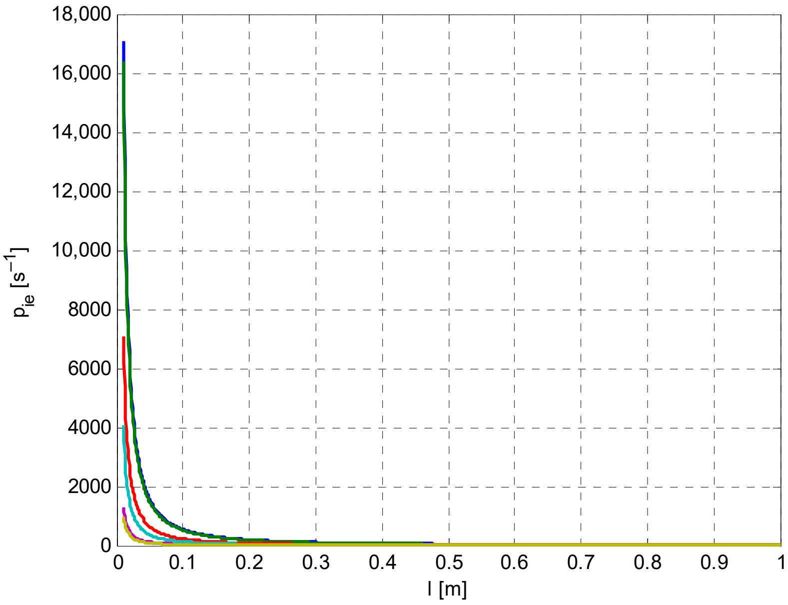

(**d1**)

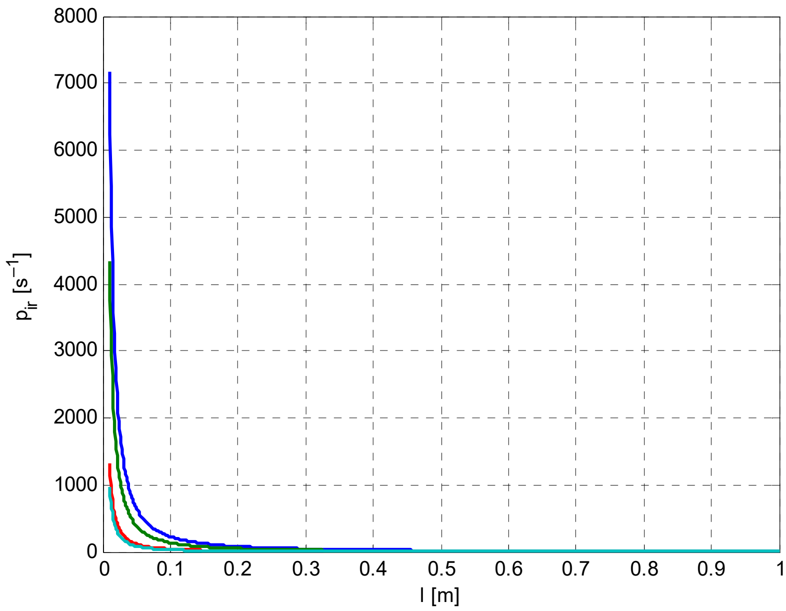

(**d2**)

Figure 8. Diagrams of variations $p_i = p_i(l)$: (**a**) first case, (**b**) second case, (**c**) third case, and (**d**) fourth case; subscript index e means that all kinematic chains are elastic ones, while subscript index r signifies that one kinematic chain consists of rigid elements. In (**a1**) only four eigenpulsations are distinct: p_1, $p_2 = p_3$, p_4, and $p_5 = p_6$; in (**b1**,**c1**) only five eigenpulsations are distinct: p_1, p_2, p_3, $p_4 = p_5$, and p_6, while in (**d1**) all six eigenpulsations are distinct. The first three considered cases are cases of degeneracy (the first is of double degeneracy, while the second and the third cases are of simple degeneracy). The last case is a regular one. The degeneracy does not imply a diminishing of the number of eigenvalues in the situation of a kinematic chain with rigid elements (see (**a2**,**b2**,**c2**,**d2**)).

All curves have decreasing shapes, with a vertical asymptote at $l = 0$, and corresponding horizontal asymptotes for $l \to \infty$. These results are expected to be obtained due to the contribution of the length l in the expressions of the components of the matrices $\left[\mathbf{K}_{system}\right]$

and, consequently, the expressions of different coefficients of the matrix differential systems of equations.

We also have degeneracy cases, which imply that not all curves may be seen in all diagrams.

6.7. Dependency on the Mass of the Shell

In this situation we consider the same four cases as in the Section 6.6.

Again the codifications for the subscript indices e and r, and the codification of the colors hold true.

The diagrams of variation are captured in Figure 9. The mass of the shell varies between 1 kg and 100 kg. The codification of colors remains the same.

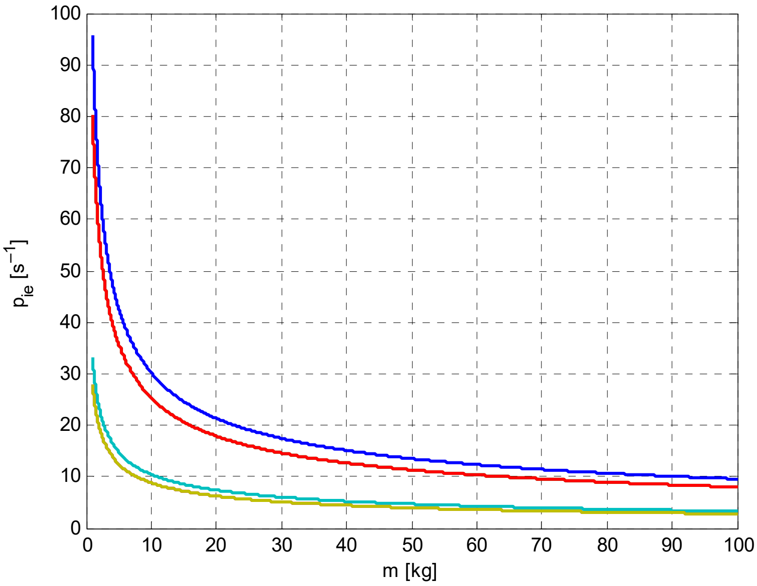

(**a1**)

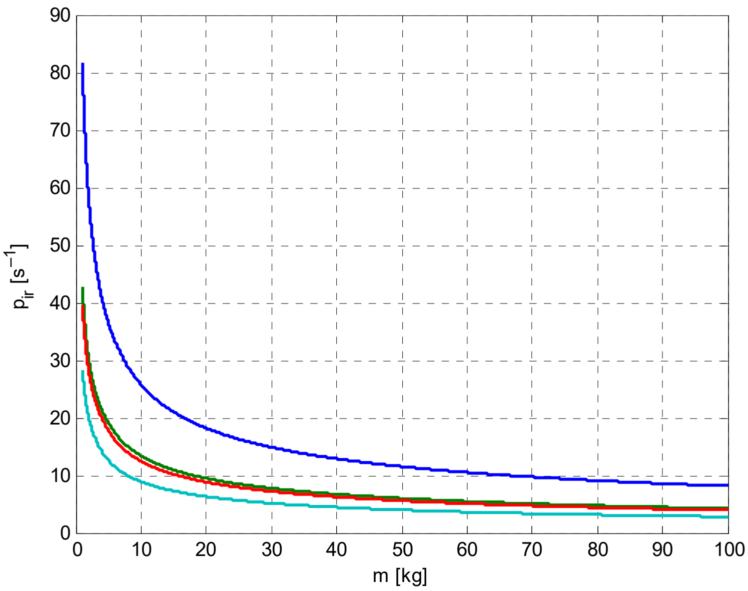

(**a2**)

Figure 9. *Cont.*

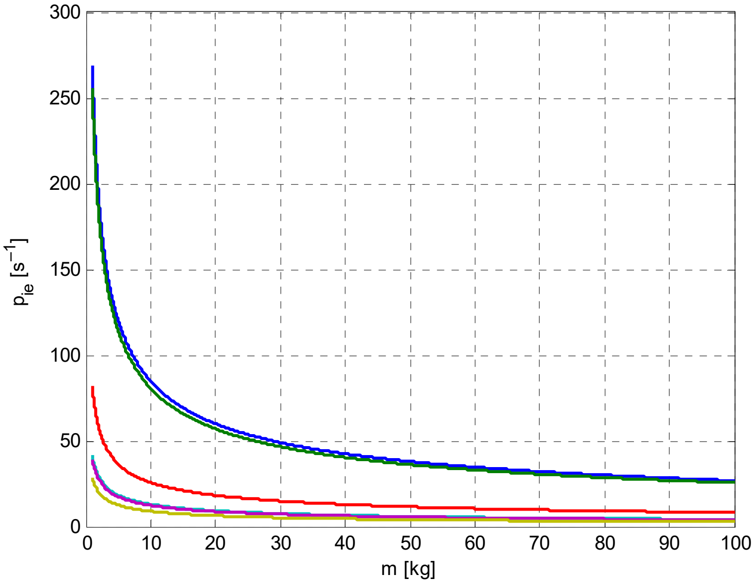

(**b1**)

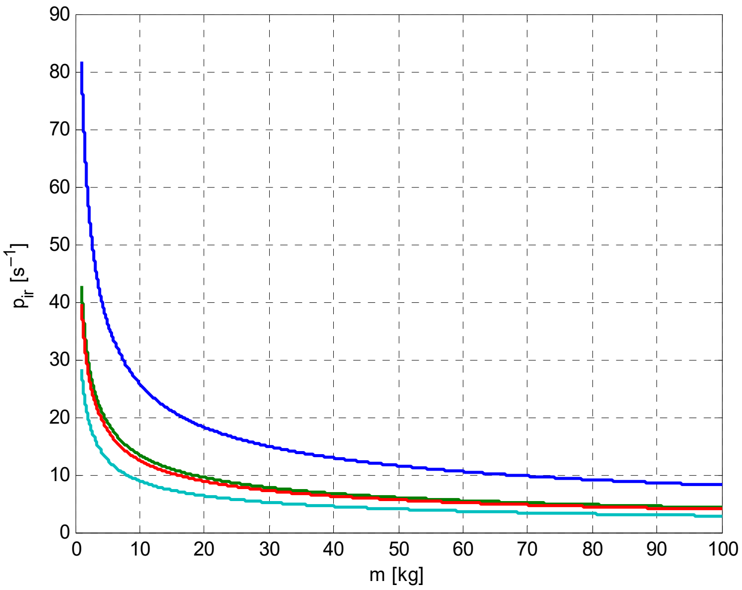

(**b2**)

Figure 9. *Cont.*

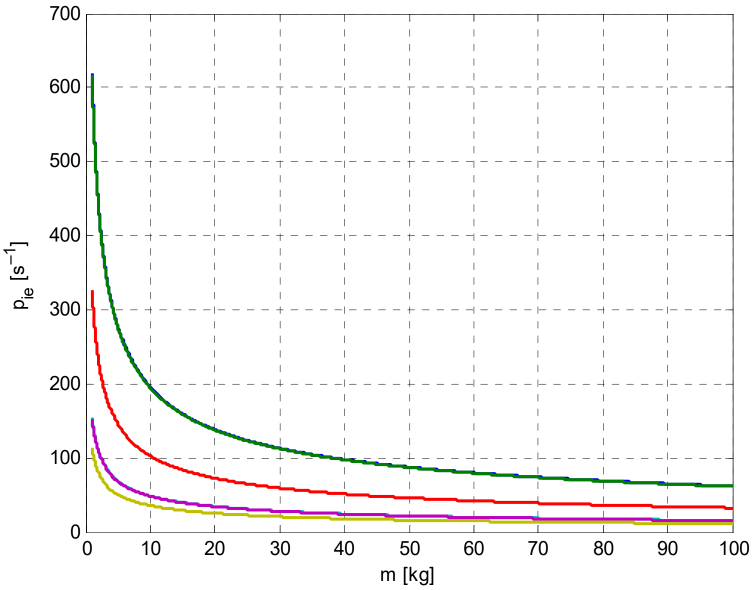

(**c1**)

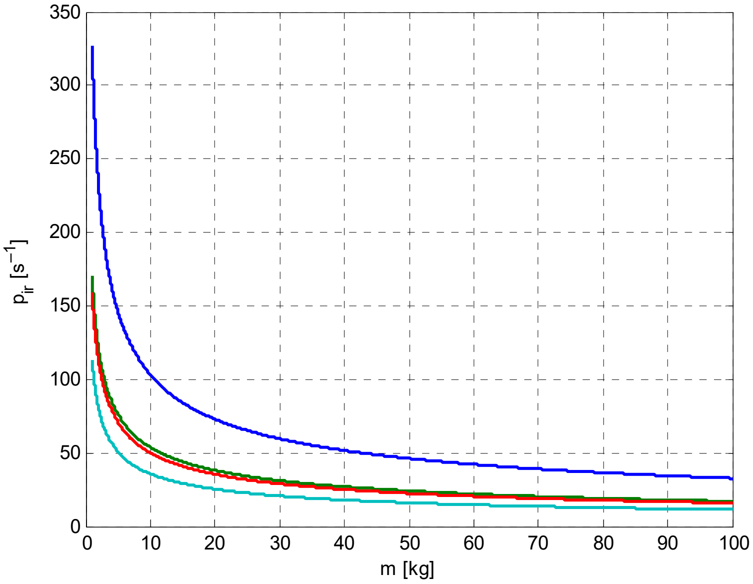

(**c2**)

Figure 9. *Cont.*

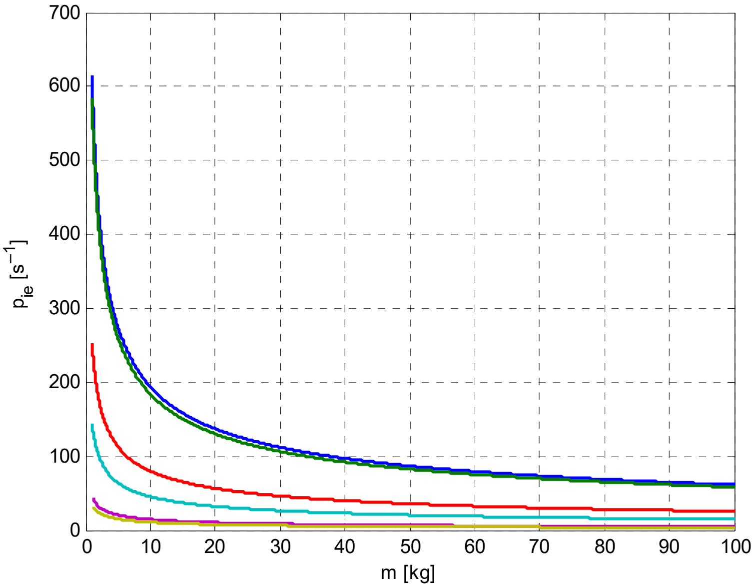

(**d1**)

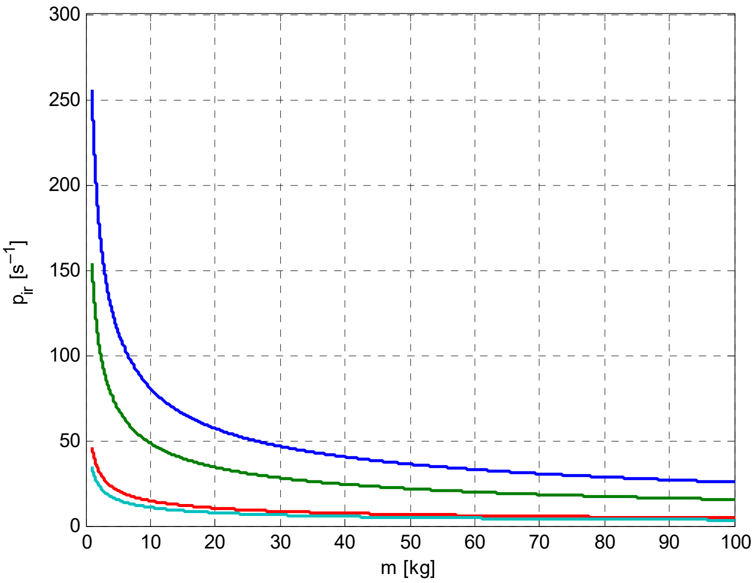

(**d2**)

Figure 9. Diagrams of variations $p_i = p_i(m)$: (**a**) first case, (**b**) second case, (**c**) third case, and (**d**) fourth case; subscript index e means that all kinematic chains are elastic ones, while subscript index r signifies that one kinematic chain consists of rigid elements. In (**a1**) only four eigenpulsations are distinct: p_1, $p_2 = p_3$, p_4, and $p_5 = p_6$; in (**b1**,**c1**) only five eigenpulsations are distinct: p_1, p_2, p_3, $p_4 = p_5$, and p_6, while in (**d1**) all six eigenpulsations are distinct. The first three considered cases are cases of degeneracy (the first is of double degeneracy, while the second and the third cases are of simple degeneracy). The last case is a regular one. The degeneracy does not imply a diminishing of the number of eigenvalues in the situation of a kinematic chain with rigid elements (see **a2**,**b2**,**c2**,**d2**).

All diagrams are decreasing curves as one expected. The curves have parabolic shapes. The results are explained by the contribution of the mass m in the expressions of the components of the matrices $\left[\mathbf{K}_{system}\right]$ and, consequently, the expressions of different coefficients of the matrix differential systems of equations.

We also have degeneracy cases, which imply that all curves may be seen in all diagrams.

6.8. Dependency on the Elasticity Modulus

E and G denote the generic values of the elasticity modulus and shear modulus, respectively, $G = \frac{E}{1+\nu}$, $\nu = 0.33$. We consider the following cases: the first case is defined by $E_1 = E_2 = E_3 = E$ and $G_1 = G_2 = G_3 = E$; the second case is defined by $E_1 = E$, $E_2 = E_3 = \frac{E}{2}$ and $G_1 = G$, $G_2 = G_3 = \frac{G}{2}$; the third case is characterized by $E_1 = E$, $E_2 = E_3 = \frac{E}{4}$ and $G_1 = G$, $G_2 = G_3 = \frac{G}{4}$; the fourth case is characterized by $E_1 = E$, $E_2 = \frac{E}{2}$, $E_3 = \frac{E}{5}$ and $G_1 = G$, $G_2 = \frac{G}{2}$, $G_3 = \frac{G}{5}$. The rest of the parameters are those from the standard case.

Again the codifications for the subscript indices e and r hold true.

The diagrams of variation are captured in Figure 10. The elasticity modulus varies between 10^8 N/m^2 and 3×10^{11} N/m^2. The codification of colors remains the same.

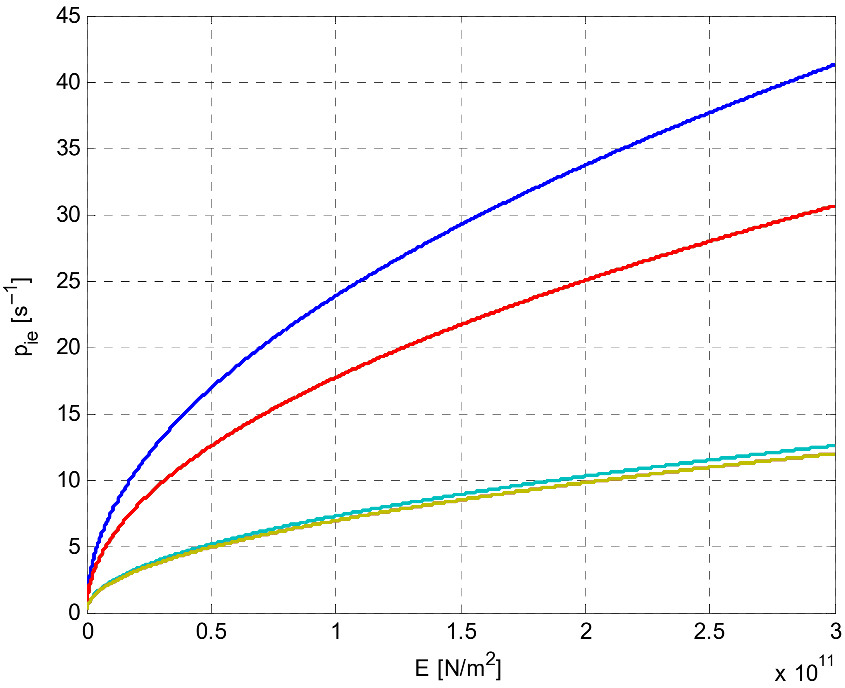

(a1)

Figure 10. *Cont.*

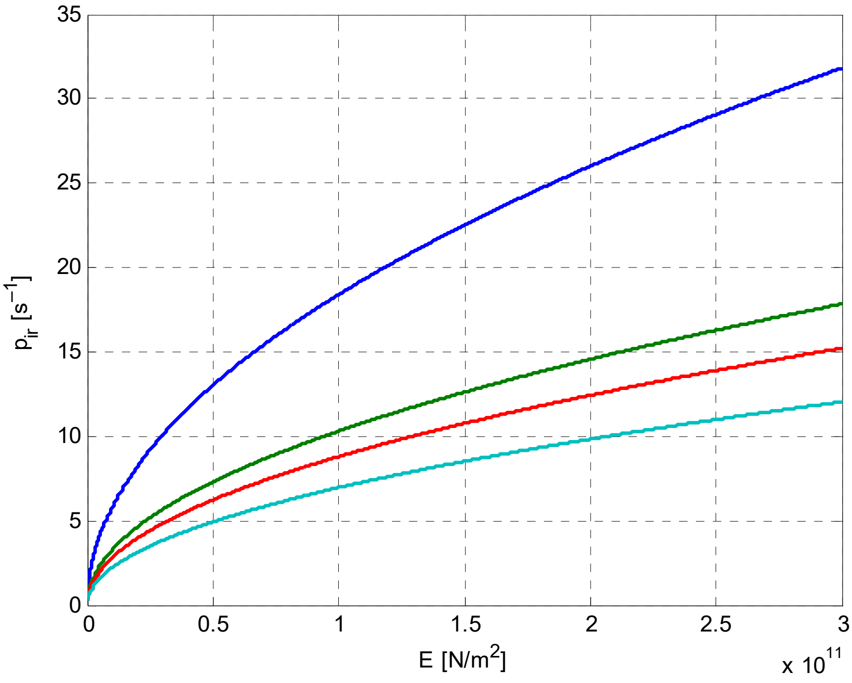

(**a2**)

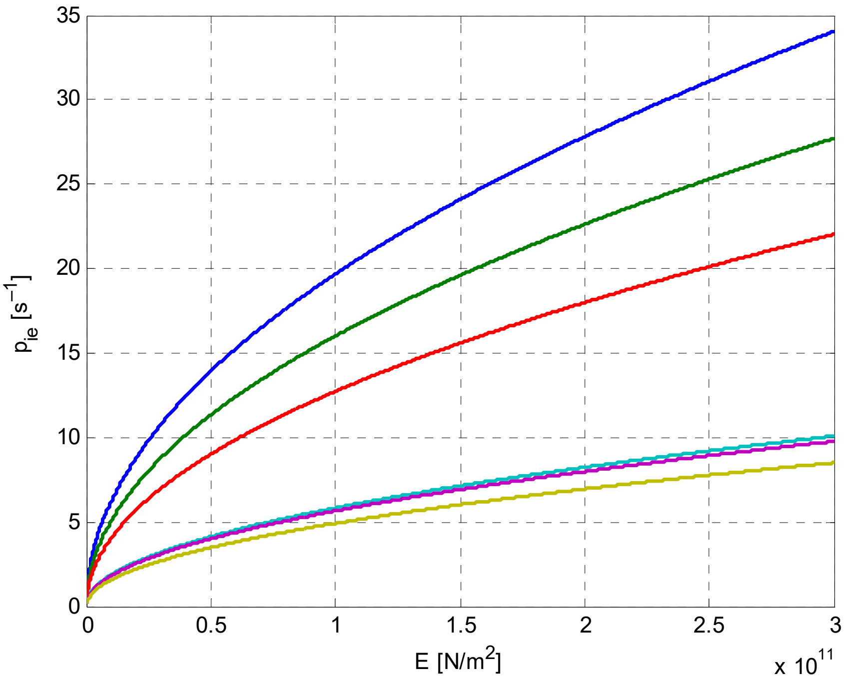

(**b1**)

Figure 10. *Cont.*

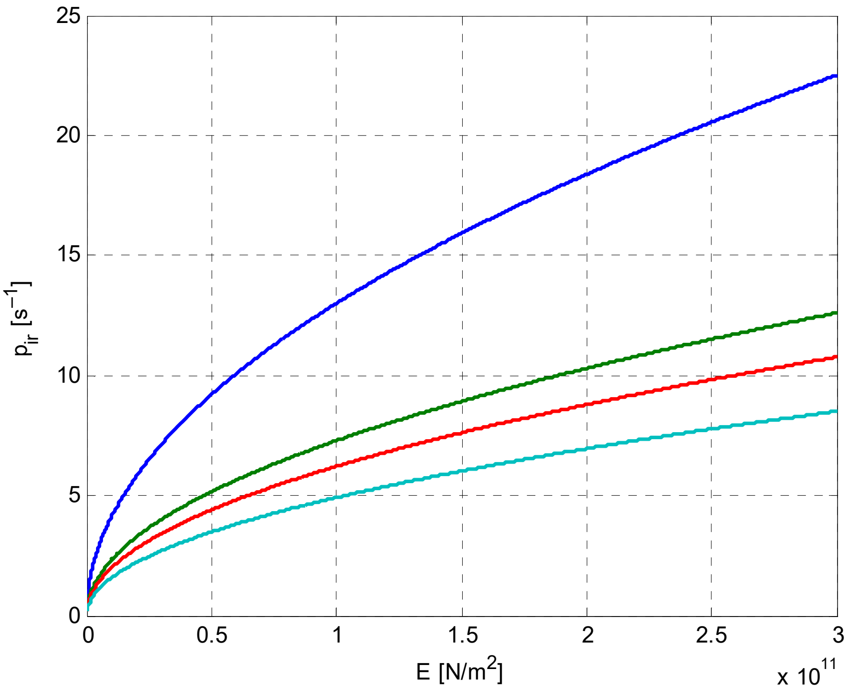

(**b2**)

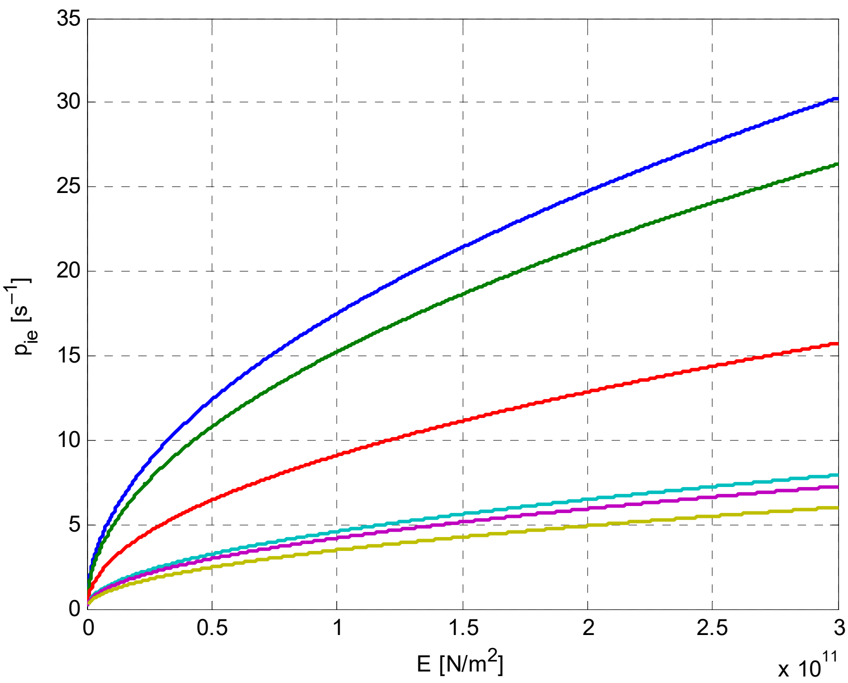

(**c1**)

Figure 10. *Cont.*

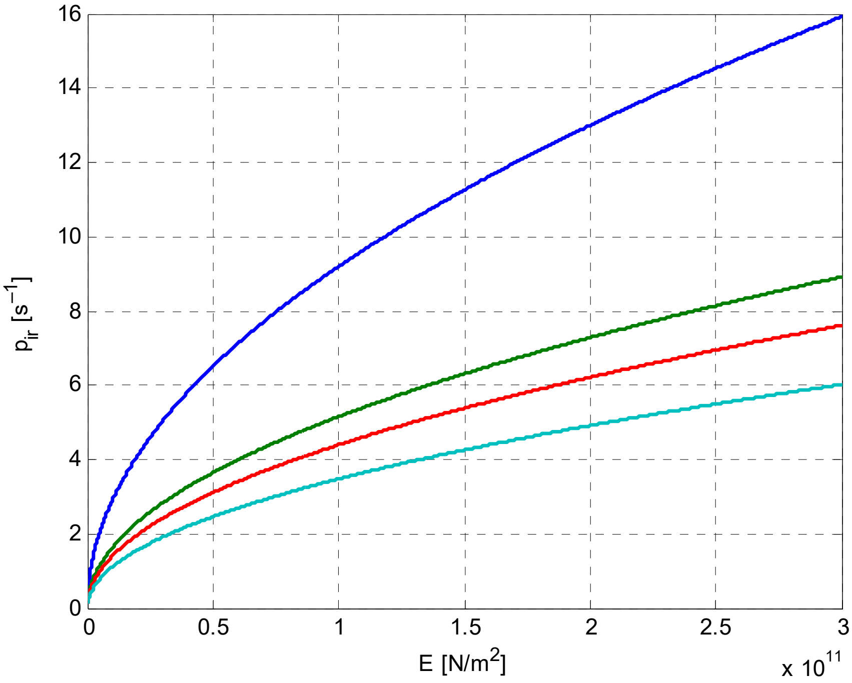

(**c2**)

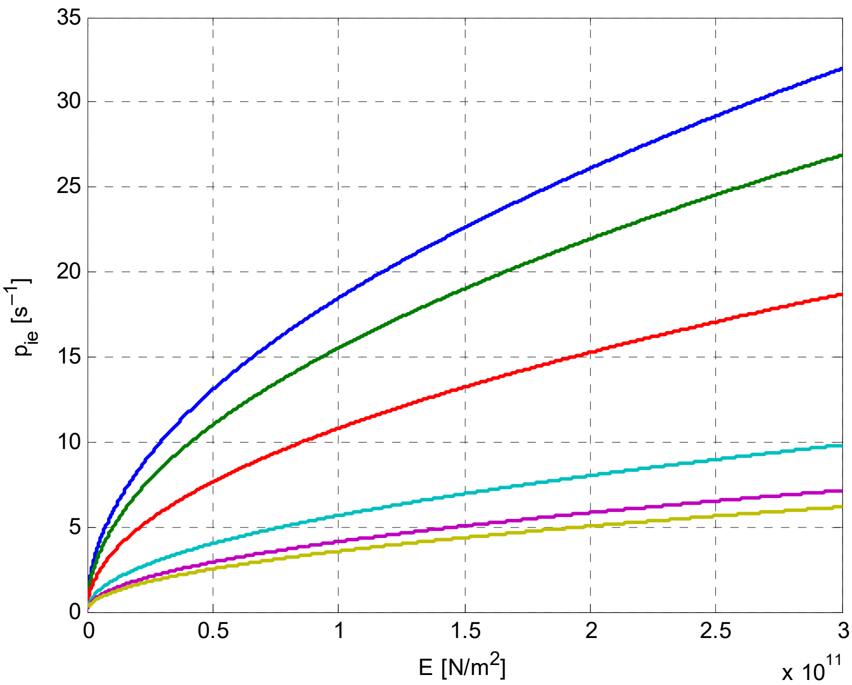

(**d1**)

Figure 10. *Cont.*

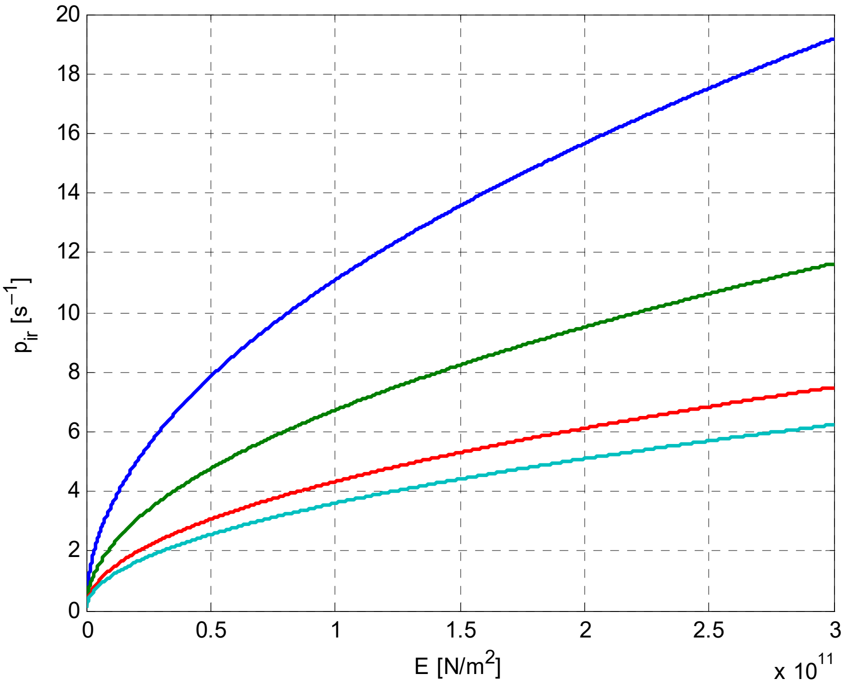

(d2)

Figure 10. Diagrams of variations $p_i = p_i(E)$: (**a**) first case, (**b**) second case, (**c**) third case, and (**d**) fourth case; subscript index e means that all kinematic chains are elastic ones, while subscript index r signifies that one kinematic chain consists of rigid elements. In (**a1**) only four eigenpulsations are distinct: p_1, $p_2 = p_3$, p_4, and $p_5 = p_6$; in (**b1**,**c1**) only five eigenpulsations are distinct: p_1, p_2, p_3, $p_4 = p_5$, and p_6; in (**d1**) all six eigenpulsations are distinct. The first three considered cases are cases of degeneracy (the first is of double degeneracy, while the second and the third are of simple degeneracy). The last case is a regular one. The degeneracy does not imply a diminishing of the number of eigenvalues in the situation of a kinematic chain with rigid elements (see **a2**,**b2**,**c2**,**d2**).

In this situation, the curves have shapes similar to the square root function. The explanation of these results is similar to the previous ones.

6.9. Forced Vibrations

We will consider the following cases. In all situations the force F_1 acts upon the shell at the point A_1 and it is situated along the OX-axis, the force F_2 acts at the point A_2 and it is situated along the OY-axis, while the force M_3 acts at the point A_3 and it is situated along the OZ-axis. We may state $\mathbf{F}_1 = F_1\mathbf{i}$, $\mathbf{F}_2 = F_2\mathbf{j}$ and $\mathbf{F}_3 = F_3\mathbf{k}$. Taking into account that $\mathbf{OA}_1 = \frac{l}{2}\mathbf{i}$, $\mathbf{OA}_2 = -\frac{l}{4}\mathbf{i} + \frac{l\sqrt{3}}{4}\mathbf{j}$, $\mathbf{OA}_3 = -\frac{l}{4}\mathbf{i} - \frac{l\sqrt{3}}{4}\mathbf{j}$, $\mathbf{A}_1\mathbf{A}_2 = -\frac{3l}{4}\mathbf{i} + \frac{l\sqrt{3}}{4}\mathbf{j}$, $\mathbf{A}_1\mathbf{A}_3 = -\frac{3l}{4}\mathbf{i} - \frac{l\sqrt{3}}{4}\mathbf{j}$, $\mathbf{OA}_1 \times \mathbf{F}_1 = 0$, $\mathbf{OA}_2 \times \mathbf{F}_2 = -F_2\frac{l}{4}\mathbf{k}$, $\mathbf{OA}_3 \times \mathbf{F}_3 = -F_3\frac{l\sqrt{3}}{4}\mathbf{i} + F_3\frac{l}{4}\mathbf{j}$, $\mathbf{A}_1\mathbf{A}_2 \times \mathbf{F}_2 = -3F_2\frac{l}{4}\mathbf{k}$, $\mathbf{A}_1\mathbf{A}_3 \times \mathbf{F}_3 = -F_3\frac{l\sqrt{3}}{4}\mathbf{i} + 3F_3\frac{l}{4}\mathbf{j}$, this results in the screw coordinates of the forces in the case when all the kinematic chains are elastic ones

$$\{\mathbf{F}\} = \begin{bmatrix} F_1 & F_2 & F_3 & -F_3\frac{l\sqrt{3}}{4} & F_3\frac{l}{4} & -F_2\frac{l}{4} \end{bmatrix}^{\mathrm{T}} \tag{27}$$

and in the case when the first kinematic chain is a rigid one

$$\{\mathbf{F}\} = \begin{bmatrix} F_1 & F_2 & F_3 & -F_3\frac{l\sqrt{3}}{4} & 3F_3\frac{l}{4} & -3F_2\frac{l}{4} \end{bmatrix}^{\mathrm{T}} \tag{28}$$

respectively.

Other approaches based on Newton–Euler equations are detailed in [16,20], while in [17] the equations of motion are obtained using the Kane equations.

Reference [51] limits the study to the first few eigenpulsations and concludes that the resonance does not appear for the considered case.

In [21] only the largest eigenvalue is considered for the study of the stability.

We can see that the behavior of the system is more complex and the beating phenomenon may be caused by one or more eigenvalues, or by a subharmonic or a superharmonic resonance.

For all cases the following parameters are considered to have constant values: $m = 10$ kg, $E_1 = E_2 = E_3 = E$, $G_1 = G_2 = G_3 = G$, with $E = 2.1 \times 10^{11}$ N/m^2, and $G = 8 \times 10^{10}$ N/m^2.

The expressions of the forces F_1, F_2, and F_3 are as follows

$$F_1 = F_{01} \sin(\omega_1 t),\ F_2 = F_{02}[1 + \sin(\omega_2 t)], F_3 = F_{03}[1 + \sin(\omega_3 t) + \sin(\omega_4 t)] \quad (29)$$

where the values of the parameters F_{01}, F_{02}, F_{03}, ω_1, ω_2, ω_3, and ω_4 are specified in each case.

The first case is defined by $F_{01} = 1$ N, $F_{02} = 2$ N, $F_{03} = 3$ N, $\omega_1 = 20\pi$ s^{-1}, $\omega_2 = 30\pi$ s^{-1}, $\omega_3 = 40\pi$ s^{-1}, $\omega_4 = 50\pi$ s^{-1}, $l = 0.2$ m, $d_1 = 0.01$ m, $d_2 = 0.01$ m, $d_3 = 0.01$ m. The diagrams are captured in Figure 11.

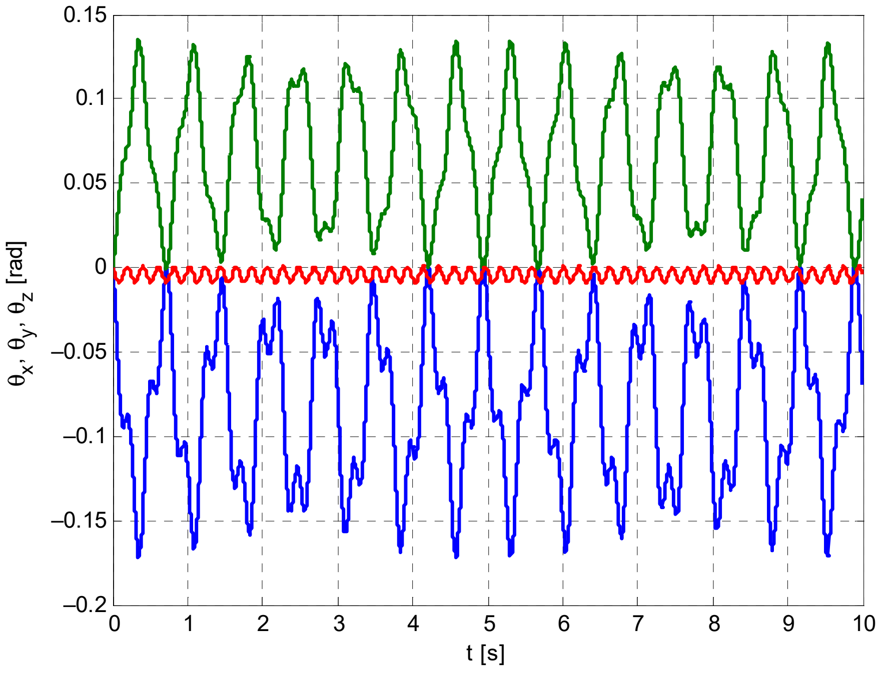

(**a**)

Figure 11. *Cont.*

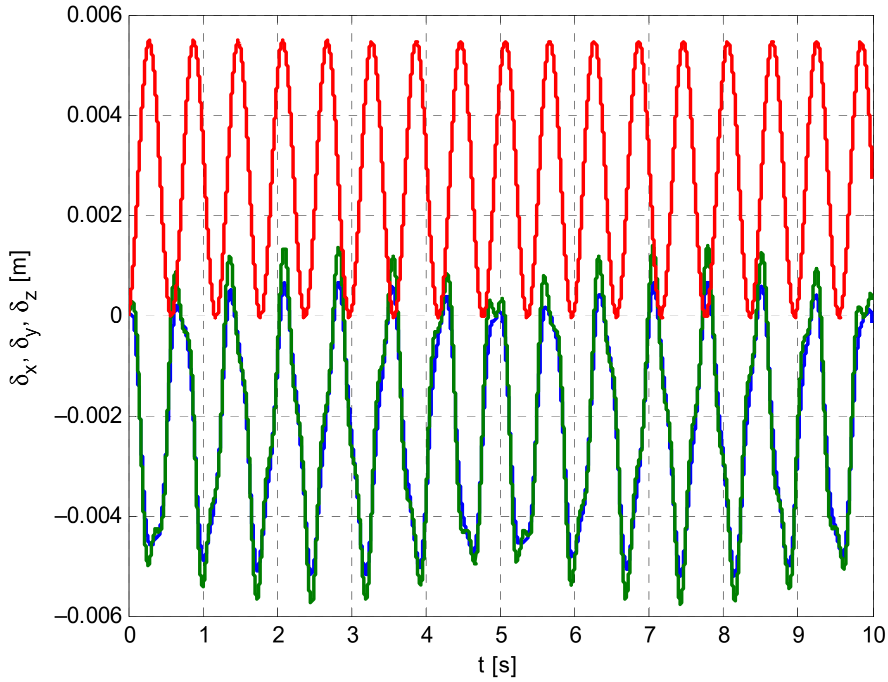

(**b**)

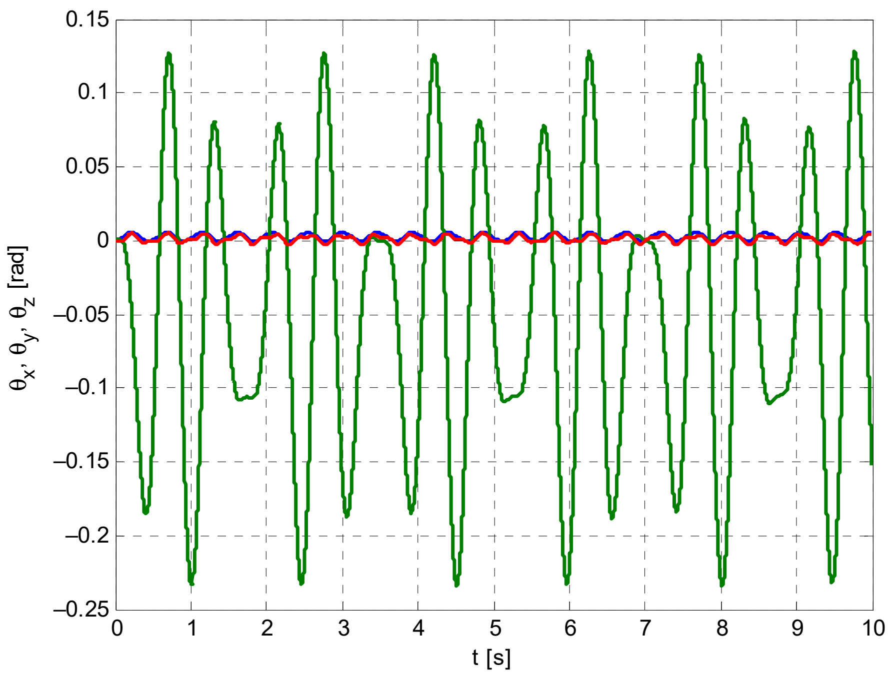

(**c**)

Figure 11. *Cont.*

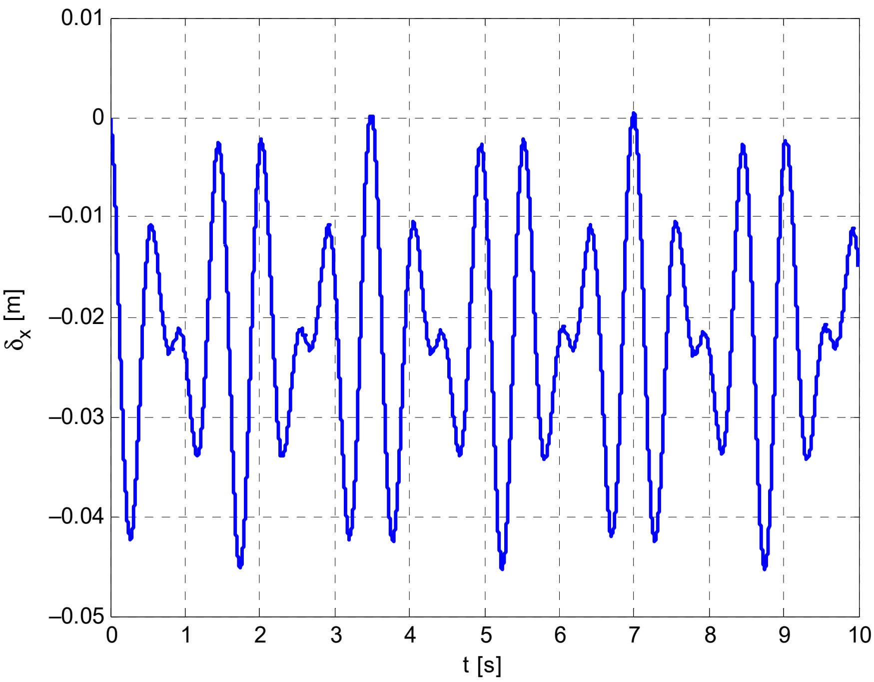

(**d**)

Figure 11. Time histories in the first case: (**a**) $\theta_x = \theta_x(t)$ (blue), $\theta_y = \theta_y(t)$ (green), $\theta_z = \theta_z(t)$ (red) (all kinematic chains are elastic), (**b**) $\delta_x = \delta_x(t)$ (blue), $\delta_y = \delta_y(t)$ (green), $\delta_z = \delta_z(t)$ (red) (all kinematic chains are elastic), (**c**) $\theta_x = \theta_x(t)$ (blue), $\theta_y = \theta_y(t)$ (green), $\theta_z = \theta_z(t)$ (red) (one kinematic chain is rigid), and (**d**) $\delta_x = \delta_x(t)$ (one kinematic chain is rigid). This case is one of double degeneracy.

The eigenpulsations for the situation in which all kinematic chains are elastic ones are $p_1 \approx 30.27\ \mathrm{s}^{-1} \approx 9.64\pi\ \mathrm{s}^{-1}$, $p_2 = p_3 \approx 25.36\ \mathrm{s}^{-1} \approx 8.07\pi\ \mathrm{s}^{-1}$, $p_4 \approx 10.51\ \mathrm{s}^{-1} \approx 3.35\pi\ \mathrm{s}^{-1}$, and $p_5 = p_6 \approx 8.87\ \mathrm{s}^{-1} \approx 2.82\pi\ \mathrm{s}^{-1}$, while for the situation in which one kinematic chain consists of rigid elements the eigenpulsations read $p_1 \approx 25.83\ \mathrm{s}^{-1} \approx 8.22\pi\ \mathrm{s}^{-1}$, $p_2 \approx 13.49\ \mathrm{s}^{-1} \approx 4.29\pi\ \mathrm{s}^{-1}$, $p_3 \approx 12.54\ \mathrm{s}^{-1} \approx 3.99\pi\ \mathrm{s}^{-1}$, and $p_4 \approx 8.96\ \mathrm{s}^{-1} \approx 2.85\pi\ \mathrm{s}^{-1}$. This case is a case of degeneracy (see the previous paragraphs).

The curves of variations are periodical ones.

For the second case the parameters are $F_{01} = 1$ N, $F_{02} = 2$ N, $F_{03} = 3$ N, $\omega_1 = 20\pi\ \mathrm{s}^{-1}$, $\omega_2 = 30\pi\ \mathrm{s}^{-1}$, $\omega_3 = 40\pi\ \mathrm{s}^{-1}$, $\omega_4 = 50\pi\ \mathrm{s}^{-1}$, $l = 0.2$ m, $d_1 = 0.02$ m, $d_2 = 0.01$ m, and $d_3 = 0.01$ m. The diagrams are captured in Figure 12.

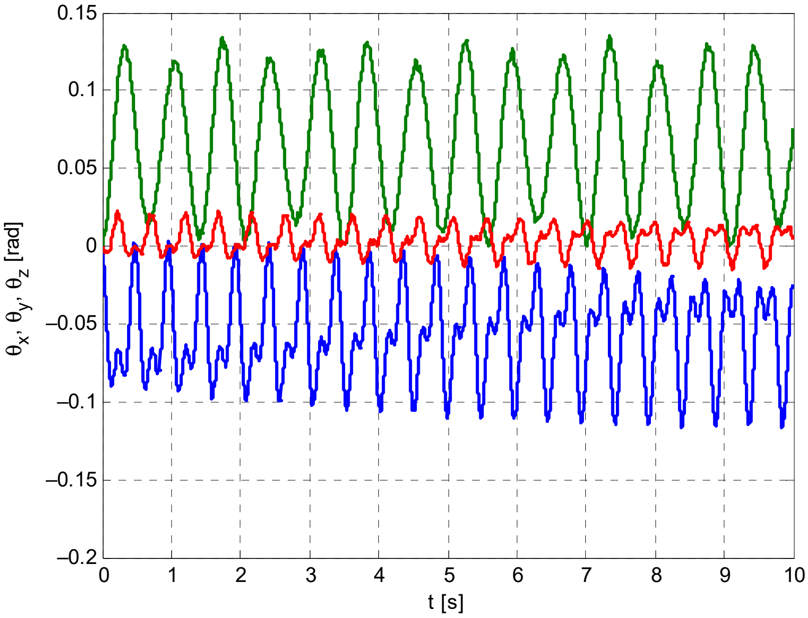

(**a**)

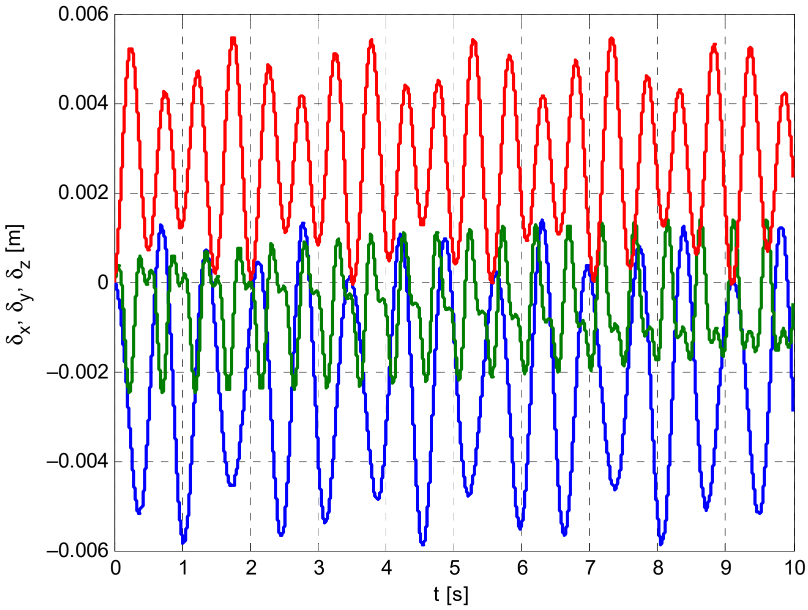

(**b**)

Figure 12. *Cont.*

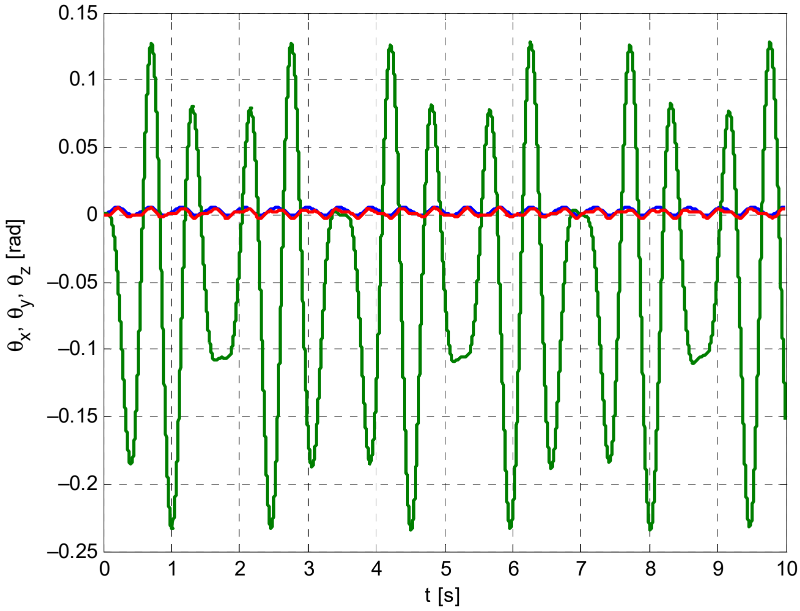

(**c**)

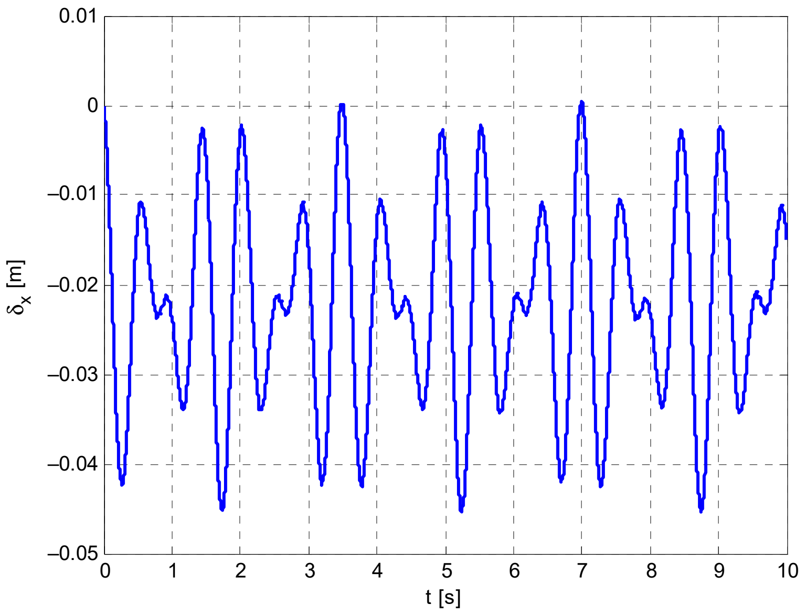

(**d**)

Figure 12. Time histories in the second case: (**a**) $\theta_x = \theta_x(t)$ (blue), $\theta_y = \theta_y(t)$ (green), $\theta_z = \theta_z(t)$ (red) (all kinematic chains are elastic), (**b**) $\delta_x = \delta_x(t)$ (blue), $\delta_y = \delta_y(t)$ (green), $\delta_z = \delta_z(t)$ (red) (all kinematic chains are elastic), (**c**) $\theta_x = \theta_x(t)$ (blue), $\theta_y = \theta_y(t)$ (green), $\theta_z = \theta_z(t)$ (red) (one kinematic chain is rigid), and (**d**) $\delta_x = \delta_x(t)$ (one kinematic chain is rigid). This case is one of single degeneracy.

The eigenpulsations for the situation in which all kinematic chains are elastic ones are $p_1 \approx 85.00\ \mathrm{s}^{-1} \approx 27.06\pi\ \mathrm{s}^{-1}$, $p_2 \approx 80.80\ \mathrm{s}^{-1} \approx 25.72\pi\ \mathrm{s}^{-1}$, $p_3 \approx 25.81\ \mathrm{s}^{-1} \approx 8.21\pi\ \mathrm{s}^{-1}$, $p_4 \approx 13.06\ \mathrm{s}^{-1} \approx 4.16\pi\ \mathrm{s}^{-1}$, $p_5 \approx 12.41\ \mathrm{s}^{-1} \approx 3.95\pi\ \mathrm{s}^{-1}$, and $p_6 \approx 8.96\ \mathrm{s}^{-1} \approx 2.85\pi\ \mathrm{s}^{-1}$, while for the situation in which one kinematic chain consists of rigid elements the eigenpulsations read $p_1 \approx 25.83\ \mathrm{s}^{-1} \approx 8.22\pi\ \mathrm{s}^{-1}$, $p_2 \approx 13.49\ \mathrm{s}^{-1} \approx 4.29\pi\ \mathrm{s}^{-1}$, $p_3 \approx 12.54\ \mathrm{s}^{-1} \approx 3.99\pi\ \mathrm{s}^{-1}$, and $p_4 \approx 8.96\ \mathrm{s}^{-1} \approx 2.85\pi\ \mathrm{s}^{-1}$. This case is also of degeneracy because $d_2 = d_3$. Moreover, we may see that the eigenpulsations in the case when one kinematic chain consists of rigid elements are equal to those obtained in the same situation in the first case.

The curves of variations are also periodical ones.

For the third case the parameters are $F_{01} = 1$ N, $F_{02} = 2$ N, $F_{03} = 3$ N, $\omega_1 = 20\pi\,\mathrm{s}^{-1}$, $\omega_2 = 30\pi\,\mathrm{s}^{-1}$, $\omega_3 = 40\pi\,\mathrm{s}^{-1}$, $\omega_4 = 50\pi\,\mathrm{s}^{-1}$, $l = 0.2$ m, $d_1 = 0.03$ m, $d_2 = 0.02$ m, and $d_3 = 0.02$ m. The diagrams are presented in Figure 13.

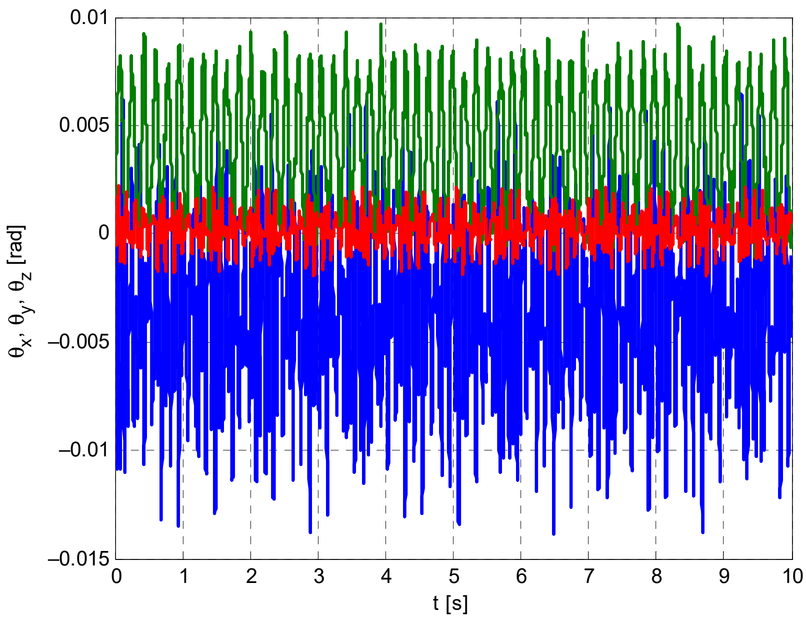

(**a**)

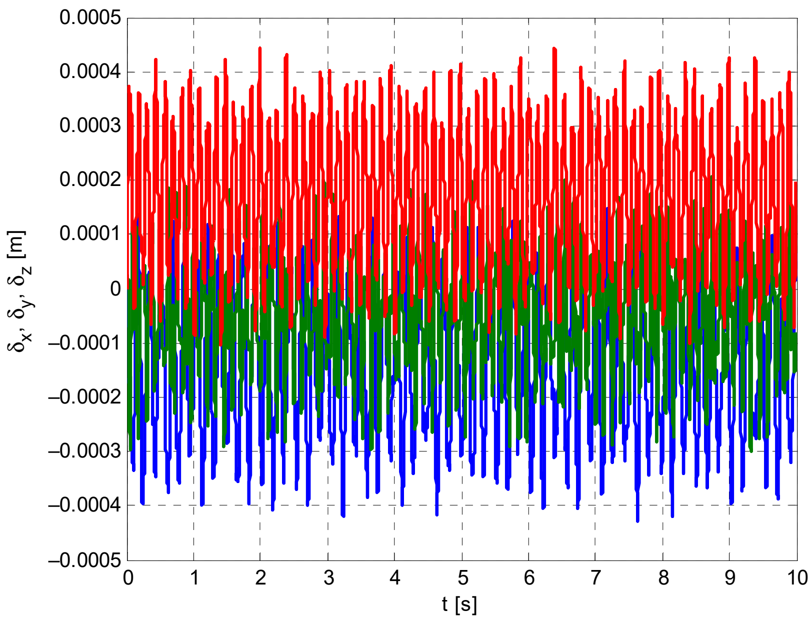

(**b**)

Figure 13. *Cont*.

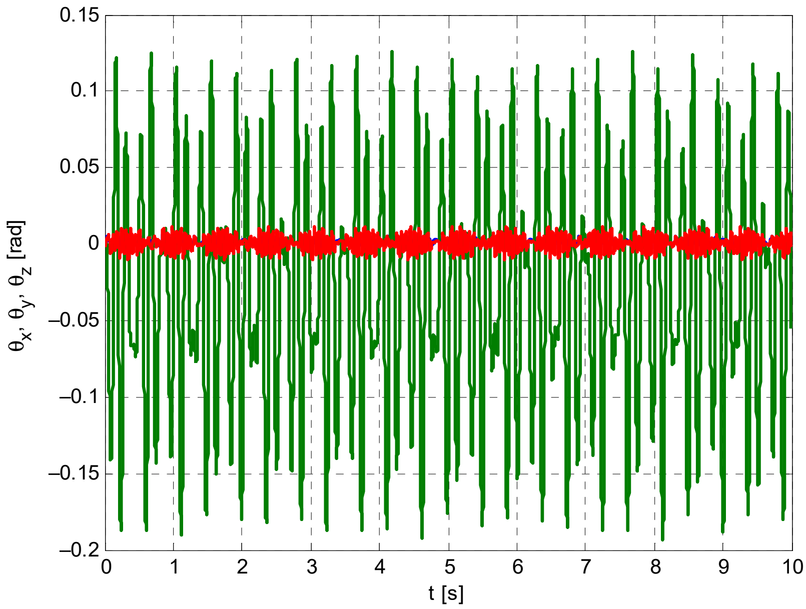

(**c**)

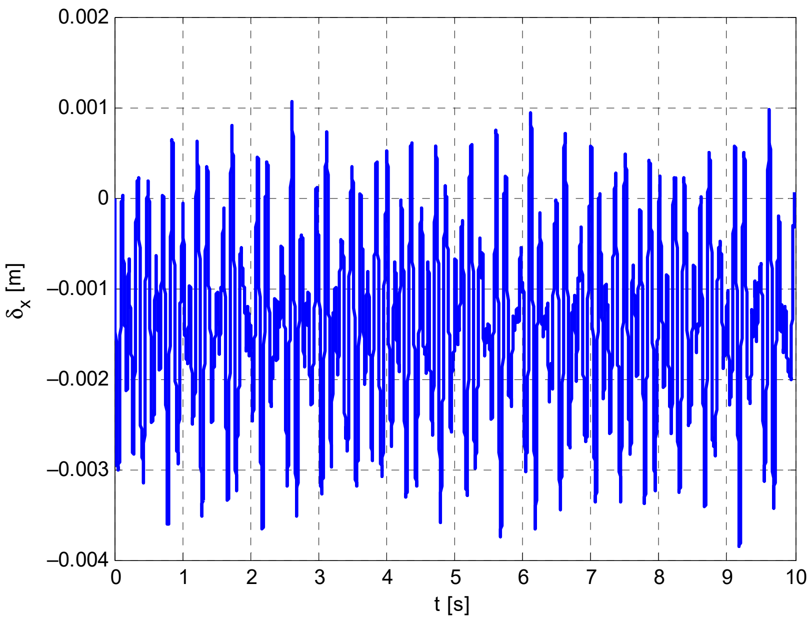

(**d**)

Figure 13. Time histories in the third case: (**a**) $\theta_x = \theta_x(t)$ (blue), $\theta_y = \theta_y(t)$ (green), $\theta_z = \theta_z(t)$ (red) (all kinematic chains are elastic), (**b**) $\delta_x = \delta_x(t)$ (blue), $\delta_y = \delta_y(t)$ (green), $\delta_z = \delta_z(t)$ (red) (all kinematic chains are elastic), (**c**) $\theta_x = \theta_x(t)$ (blue), $\theta_y = \theta_y(t)$ (green), $\theta_z = \theta_z(t)$ (red) (one kinematic chain is rigid), and (**d**) $\delta_x = \delta_x(t)$ (one kinematic chain is rigid). This case is also a case of single degeneracy. Moreover, the beating phenomenon is presented.

The eigenpulsations in the case of all elastic kinematic chains read $p_1 \approx 195.95\ \mathrm{s}^{-1} \approx 62.37\pi\ \mathrm{s}^{-1}$, $p_2 \approx 195.03\ \mathrm{s}^{-1} \approx 62.08\pi\ \mathrm{s}^{-1}$, $p_3 \approx 103.01\ \mathrm{s}^{-1} \approx 32.79\pi\ \mathrm{s}^{-1}$, $p_4 \approx 48.81\ \mathrm{s}^{-1} \approx 15.54\pi\ \mathrm{s}^{-1}$, $p_5 \approx 48.50\ \mathrm{s}^{-1} \approx 15.44\pi\ \mathrm{s}^{-1}$, and $p_6 \approx 35.82\ \mathrm{s}^{-1} \approx 11.40\pi\ \mathrm{s}^{-1}$, while in the case when one kinematic chain consists of rigid elements the eigenpulsations are $p_1 \approx 103.32\ \mathrm{s}^{-1} \approx 32.89\pi\ \mathrm{s}^{-1}$, $p_2 \approx 53.96\ \mathrm{s}^{-1} \approx 17.18\pi\ \mathrm{s}^{-1}$, $p_3 \approx 50.18\ \mathrm{s}^{-1} \approx 15.97\pi\ \mathrm{s}^{-1}$, and $p_4 \approx 35.86\ \mathrm{s}^{-1} \approx 11.41\pi\ \mathrm{s}^{-1}$. Because some eigenpulsations are very closed to $2\omega_2$ or $\frac{\omega_2}{2}$, the beating phenomenon appears in the next diagrams. The curves are periodical ones.

The fourth case is characterized by $F_{01} = 1$ N, $F_{02} = 2$ N, $F_{03} = 3$ N, $\omega_1 = 20\pi\ \mathrm{s}^{-1}$, $\omega_2 = 30\pi\ \mathrm{s}^{-1}$, $\omega_3 = 40\pi\ \mathrm{s}^{-1}$, $\omega_4 = 50\pi\ \mathrm{s}^{-1}$, $l = 0.2$ m, $d_1 = 0.03$ m, $d_2 = 0.01$ m, and $d_3 = 0.02$ m. The diagrams are presented in Figure 14.

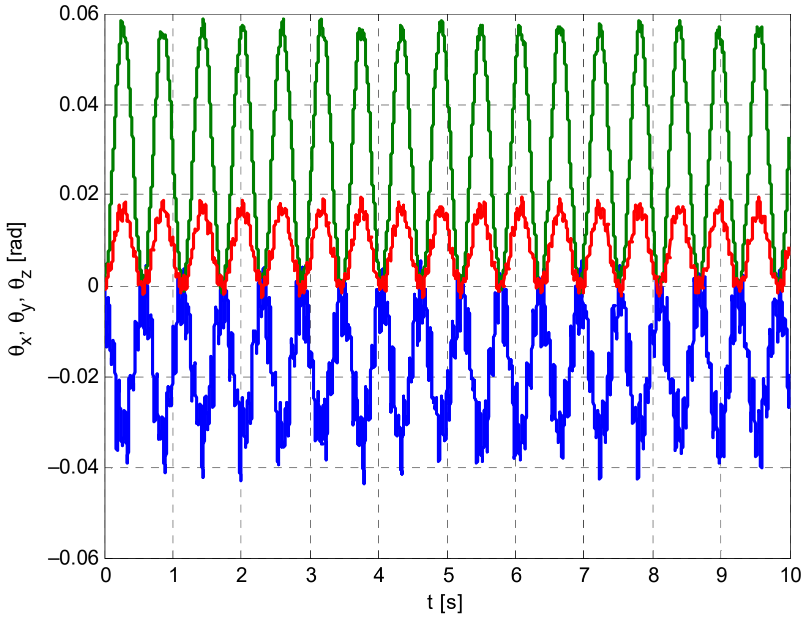

(**a**)

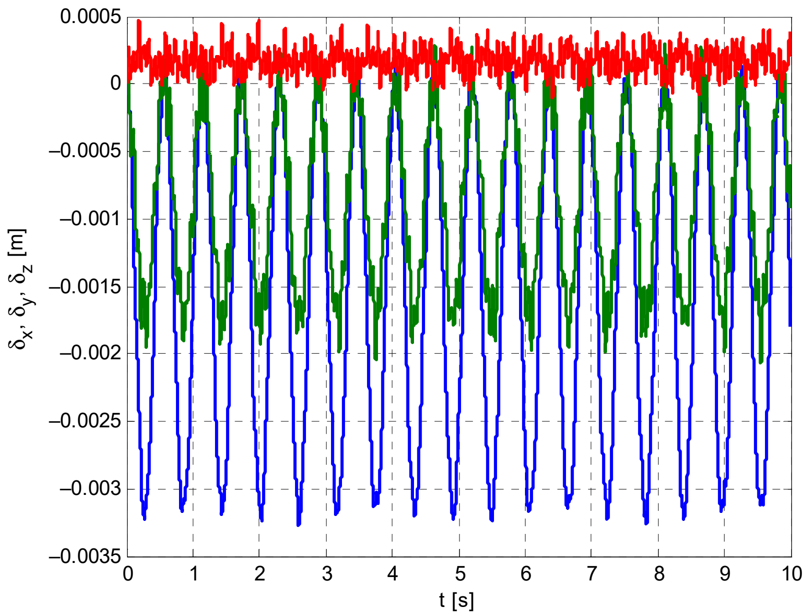

(**b**)

Figure 14. *Cont.*

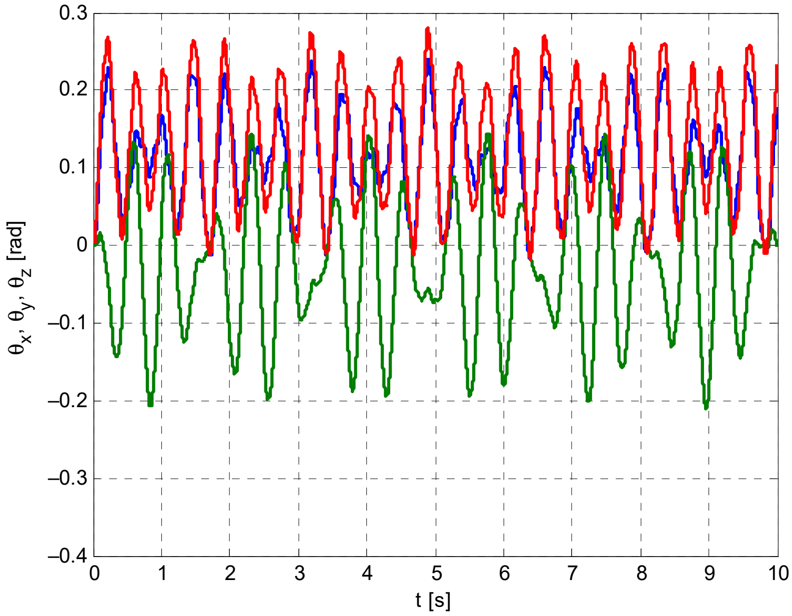

(**c**)

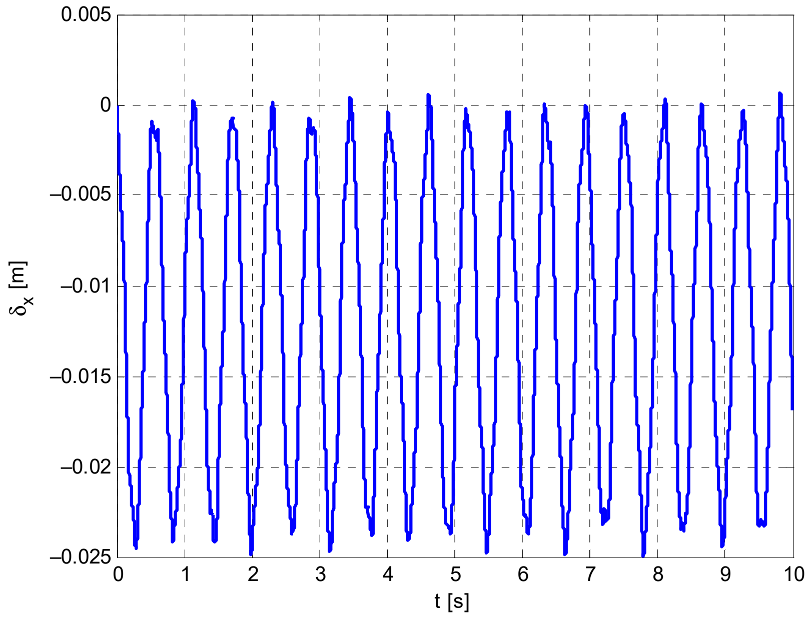

(**d**)

Figure 14. Time histories in the fourth case: (**a**) $\theta_x = \theta_x(t)$ (blue), $\theta_y = \theta_y(t)$ (green), $\theta_z = \theta_z(t)$ (red) (all kinematic chains are elastic), (**b**) $\delta_x = \delta_x(t)$ (blue), $\delta_y = \delta_y(t)$ (green), $\delta_z = \delta_z(t)$ (red) (all kinematic chains are elastic), (**c**) $\theta_x = \theta_x(t)$ (blue), $\theta_y = \theta_y(t)$ (green), $\theta_z = \theta_z(t)$ (red) (one kinematic chain is rigid), and (**d**) $\delta_x = \delta_x(t)$ (one kinematic chain is rigid). This case is a regular one (no degeneracy); the beating phenomenon is present.

The eigenpulsations are now: $p_1 \approx 194.38\ \text{s}^{-1} \approx 61.88\pi\ \text{s}^{-1}$, $p_2 \approx 184.60\ \text{s}^{-1} \approx 58.76\pi\ \text{s}^{-1}$, $p_3 \approx 80.14\ \text{s}^{-1} \approx 25.51\pi\ \text{s}^{-1}$, $p_4 \approx 45.66\ \text{s}^{-1} \approx 14.53\pi\ \text{s}^{-1}$, $p_5 \approx 14.66\ \text{s}^{-1} \approx 4.67\pi\ \text{s}^{-1}$, $p_6 \approx 10.82\ \text{s}^{-1} \approx 3,44\pi\ \text{s}^{-1}$, and $p_1 \approx 80.86\ \text{s}^{-1} \approx 25.47\pi\ \text{s}^{-1}$, $p_2 \approx 48.64\ \text{s}^{-1} \approx 15.48\pi\ \text{s}^{-1}$, $p_3 \approx 14.69\ \text{s}^{-1} \approx 4.68\pi\ \text{s}^{-1}$, $p_4 \approx 10.86\ \text{s}^{-1} \approx 3.45\pi\ \text{s}^{-1}$ for the case when all kinematic chains are elastic ones, and the case when one kinematic chain consists of rigid elements, respectively. Again, because some eigenpulsations are very closed to $2\omega_2$ or $\frac{\omega_2}{2}$, the beating phenomenon appears in the next diagrams. The curves are also periodical ones.

The fifth case is characterized by $F_{01} = 1$ N, $F_{02} = 2$ N, $F_{03} = 3$ N, $\omega_1 = 20\pi$ s^{-1}, $\omega_2 = 30\pi$ s^{-1}, $\omega_3 = 40\pi$ s^{-1}, $\omega_4 = 50\pi$ s^{-1}, $l = 0.5$ m, $d_1 = 0.01$ m, $d_2 = 0.01$ m, and $d_3 = 0.01$ m. The diagrams are presented in Figure 15.

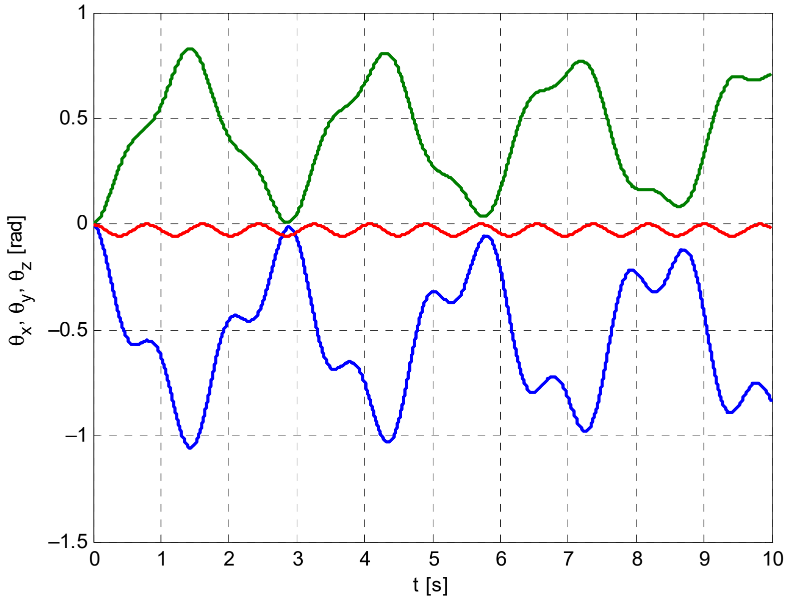

(**a**)

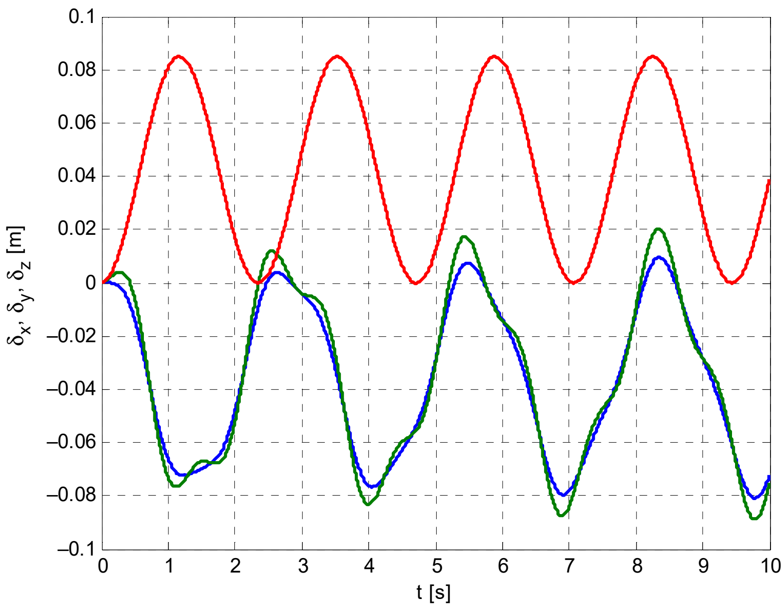

(**b**)

Figure 15. *Cont.*

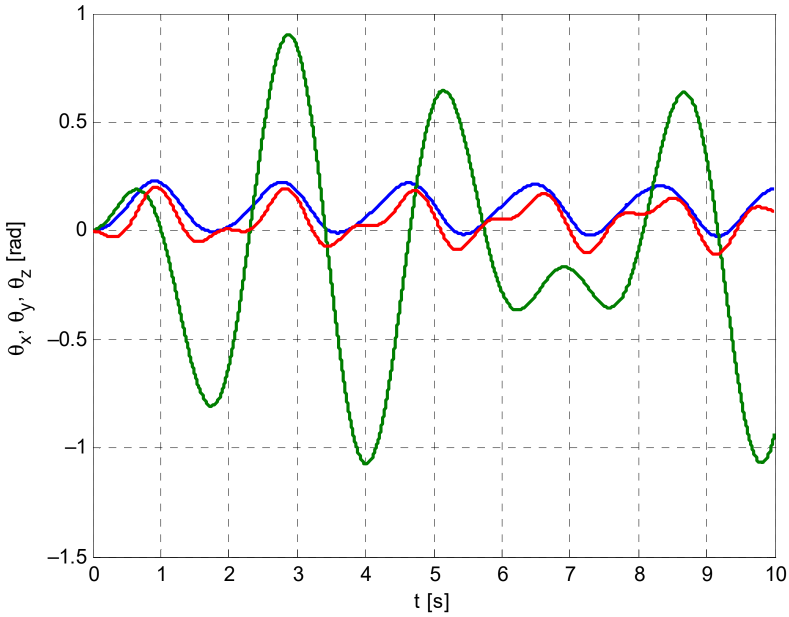

(**c**)

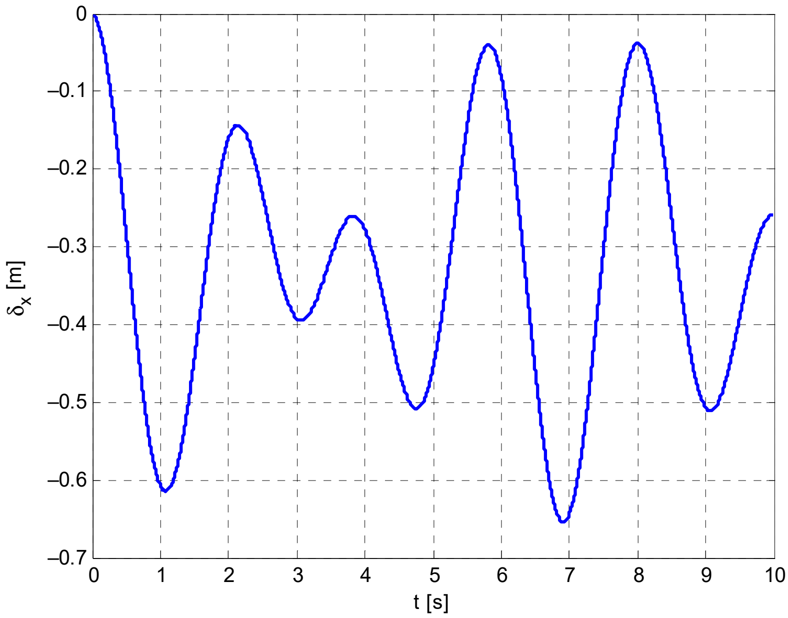

(**d**)

Figure 15. Time histories in the fifth case: (**a**) $\theta_x = \theta_x(t)$ (blue), $\theta_y = \theta_y(t)$ (green), $\theta_z = \theta_z(t)$ (red) (all kinematic chains are elastic), (**b**) $\delta_x = \delta_x(t)$ (blue), $\delta_y = \delta_y(t)$ (green), $\delta_z = \delta_z(t)$ (red) (all kinematic chains are elastic), (**c**) $\theta_x = \theta_x(t)$ (blue), $\theta_y = \theta_y(t)$ (green), $\theta_z = \theta_z(t)$ (red) (one kinematic chain is rigid), and (**d**) $\delta_x = \delta_x(t)$ (one kinematic chain is rigid). This case is one of double degeneracy.

The eigenpulsations are $p_1 \approx 7.66\ \mathrm{s}^{-1} \approx 2.44\pi\ \mathrm{s}^{-1}$, $p_2 = p_3 \approx 6.42\ ^{-1} \approx 2.04\pi\ \mathrm{s}^{-1}$, $p_4 \approx 2.66\ \mathrm{s}^{-1} \approx 0.85\pi\ \mathrm{s}^{-1}$, and $p_5 = p_6 \approx 2.24\ \mathrm{s}^{-1} \approx 0.71\pi\ \mathrm{s}^{-1}$ when all the kinematic chains are elastic ones, and $p_1 \approx 6.53\ \mathrm{s}^{-1} \approx 2.08\pi\ \mathrm{s}^{-1}$, $p_2 \approx 3.41\ \mathrm{s}^{-1} \approx 1.09\pi\ \mathrm{s}^{-1}$, $p_3 = 3.17\ \mathrm{s}^{-1} \approx 1.01\pi\ \mathrm{s}^{-1}$, and $p_4 \approx 2.27\ \mathrm{s}^{-1} \approx 0.72\pi\ \mathrm{s}^{-1}$ when one kinematic chain consists of rigid elements (see also the Section 6.2).

The curves of variation are periodical ones.

The sixth case is defined by $F_{01} = 1$ N, $F_{02} = 2$ N, $F_{03} = 3$ N, $\omega_1 = 20\pi$ s^{-1}, $\omega_2 = 20\pi$ s^{-1}, $\omega_3 = 20\pi$ s^{-1}, $\omega_4 = 20\pi$ s^{-1}, $l = 0.2$ m, $d_1 = 0.03$ m, $d_2 = 0.01$ m, and $d_3 = 0.02$ m. The diagrams are presented in Figure 16.

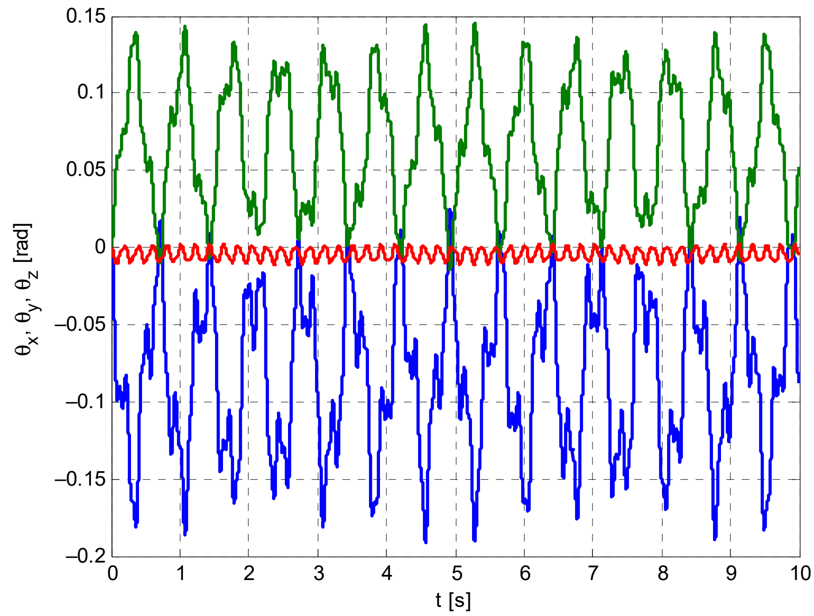

(**a**)

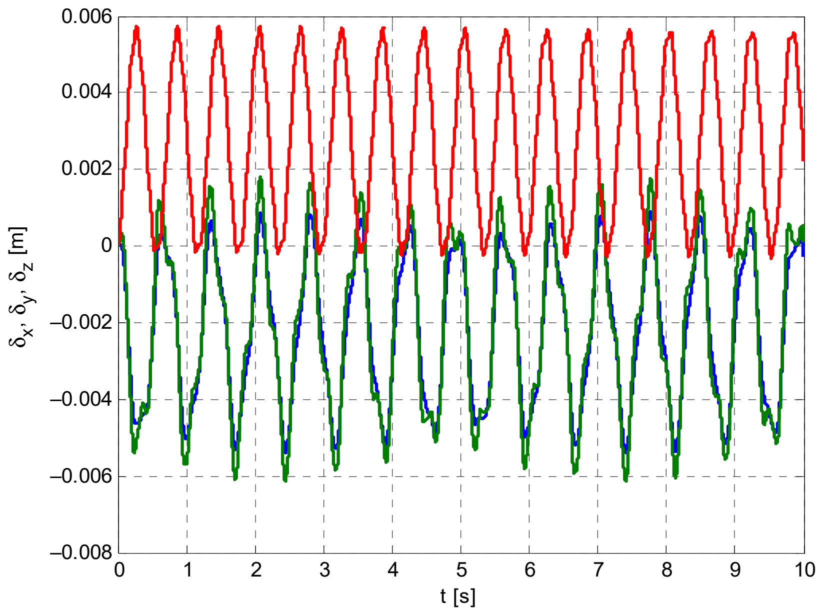

(**b**)

Figure 16. *Cont.*

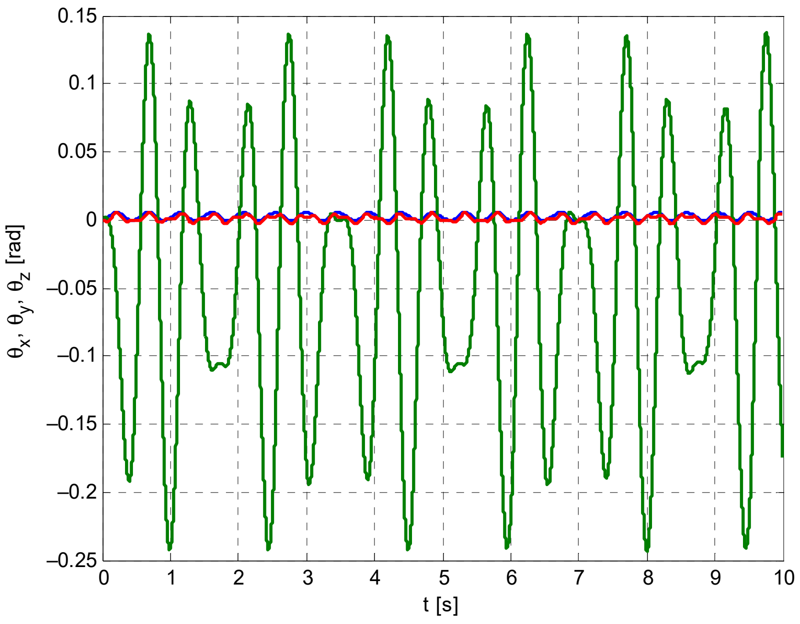

(**c**)

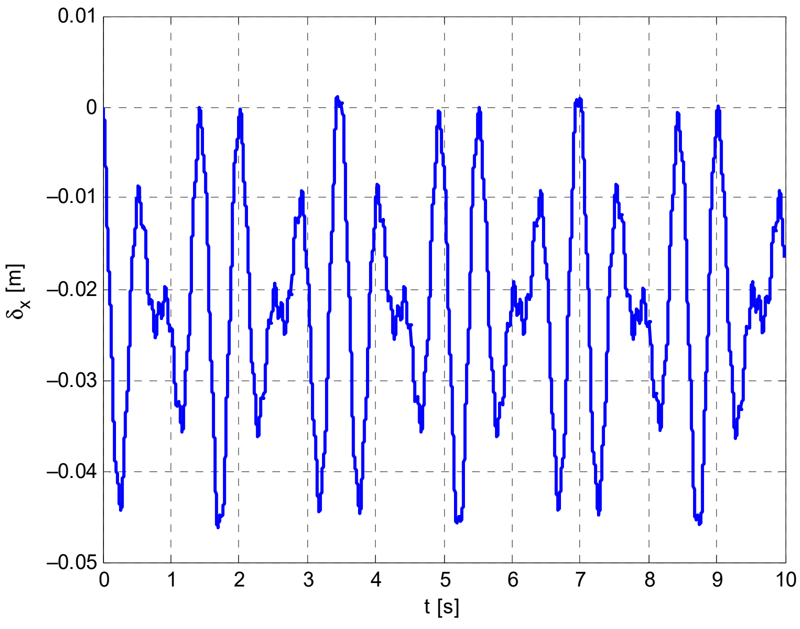

(**d**)

Figure 16. Time histories in the sixth case: (**a**) $\theta_x = \theta_x(t)$ (blue), $\theta_y = \theta_y(t)$ (green), $\theta_z = \theta_z(t)$ (red) (all kinematic chains are elastic), (**b**) $\delta_x = \delta_x(t)$ (blue), $\delta_y = \delta_y(t)$ (green), $\delta_z = \delta_z(t)$ (red) (all kinematic chains are elastic), (**c**) $\theta_x = \theta_x(t)$ (blue), $\theta_y = \theta_y(t)$ (green), $\theta_z = \theta_z(t)$ (red) (one kinematic chain is rigid), and (**d**) $\delta_x = \delta_x(t)$ (one kinematic chain is rigid). This case is a regular one (no degeneracy is present).

The eigenpulsations are $p_1 \approx 194.38\ \mathrm{s}^{-1} \approx 61.88\pi\ \mathrm{s}^{-1}$, $p_2 \approx 184.60\ \mathrm{s}^{-1} \approx 58.76\pi\ \mathrm{s}^{-1}$, $p_3 \approx 80.14\ \mathrm{s}^{-1} \approx 25.51\pi\ \mathrm{s}^{-1}$, $p_4 \approx 45.66\ \mathrm{s}^{-1} \approx 14.53\pi\ \mathrm{s}^{-1}$, $p_5 \approx 14.66\ \mathrm{s}^{-1} \approx 4.67\pi\ \mathrm{s}^{-1}$, $p_6 \approx 10.82\ \mathrm{s}^{-1} \approx 3{,}44\pi\ \mathrm{s}^{-1}$, and $p_1 \approx 80.86\ \mathrm{s}^{-1} \approx 25.47\pi\ \mathrm{s}^{-1}$, $p_2 \approx 48.64\ \mathrm{s}^{-1} \approx 15.48\pi\ \mathrm{s}^{-1}$, $p_3 \approx 14.69\ \mathrm{s}^{-1} \approx 4.68\pi\ \mathrm{s}^{-1}$, $p_4 \approx 10.86\ \mathrm{s}^{-1} \approx 3.45\pi\ \mathrm{s}^{-1}$ for the case when all kinematic chains are elastic ones, and the case when one kinematic chain consists of rigid elements, respectively (see also the fourth case). In this situation we do not have the beating phenomenon. The curves are also periodical ones.

Finally, the seventh case is defined by $F_{01} = 1$ N, $F_{02} = 2$ N, $F_{03} = 3$ N, $\omega_1 = 20\pi\ \mathrm{s}^{-1}$, $\omega_2 = 30\pi\ \mathrm{s}^{-1}$, $\omega_3 = 40\pi\ \mathrm{s}^{-1}$, $\omega_4 = 50\pi\ \mathrm{s}^{-1}$, $l = 0.5$ m, $d_1 = 0.03$ m, $d_2 = 0.01$ m, and $d_3 = 0.02$ m. The diagrams are captured in Figure 17.

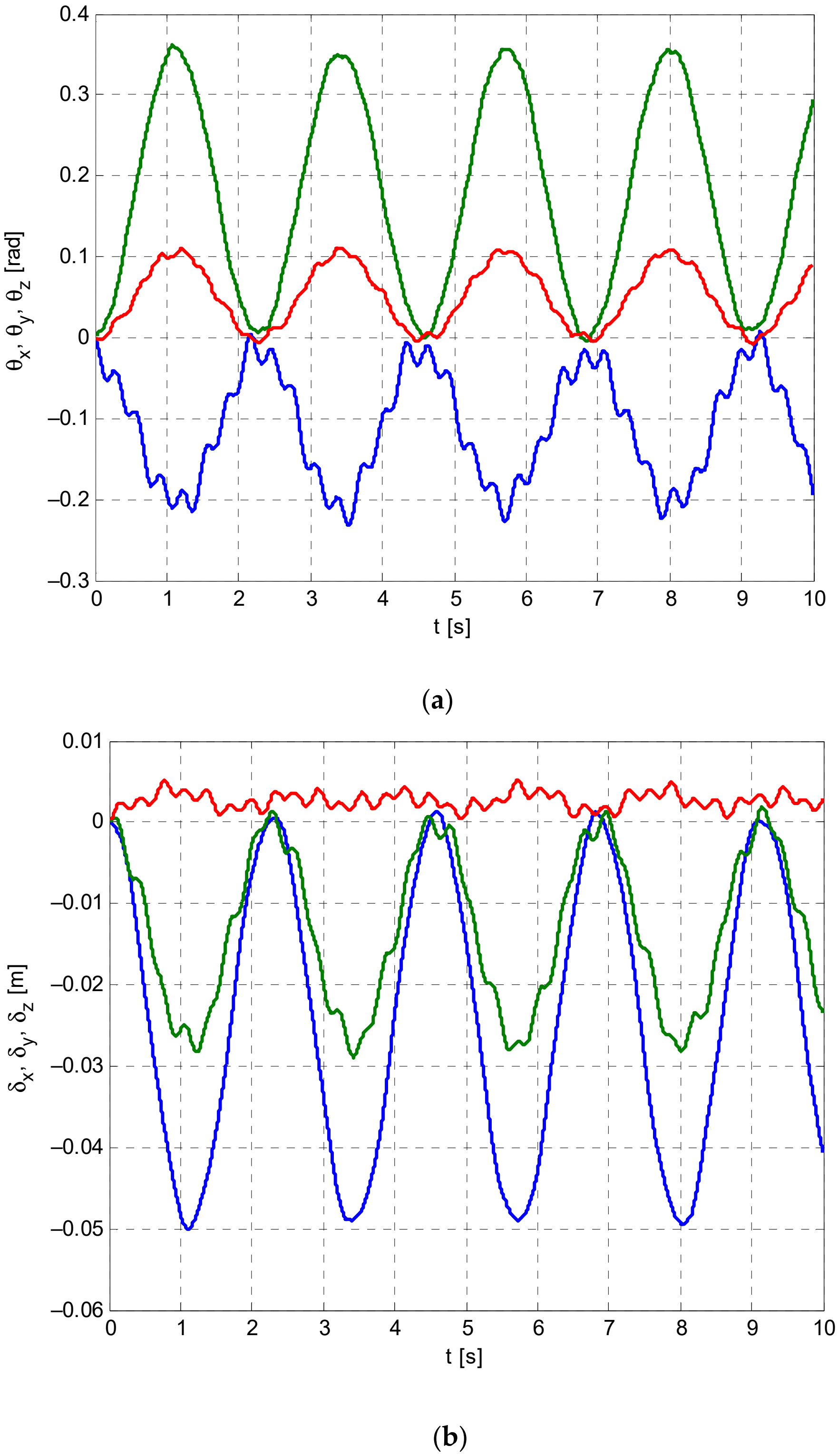

Figure 17. *Cont.*

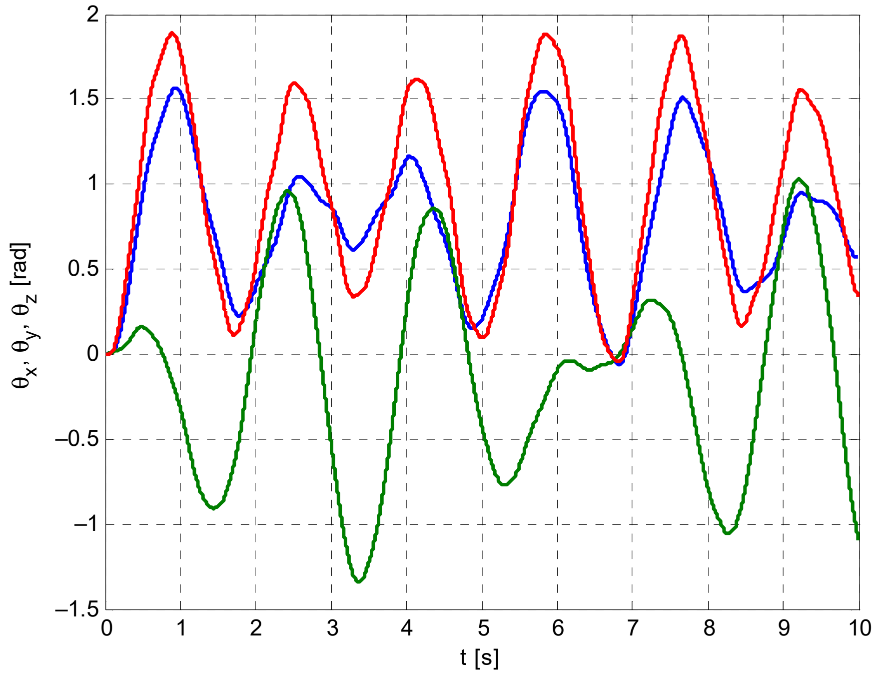

(**c**)

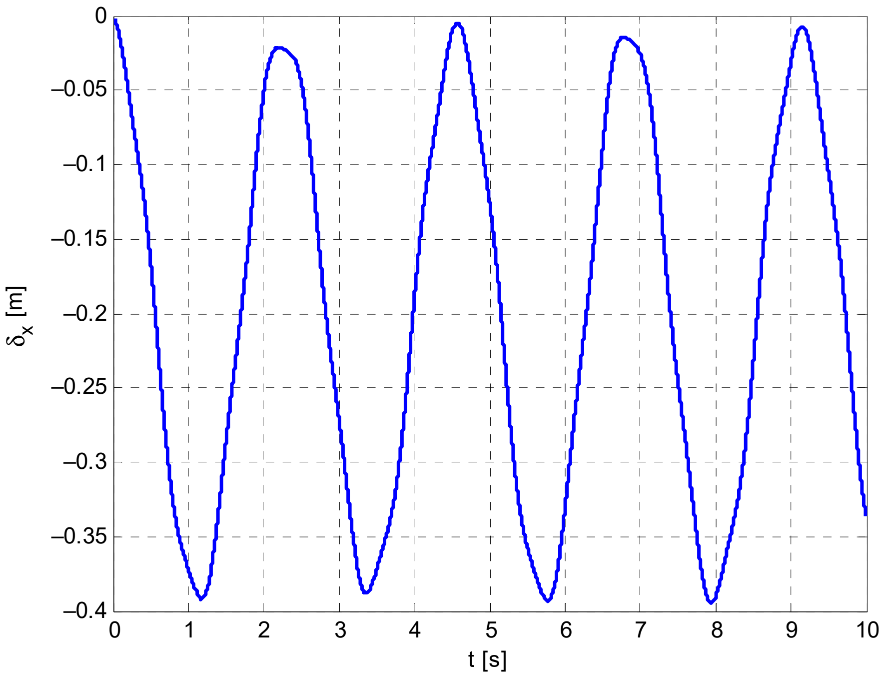

(**d**)

Figure 17. Time histories in the seventh case: (**a**) $\theta_x = \theta_x(t)$ (blue), $\theta_y = \theta_y(t)$ (green), $\theta_z = \theta_z(t)$ (red) (all kinematic chains are elastic), (**b**) $\delta_x = \delta_x(t)$ (blue), $\delta_y = \delta_y(t)$ (green), $\delta_z = \delta_z(t)$ (red) (all kinematic chains are elastic), (**c**) $\theta_x = \theta_x(t)$ (blue), $\theta_y = \theta_y(t)$ (green), $\theta_z = \theta_z(t)$ (red) (one kinematic chain is rigid), and (**d**) $\delta_x = \delta_x(t)$ (one kinematic chain is rigid). This case is a regular one (no degeneracy is present). The beating phenomenon appears only in the situation in which all kinematic chains are elastic ones.

The eigenpulsations for the situation in which all kinematic chains are elastic ones read $p_1 \approx 155.52\ \mathrm{s}^{-1} \approx 49.50\pi\ \mathrm{s}^{-1}$, $p_2 \approx 147.69\ \mathrm{s}^{-1} \approx 47.01\pi\ \mathrm{s}^{-1}$, $p_3 \approx 64.11\ \mathrm{s}^{-1} \approx 20.41\pi\ \mathrm{s}^{-1}$, $p_4 \approx 36.54\ \mathrm{s}^{-1} \approx 11.63\pi\ \mathrm{s}^{-1}$, $p_5 \approx 11.70\ \mathrm{s}^{-1} \approx 3.73\pi\ \mathrm{s}^{-1}$, and $p_6 \approx 8.66\ \mathrm{s}^{-1} \approx 2.76\pi\ \mathrm{s}^{-1}$, while for the situation in which one kinematic chain consists of rigid elements the eigenpulsations are $p_1 \approx 20.46\ \mathrm{s}^{-1} \approx 6.51\pi\ \mathrm{s}^{-1}$, $p_2 \approx 12.31\ \mathrm{s}^{-1} \approx 3.92\pi\ \mathrm{s}^{-1}$, $p_3 \approx 3.72\ \mathrm{s}^{-1} \approx 1.18\pi\ \mathrm{s}^{-1}$, and $p_4 \approx 2.75\ \mathrm{s}^{-1} \approx 0.87\pi\ \mathrm{s}^{-1}$. Because in the case when all kinematic chains are elastic ones two eigenpulsations are closed to ω_1 and ω_4, the phenomenon of beating appears in this case. This statement does not hold true for the case in which one kinematic chain consists of rigid elements.

The curves of variation are also periodical ones.

Similar results are presented in [43] for the situation with damping. Periodicity of the vibrations was also reported in [49].

7. Conclusions

In this paper we considered a rigid solid hung by kinematic chains in the most general case. When all kinematic chains are elastic ones we determined the general matrix equation of free vibration and we proved that in the case in which the mechanical system presents certain symmetries, the system of differential equations separates into new systems (the situation of degeneracy) from which one may determine the eigenpulsations. The same statement holds true for the situation in which one kinematic chain consists of rigid elements. In the most general case, the system has six or four different eigenpulsations, respectively.

Some degrees of freedom are common to both cases, but there exists no formula to calculate the eigenpulsations of one case knowing the values of the eigenpulsations of the other case.

If the system is acted on by harmonic forces, it is possible to obtain the beating phenomenon in both cases (all kinematic chains are elastic, and one kinematic chain is rigid, respectively), or in only one case. The motion is always a periodic one.

The calculations are performed using the screw coordinates and the corresponding results are presented in matrix form. The method presented here may be used for any rigid solid hung by kinematic chains, no matter if the kinematic chains form a symmetrical or an unsymmetrical structure. There is no limit for the number of kinematic chains. Moreover, these kinematic chains may be different.

The case for more than one rigid kinematic chain is more complicated because one has to determine the possible motions of the rigid solid considering only these kinematic chains. This will be our future goal.

Author Contributions: Conceptualization, A.-F.S., N.P., N.-D.S., L.M. and V.C.; methodology, A.-F.S., N.P., N.-D.S., L.M. and V.C.; software, A.-F.S., N.P., N.-D.S., L.M. and V.C.; validation, A.-F.S., N.P., N.-D.S., L.M. and V.C.; formal analysis, A.-F.S., N.P., N.-D.S., L.M,. and V.C.; investigation, A.-F.S., N.P., N.-D.S., L.M. and V.C.; resources, A.-F.S., N.P., N.-D.S., L.M. and V.C.; data curation, A.-F.S., N.P., N.-D.S., L.M. and V.C.; writing—original draft preparation, A.-F.S., N.P., N.-D.S., L.M. and V.C.; writing—review and editing, A.-F.S., N.P., N.-D.S., L.M. and V.C.; visualization, A.-F.S., N.P., N.-D.S., L.M. and V.C.; supervision, A.-F.S., N.P., N.-D.S., L.M. and V.C.; project administration, A.-F.S., N.P., N.-D.S., L.M. and V.C.; funding acquisition, A.-F.S., N.P., N.-D.S., L.M. and V.C. All authors have read and agreed to the published version of the manuscript.

Funding: This work was supported by a grant of the Romanian Ministry of Research and Innovation PNCDI III project PN-III-P2-2.1-PED-2019-0085 CONTRACT 447PED/2020.

Conflicts of Interest: The authors declare no conflict of interest.

Nomenclature

$OXYZ$	the general reference system (the system of the principal axes of inertia for the rigid solid
$[\mathbf{R}_B]$, g, …, $[\mathbf{R}_G]$, …	the rotational matrices of the local references systems with respect to the general reference system
$X_B, Y_B, Z_B, X_C, Y_C, Z_C, \ldots, X_G$, $Y_G, Z_G, \ldots$	the coordinates of the points $B, C, \ldots, G, \ldots$ relative to the general reference system
$[\mathbf{G}_B], [\mathbf{G}_C], \ldots, [\mathbf{G}_G], \ldots$	the translational matrices in the form $[\mathbf{G}_B] = \begin{bmatrix} 0 & -Z_B & Y_B \\ Z_B & 0 & -X_B \\ Y_B & X_B & 0 \end{bmatrix}, \ldots$
$[\mathbf{T}_B], [\mathbf{T}_C], \ldots, [\mathbf{T}_G], \ldots$	the matrices of position given by $[\mathbf{T}_B] = \begin{bmatrix} [\mathbf{R}_B] & [0] \\ [\mathbf{G}_B][\mathbf{R}_B] & [\mathbf{R}_B] \end{bmatrix}, \ldots$
$\boldsymbol{\theta}, \boldsymbol{\delta}$	the small angular displacement, and the small linear displacement, respectively, of the rigid solid
$\theta_X, \theta_Y, \theta_Z$, and $\delta_X, \delta_Y, \delta_Z$	the projections of the vectors $\boldsymbol{\theta}$, and $\boldsymbol{\delta}$, respectively, onto the axes OX, OY, and OZ
$\{\boldsymbol{\Delta}\}$	the column matrix of the displacements of the rigid solid, $\{\boldsymbol{\Delta}\} = \begin{bmatrix} \theta_X & \theta_Y & \theta_Z & \delta_X & \delta_Y & \delta_Z \end{bmatrix}^{\mathrm{T}}$
$\{\boldsymbol{\xi}_B\}$	the column matrices of the possible displacements $\xi_B^{(1)}, \xi_B^{(2)}, \ldots$, at the kinematic joint B, in the motion of the element BC with respect to the element AB,$\{\boldsymbol{\xi}_B\} = \begin{bmatrix} \xi_B^{(1)} & \xi_B^{(2)} & \ldots \end{bmatrix}^{\mathrm{T}}$
$[\mathbf{u}_B]$	the matrix of the screw coordinates of the kinematic joint B
$[\mathbf{U}_B]$	the matrix given by$[\mathbf{U}_B] = [\mathbf{T}_B][\mathbf{u}_B]$
E, G	the Young modulus, and the shear modulus, respectively, of a bar
A, and I_x, I_y, I_z	the area, and the moments of inertia, respectively, of the homogeneous bar
l	the length of a homogeneous bar
$[\mathbf{k}]$	the rigidity matrix of a bar relative to the local reference system
$[\mathbf{h}]$	the flexibility matrix of a bar relative to the local reference system
$[\boldsymbol{\eta}]$	the matrix given by$[\boldsymbol{\eta}] = \begin{bmatrix} 0&0&0&1&0&0 \\ 0&0&0&0&1&0 \\ 0&0&0&0&0&1 \\ 1&0&0&0&0&0 \\ 0&1&0&0&0&0 \\ 0&0&1&0&0&0 \end{bmatrix}$
m, and J_X, J_Y, J_Z	the mass, and the central principal moments of inertia, respectively, of the rigid solid
$[\mathbf{M}]$	the matrix$[\mathbf{M}] = \begin{bmatrix} 0&0&0&m&0&0 \\ 0&0&0&0&m&0 \\ 0&0&0&0&0&m \\ J_X&0&0&0&0&0 \\ 0&J_Y&0&0&0&0 \\ 0&0&J_Z&0&0&0 \end{bmatrix}$

Appendix A

Let us consider a bar AB and a system of coordinates $Axyz$, where the axis Ax is along the bar. The displacements of the end A are d_{Ax} (translation along the Ax axis, θ_{Ax} (rotation about the same axis), d_{Ay} (translation along the Ay axis), θ_{Ay} (rotation about the Ay axis), d_{Az}, and θ_{Az} (translation along and rotation about the Az axis). Analogically, the displacements of the point B are d^*_{Bx}, θ^*_{Bx}, d^*_{By}, θ^*_{By}, d^*_{Bz}, and θ^*_{Bz}.

The axial force (along the Ax axis) is given by

$$f_{Ax} = \frac{EA}{l}(d_{Ax} - d^*_{Bx}) \tag{A1}$$

while the torsional moments (about the same axis) reads

$$m_{Ax} = \frac{GI_x}{l}(\theta_{Ax} - \theta^*_{Bx}) \tag{A2}$$

With the aid of the Euler–Bernoulli relation

$$EI_z\frac{\mathrm{d}^2y}{\mathrm{d}x^2} = -m_z(x) \tag{A3}$$

where

$$m_z(x) = m_{Az} - f_{Ay}x \tag{A4}$$

and taking into account that

$$\theta_z = \frac{\mathrm{d}y}{\mathrm{d}x} \tag{A5}$$

and the initial conditions (at $x = 0$, $y = d_{Ay}$, and $\theta_z = \theta_{Az}$, while at $x = l$, $y = d^*_{By}$, and $\theta_z = \theta^*_{Bz}$), it results in the relations

$$f_{Ay} = \frac{6EI_z}{l^2}\theta_{Az} + \frac{6EI_z}{l^2}\theta^*_{Bz} + \frac{12EI_z}{l^3}d_{Ay} + \frac{12EI_z}{l^3}d^*_{By} \tag{A6}$$

$$m_{Az} = \frac{4EI_z}{l}\theta_{Az} + \frac{2EI_z}{l}\theta^*_{Bz} + \frac{6EI_z}{l^2}d_{Ay} - \frac{6EI_z}{l^2}d^*_{By} \tag{A7}$$

Analogically, one obtains

$$f_{Az} = -\frac{6EI_y}{l^2}\theta_{Ay} - \frac{6EI_y}{l^2}\theta^*_{By} + \frac{12EI_y}{l^3}d_{Az} - \frac{12EI_y}{l^3}d^*_{Bz} \tag{A8}$$

$$m_{Ay} = \frac{4EI_y}{l}\theta_{Ay} + \frac{2EI_y}{l}\theta^*_{By} - \frac{6EI_y}{l^2}d_{Az} + \frac{6EI_y}{l^2}d^*_{Bz} \tag{A9}$$

Using the previous expressions, one obtains

$$\{\mathbf{f}_A\} = [\mathbf{k}_{AB}]\{\mathbf{d}_A\} - [\mathbf{k}^*_{AB}]\{\mathbf{d}^*_B\} \tag{A10}$$

Knowing that

$$\{\mathbf{d}^*_B\} = [\mathbf{T}^*_{AB}]^{-1}\{\mathbf{d}_B\} \tag{A11}$$

$$[\mathbf{k}_{AB}] = [\mathbf{k}^*_{AB}][\mathbf{T}^*_{AB}]^{-1} \tag{A12}$$

this results in

$$\{\mathbf{f}_A\} = [\mathbf{k}_{AB}]\{\{\mathbf{d}_A\} - \{\mathbf{d}_B\}\} \tag{A13}$$

Defining now the relative displacement

$$\{\mathbf{d}_{AB}\} = \{\mathbf{d}_A\} - \{\mathbf{d}_B\} \tag{A14}$$

results in

$$\{\mathbf{f}_A\} = [\mathbf{k}_{AB}]\{\mathbf{d}_{AB}\} \tag{A15}$$

Appendix B

The complete calculation for the first case is given below.

For the kinematic chain $A_1B_1C_1$ the calculation schema is captured in Figure A1.

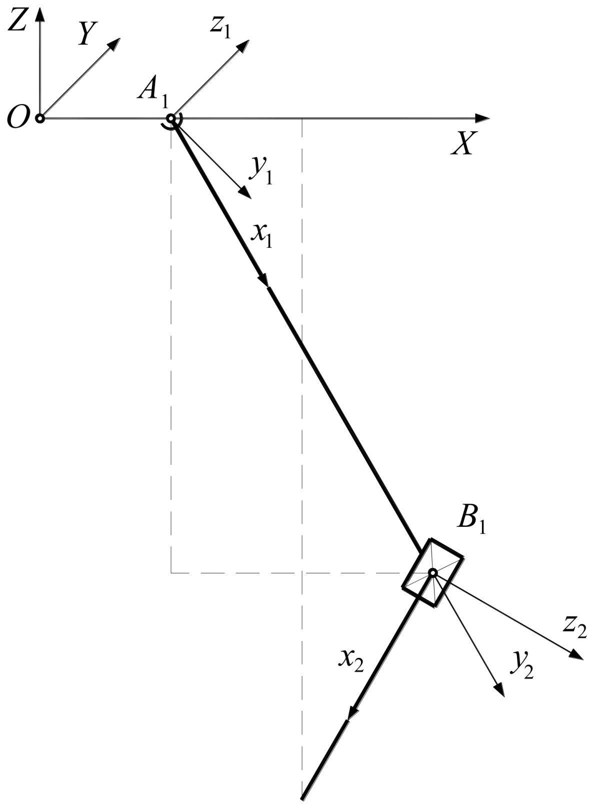

Figure A1. Calculation schema.

It successively results in

$$[\mathbf{R}_{A_1}] = \begin{bmatrix} 0.5 & 0 & 0.866 \\ 0 & 1 & 0 \\ -0.866 & 0 & 0.5 \end{bmatrix},\ [\mathbf{G}_{A_1}] = \begin{bmatrix} 0 & 0 & 0 \\ 0 & 0 & -0.1 \\ 0 & 0.1 & 0 \end{bmatrix},$$

$$[\mathbf{T}_{A_1}] = \begin{bmatrix} 0.5 & 0 & 0.866 & 0 & 0 & 0 \\ 0 & 1 & 0 & 0 & 0 & 0 \\ -0.866 & 0 & 0.5 & 0 & 0 & 0 \\ 0 & 0 & 0 & 0.5 & 0 & 0.866 \\ 0.087 & 0 & -0.05 & 0 & 1 & 0 \\ 0 & 0.1 & 0 & -0.866 & 0 & 0.5 \end{bmatrix},$$

$$[\mathbf{R}_{B_1}] = \begin{bmatrix} -0.5 & 0 & 0.866 \\ 0 & 1 & 0 \\ -0.866 & 0 & -0.5 \end{bmatrix},\ [\mathbf{G}_{B_1}] = \begin{bmatrix} 0 & 0.346 & 0 \\ -0.346 & 0 & -0.3 \\ 0 & 0.3 & 0 \end{bmatrix},$$

$$[\mathbf{T}_{B_1}] = \begin{bmatrix} -0.5 & 0 & 0.866 & 0 & 0 & 0 \\ 0 & 1 & 0 & 0 & 0 & 0 \\ -0.866 & 0 & -0.5 & 0 & 0 & 0 \\ 0 & 0.346 & 0 & -0.5 & 0 & 0.866 \\ 0.433 & 0 & -0.15 & 0 & 1 & 0 \\ 0 & 0.3 & 0 & -0.866 & 0 & -0.5 \end{bmatrix},$$

$$[\mathbf{R}_{A_2}] = \begin{bmatrix} -0.25 & -0.866 & -0.433 \\ 0.433 & -0.5 & 0.75 \\ -0.866 & 0 & 0.5 \end{bmatrix}, \; [\mathbf{G}_{A_2}] = \begin{bmatrix} 0 & 0 & 0.087 \\ 0 & 0 & 0.05 \\ -0.087 & -0.05 & 0 \end{bmatrix},$$

$$[\mathbf{T}_{A_2}] = \begin{bmatrix} -0.25 & -0.866 & -0.433 & 0 & 0 & 0 \\ 0.433 & -0.5 & 0.75 & 0 & 0 & 0 \\ -0.866 & 0 & 0.5 & 0 & 0 & 0 \\ -0.075 & 0 & 0.043 & -0.25 & -0.866 & -0.433 \\ -0.433 & 0 & 0.025 & 0.433 & -0.5 & 0.75 \\ 0 & 0.1 & 0 & -0.866 & 0 & 0.5 \end{bmatrix},$$

$$[\mathbf{R}_{B_2}] = \begin{bmatrix} 0.25 & -0.866 & -0.433 \\ -0.433 & -0.5 & 0.75 \\ -0.866 & 0 & -0.5 \end{bmatrix}, \; [\mathbf{G}_{B_2}] = \begin{bmatrix} 0 & 0.346 & 0.260 \\ -0.346 & 0 & 0.15 \\ -0.260 & -0.15 & 0 \end{bmatrix},$$

$$[\mathbf{T}_{B_2}] = \begin{bmatrix} 0.25 & -0.866 & -0.433 & 0 & 0 & 0 \\ -0.433 & -0.5 & 0.75 & 0 & 0 & 0 \\ -0.866 & 0 & -0.5 & 0 & 0 & 0 \\ -0.375 & 0.173 & 0.130 & 0.25 & -0.866 & -0.433 \\ -0.217 & 0.3 & 0.075 & -0.433 & -0.5 & 0.75 \\ 0 & 0.3 & 0 & 0.866 & 0 & -0.5 \end{bmatrix},$$

$$[\mathbf{R}_{A_3}] = \begin{bmatrix} -0.25 & 0.866 & -0.433 \\ -0.433 & -0.5 & -0.75 \\ -0.866 & 0 & 0.5 \end{bmatrix}, \; [\mathbf{G}_{A_3}] = \begin{bmatrix} 0 & 0 & -0.087 \\ 0 & 0 & 0.05 \\ 0.087 & -0.05 & 0 \end{bmatrix},$$

$$[\mathbf{T}_{A_3}] = \begin{bmatrix} -0.25 & 0.866 & -0.433 & 0 & 0 & 0 \\ -0.433 & -0.5 & -0.75 & 0 & 0 & 0 \\ -0.866 & 0 & 0.5 & 0 & 0 & 0 \\ 0.075 & 0 & -0.0433 & -0.25 & 0.866 & -0.433 \\ -0.043 & 0 & 0.025 & -0.433 & -0.5 & -0.75 \\ 0 & 0.1 & 0 & -0.866 & 0 & 0.5 \end{bmatrix},$$

$$[\mathbf{R}_{B_3}] = \begin{bmatrix} 0.25 & 0.866 & -0.433 \\ 0.433 & -0.5 & -0.75 \\ -0.866 & 0 & -0.5 \end{bmatrix}, \; [\mathbf{G}_{B_3}] = \begin{bmatrix} 0 & 0.346 & -0.260 \\ -0.346 & 0 & 0.15 \\ 0.260 & -0.15 & 0 \end{bmatrix},$$

$$[\mathbf{T}_{B_3}] = \begin{bmatrix} 0.25 & 0.866 & -0.433 & 0 & 0 & 0 \\ 0.433 & -0.5 & -0.75 & 0 & 0 & 0 \\ -0.866 & 0 & -0.5 & 0 & 0 & 0 \\ 0.375 & -0.173 & -0.130 & 0.25 & 0.866 & -0.433 \\ -0.217 & -0.3 & 0.075 & 0.433 & -0.5 & -0.75 \\ 0 & 0.3 & 0 & -0.866 & 0 & -0.5 \end{bmatrix},$$

$$[\mathbf{u}_{A_1}] = [\mathbf{u}_{A_2}] = [\mathbf{u}_{A_3}] = \begin{bmatrix} 1 & 0 & 0 \\ 0 & 1 & 0 \\ 0 & 0 & 1 \\ 0 & 0 & 0 \\ 0 & 0 & 0 \\ 0 & 0 & 0 \end{bmatrix},$$

$$[\mathbf{U}_{A_1}] = \begin{bmatrix} 0.5 & 0 & 0.866 \\ 0 & 1 & 0 \\ -0.866 & 0 & 0.5 \\ 0 & 0 & 0 \\ 0.087 & 0 & -0.05 \\ 0 & 0.1 & 0 \end{bmatrix},$$

$$[\mathbf{U}_{A_2}] = \begin{bmatrix} -0.25 & -0.866 & -0.433 \\ 0.433 & -0.5 & 0.75 \\ -0.866 & 0 & 0.5 \\ -0.075 & 0 & 0.043 \\ -0.043 & 0 & 0.025 \\ 0 & 0.1 & 0 \end{bmatrix},$$

$$[\mathbf{U}_{A_3}] = \begin{bmatrix} -0.25 & 0.866 & -0.433 \\ -0.433 & -0.5 & -0.75 \\ -0.866 & 0 & 0.5 \\ 0.075 & 0 & -0.043 \\ -0.043 & 0 & 0.025 \\ 0 & 0.1 & 0 \end{bmatrix},$$

$$[\mathbf{u}_{B_1}] = [\mathbf{u}_{B_2}] = [\mathbf{u}_{B_3}] = \begin{bmatrix} 0 & 0 & 0 & 1 & 0 & 0 \end{bmatrix}^{\mathrm{T}},$$

$$[\mathbf{U}_{B_1}] = \begin{bmatrix} 0 \\ 0 \\ 0 \\ -0.5 \\ 0 \\ -0.866 \end{bmatrix},\ [\mathbf{U}_{B_2}] = \begin{bmatrix} 0 \\ 0 \\ 0 \\ 0.25 \\ -0.433 \\ -0.866 \end{bmatrix},\ [\mathbf{U}_{B_3}] = \begin{bmatrix} 0 \\ 0 \\ 0 \\ 0.25 \\ 0.433 \\ -0.866 \end{bmatrix},$$

$$[\mathbf{k}_{A_1B_1}] = [\mathbf{k}_{A_2B_2}] = [\mathbf{k}_{A_3B_3}]$$
$$= \begin{bmatrix} 0 & 0 & 0 & 8.247\times10^7 & 0 & 0 \\ 0 & 0 & 1.546\times10^4 & 0 & 1.546\times10^5 & 0 \\ 0 & -1.546\times10^4 & 0 & 0 & 0 & 1.546\times10^5 \\ 392.7 & 0 & 0 & 0 & 0 & 0 \\ 0 & 2061.7 & 0 & 0 & 0 & -1.564\times10^4 \\ 0 & 0 & 20647 & 0 & 1.564\times10^4 & 0 \end{bmatrix},$$

$$[\mathbf{k}_{B_1C_1}] = [\mathbf{k}_{B_2C_2}] = [\mathbf{k}_{B_3C_3}]$$
$$= \begin{bmatrix} 0 & 0 & 0 & 4.123\times10^7 & 0 & 0 \\ 0 & 0 & 3.866\times10^3 & 0 & 1.933\times10^4 & 0 \\ 0 & -3.866\times10^3 & 0 & 0 & 0 & 1.933\times10^4 \\ 196.3 & 0 & 0 & 0 & 0 & 0 \\ 0 & 1.03\times10^3 & 0 & 0 & 0 & -3.865\times10^3 \\ 0 & 0 & 1.03\times10^3 & 0 & 3.865\times10^3 & 0 \end{bmatrix},$$

$$[\mathbf{K}_{A_1B_1}]$$
$$= \begin{bmatrix} 0 & 3.551\times10^6 & 0 & 2.073\times10^7 & 0 & -3.564\times10^7 \\ 1.399\times10^4 & 0 & 2.319\times10^4 & 0 & 1.546\times10^5 & 0 \\ 0 & -6.020\times10^6 & 0 & -3.564\times10^7 & 0 & 6.189\times10^7 \\ 1.644\times10^3 & 0 & 2.062\times10^3 & 0 & 1.339\times10^4 & 0 \\ 0 & 6.225\times10^5 & 0 & 3.550\times10^6 & 0 & -6.020\times10^6 \\ 2.062\times10^3 & 0 & 3.902\times10^3 & 0 & 2.319\times10^4 & 0 \end{bmatrix},$$

$$
\begin{aligned}
&\left[\mathbf{K}_{A_2B_2}\right]\\
&= \begin{bmatrix}
-1.543\times10^{6} & 8.777\times10^{5} & -2.009\times10^{4} & 5.299\times10^{6} & -8.911\times10^{6} & 1.782\times10^{7}\\
-2.660\times10^{6} & -1.543\times10^{6} & -1.160\times10^{4} & -8.911\times10^{6} & 1.559\times10^{7} & -3.087\times10^{7}\\
5.366\times10^{6} & 3.098\times10^{6} & 0 & 1.782\times10^{7} & -3.087\times10^{7} & 6.189\times10^{7}\\
4.673\times10^{5} & 2.688\times10^{5} & -1.031\times10^{3} & 1.543\times10^{6} & -2.660\times10^{6} & 5.366\times10^{6}\\
2.688\times10^{5} & 1.569\times10^{5} & 1.786\times10^{3} & 8.777\times10^{5} & -1.543\times10^{6} & 3.098\times10^{6}\\
-1.031\times10^{3} & 1.786\times10^{3} & 3.902\times10^{3} & -2.009\times10^{4} & -1.160\times10^{4} & 0
\end{bmatrix}
\end{aligned}
$$

$$
\begin{aligned}
&\left[\mathbf{K}_{A_3B_3}\right]\\
&= \begin{bmatrix}
-1.543\times10^{6} & 8.777\times10^{5} & 2.009\times10^{4} & 5.299\times10^{6} & 8.911\times10^{6} & 1.782\times10^{7}\\
-2.660\times10^{6} & 1.543\times10^{6} & -1.160\times10^{4} & 8.911\times10^{6} & 1.559\times10^{7} & 3.087\times10^{7}\\
-5.366\times10^{6} & 3.098\times10^{6} & 0 & 1.782\times10^{7} & 3.087\times10^{7} & 6.189\times10^{7}\\
4.673\times10^{5} & -2.688\times10^{5} & -1.031\times10^{3} & -1.543\times10^{6} & -2.660\times10^{6} & 5.366\times10^{6}\\
-2.688\times10^{5} & 1.569\times10^{5} & -1.786\times10^{3} & 8.777\times10^{5} & 1.543\times10^{6} & 3.098\times10^{6}\\
-1.031\times10^{3} & -1.786\times10^{3} & 3.902\times10^{3} & 2.009\times10^{4} & -1.160\times10^{4} & 0
\end{bmatrix}
\end{aligned}
$$

$$
\begin{aligned}
&\left[\mathbf{K}_{B_1C_1}\right]\\
&= \begin{bmatrix}
0 & -8.933\times10^{6} & 0 & 1.032\times10^{7} & 0 & 1.785\times10^{7}\\
1.004\times10^{4} & 0 & 3.866\times10^{3} & 0 & 1.933\times10^{4} & 0\\
0 & -1.546\times10^{7} & 0 & 1.785\times10^{7} & 0 & 3.093\times10^{7}\\
5.461\times10^{3} & 0 & 1.982\times10^{3} & 0 & 1.004\times10^{4} & 0\\
0 & 7.734\times10^{6} & 0 & -8.933\times10^{6} & 0 & -1.546\times10^{7}\\
1.982\times10^{3} & 0 & 9.848\times10^{2} & 0 & 3.866\times10^{3} & 0
\end{bmatrix},
\end{aligned}
$$

$$
\begin{aligned}
&\left[\mathbf{K}_{B_2C_2}\right]\\
&= \begin{bmatrix}
-3.864\times10^{6} & -2.241\times10^{6} & -3.348\times10^{3} & 2.595\times10^{6} & -4.462\times10^{6} & -8.923\times10^{6}\\
6.703\times10^{6} & 3.864\times10^{6} & -1.933\times10^{3} & -4.462\times10^{6} & 7.747\times10^{6} & 1.546\times10^{7}\\
1.339\times10^{7} & 7.730\times10^{6} & 0 & -8.923\times10^{6} & 1.546\times10^{7} & 3.093\times10^{7}\\
5.802\times10^{6} & 3.347\times10^{6} & -9.910\times10^{2} & -3.864\times10^{6} & 6.702\times10^{6} & 1.339\times10^{7}\\
3.347\times10^{6} & 1.938\times10^{6} & 1.717\times10^{3} & -2.241\times10^{6} & 3.864\times10^{6} & 7.730\times10^{6}\\
-9.910\times10^{2} & 1.717\times10^{3} & 9.848\times10^{2} & -3.348\times10^{3} & -1.933\times10^{3} & 0
\end{bmatrix}
\end{aligned}
$$

$$
\begin{aligned}
&\left[\mathbf{K}_{B_3C_3}\right]\\
&= \begin{bmatrix}
3.864\times10^{6} & -2.241\times10^{6} & 3.348\times10^{3} & 2.595\times10^{6} & 4.462\times10^{6} & -8.923\times10^{6}\\
6.702\times10^{6} & -3.864\times10^{6} & -1.933\times10^{3} & -4.462\times10^{6} & 7.747\times10^{6} & -1.546\times10^{7}\\
-1.339\times10^{7} & 7.730\times10^{6} & 0 & -8.923\times10^{6} & -1.546\times10^{7} & 3.093\times10^{7}\\
5.802\times10^{6} & -3.347\times10^{6} & -9.910\times10^{2} & 3.864\times10^{6} & 6.702\times10^{6} & -1.339\times10^{7}\\
-3.347\times10^{6} & 1.938\times10^{6} & -1.717\times10^{3} & 2.241\times10^{6} & -3.864\times10^{6} & 7.730\times10^{6}\\
-9.910\times10^{2} & -1.717\times10^{3} & 9.848\times10^{2} & 3.348\times10^{3} & -1.933\times10^{3} & 0
\end{bmatrix}
\end{aligned}
$$

$$
\begin{aligned}
&\left[\tilde{\mathbf{K}}_{\mathbf{A}_1C_1}\right]\\
&= \begin{bmatrix}
0 & -1.023\times10^{3} & 0 & 3.543\times10^{3} & 0 & -1.672\times10^{3}\\
1.186\times10^{3} & 0 & 6.428\times10^{2} & 0 & 3.145\times10^{3} & 0\\
0 & -9.810\times10^{3} & 0 & -1.672\times10^{3} & 0 & 5.693\times10^{3}\\
6.071\times10^{2} & 0 & 2.366\times10^{2} & 0 & 1.186\times10^{3} & 0\\
0 & 2.354\times10^{3} & 0 & -1.023\times10^{3} & 0 & -9.810\times10^{3}\\
2.366\times10^{2} & 0 & 2.708\times10^{2} & 0 & 6.428\times10^{2} & 0
\end{bmatrix},
\end{aligned}
$$

$$\left[\tilde{\mathbf{K}}_{\mathbf{A}_2 C_2}\right] = \begin{bmatrix} 7.070\times10^{1} & -1.146\times10^{3} & -5.567\times10^{2} & 3.245\times10^{3} & -1.723\times10^{2} & 8.361\times10^{2} \\ 1.064\times10^{3} & -7.070\times10^{1} & -3.214\times10^{2} & -1.723\times10^{2} & 3.444\times10^{3} & -1.448\times10^{3} \\ 8.495\times10^{3} & 4.905\times10^{3} & 0 & 8.361\times10^{2} & -1.448\times10^{3} & 5.693\times10^{4} \\ 1.917\times10^{3} & 7.565\times10^{2} & -1.183\times10^{2} & 7.070\times10^{1} & 1.064\times10^{3} & 8.495\times10^{3} \\ 7.565\times10^{2} & 1.044\times10^{3} & 2.049\times10^{2} & -1.146\times10^{3} & -7.070\times10^{1} & 4.905\times10^{3} \\ -1.183\times10^{2} & 2.049\times10^{3} & 2.708\times10^{2} & -5.567\times10^{2} & -3.214\times10^{2} & 0 \end{bmatrix}$$

$$\left[\tilde{\mathbf{K}}_{\mathbf{A}_3 C_3}\right] = \begin{bmatrix} -7.070\times10^{1} & -1.146\times10^{3} & 5.567\times10^{2} & 3.245\times10^{3} & 1.723\times10^{2} & 8.361\times10^{2} \\ 1.064\times10^{3} & 7.070\times10^{1} & -3.214\times10^{2} & 1.723\times10^{2} & 3.444\times10^{3} & 1.448\times10^{3} \\ -8.495\times10^{3} & 4.905\times10^{3} & 0 & 8.361\times10^{2} & 1.448\times10^{3} & 5.693\times10^{4} \\ 1.917\times10^{3} & -7.565\times10^{2} & -1.183\times10^{2} & -7.070\times10^{1} & 1.064\times10^{3} & -8.495\times10^{3} \\ -7.565\times10^{2} & 1.044\times10^{3} & -2.049\times10^{2} & -1.146\times10^{3} & 7.070\times10^{1} & 4.905\times10^{3} \\ -1.183\times10^{2} & -2.049\times10^{3} & 2.708\times10^{2} & 5.567\times10^{2} & -3.214\times10^{2} & 0 \end{bmatrix}$$

$$\left[\mathbf{U}_{A_1B_1}\right] = \begin{bmatrix} 0.5 & 0 & 0.866 & 0 \\ 0 & 1 & 0 & 0.343 \\ -0.866 & 0 & 0.5 & 0 \\ 0 & 0 & 0 & -0.5 \\ 0.087 & 0 & -0.05 & 0 \\ 0 & 0.1 & 0 & -0.866 \end{bmatrix},$$

$$\left[\mathbf{U}_{A_2B_2}\right] = \begin{bmatrix} -0.25 & -0.866 & -0.433 & 0 \\ 0.433 & -0.5 & 0.75 & 0 \\ -0.866 & 0 & 0.5 & 0 \\ -0.075 & 0 & 0.043 & 0.25 \\ -0.043 & 0 & 0.025 & -0.433 \\ 0 & 0.1 & 0 & -0.866 \end{bmatrix},$$

$$\left[\mathbf{U}_{A_3B_3}\right] = \begin{bmatrix} -0.25 & 0.866 & -0.433 & 0 \\ -0.433 & -0.5 & -0.75 & 0 \\ -0.866 & 0 & 0.5 & 0 \\ 0.075 & 0 & -0.043 & 0.25 \\ -0.043 & 0 & 0.025 & 0.433 \\ 0 & 0.1 & 0 & -0.866 \end{bmatrix},$$

$$\left[\mathbf{K}_{A_1C_1}\right] = \begin{bmatrix} 0 & 6.377\times10^{1} & 0 & 1.104\times10^{3} & 0 & -6.377\times10^{2} \\ 0 & 0 & 7.636\times10^{1} & 0 & 7.636\times10^{2} & 0 \\ 0 & -3.682\times10^{1} & 0 & -6.377\times10^{2} & 0 & 3.682\times10^{2} \\ 0 & 0 & 0 & 0 & 0 & 0 \\ 0 & 3.682 & 0 & 6.377\times10^{1} & 0 & -3.682\times10^{1} \\ 0 & 0 & 7.636 & 0 & 7.636\times10^{1} & 0 \end{bmatrix},$$

$$\left[\mathbf{K}_{\mathbf{A}_2 C_2}\right] = \begin{bmatrix} 2.761\times10^{1} & 1.594\times10^{1} & -6.613\times10^{1} & 8.488\times10^{2} & -1.476\times10^{2} & 3.188\times10^{2} \\ -4.782\times10^{1} & -2.761\times10^{1} & -3.818\times10^{1} & -1.476\times10^{2} & 1.019\times10^{3} & -5.522\times10^{2} \\ 3.188\times10^{1} & 1.841\times10^{1} & 0 & 3.188\times10^{2} & -5.522\times10^{2} & 3.682\times10^{2} \\ 2.761 & 1.594 & 0 & 2.761\times10^{1} & -4.782\times10^{1} & 3.188\times10^{1} \\ 1.594 & 0.920 & 0 & 1.594\times10^{1} & -2.761\times10^{1} & 1.841\times10^{1} \\ 0 & 0 & 7.636 & -6.613\times10^{1} & -3.818\times10^{1} & 0 \end{bmatrix}$$

$$
\begin{bmatrix}\mathbf{K}_{\mathbf{A}_3C_3}\end{bmatrix} = \begin{bmatrix}
-2.761\times10^{1} & 1.594\times10^{1} & 6.613\times10^{1} & 8.488\times10^{2} & 1.476\times10^{2} & 3.188\times10^{2} \\
-4.782\times10^{1} & 2.761\times10^{1} & -3.818\times10^{1} & -1.476\times10^{2} & 1.019\times10^{3} & 5.522\times10^{2} \\
-3.188\times10^{1} & 1.841\times10^{1} & 0 & 3.188\times10^{2} & 5.522\times10^{2} & 3.682\times10^{2} \\
2.761 & -1.594 & 0 & -2.761\times10^{1} & -4.782\times10^{1} & -3.188\times10^{1} \\
-1.594 & 0.920 & 0 & 1.594\times10^{1} & 2.761\times10^{1} & 1.841\times10^{1} \\
0 & 0 & 7.636 & 6.613\times10^{1} & -3.818\times10^{1} & 0
\end{bmatrix}
$$

$$
[\mathbf{M}] = \begin{bmatrix}
0 & 0 & 0 & 10 & 0 & 0 \\
0 & 0 & 0 & 0 & 10 & 0 \\
0 & 0 & 0 & 0 & 0 & 10 \\
1.25\times10^{-2} & 0 & 0 & 0 & 0 & 0 \\
0 & 1.25\times10^{-2} & 0 & 0 & 0 & 0 \\
0 & 0 & 1.25\times10^{-2} & 0 & 0 & 0
\end{bmatrix}.
$$

Appendix C

The matrix differential systems for each considered case are given below.

For the first case (Section 6.1):

(a) if we consider that all the kinematic chains contain only elastic elements, then we obtain

$$
\begin{bmatrix}\mathbf{K}_{system}\end{bmatrix} = \begin{bmatrix}
0 & 9.565\times10^{1} & 0 & 2.802\times10^{3} & 0 & 0 \\
-9.565\times10^{1} & 0 & 0 & 0 & 2.802\times10^{3} & 0 \\
0 & 0 & 0 & 0 & 0 & 1.104\times10^{3} \\
5.522 & 0 & 0 & 0 & -9.565\times10^{1} & 0 \\
0 & 5.522 & 0 & 9.565 & 0 & 0 \\
0 & 0 & 2.291\times10^{1} & 0 & 0 & 0
\end{bmatrix}
$$

and the matrix differential system

$$
\begin{cases}
\ddot{\theta}_X + 4.418\times10^{2}\theta_X - 7.652\times10^{3}\delta_Y = 0\,, \\
\ddot{\theta}_Y + 4.418\times10^{2}\theta_Y + 7.652\times10^{3}\delta_X = 0\,, \\
\ddot{\theta}_Z + 9.163\times10^{2}\theta_Z = 0\,, \\
\ddot{\delta}_X + 9.565\theta_Y + 2.802\times10^{2}\delta_X = 0\,, \\
\ddot{\delta}_Y - 9.565\theta_X + 2.802\times10^{2}\delta_Y = 0\,, \\
\ddot{\delta}_Z + 1.104\times10^{2}\delta_Z = 0\,.
\end{cases}
$$

The previous system separates into

$$
\begin{cases}
\ddot{\theta}_X + 4.418\times10^{2}\theta_X - 7.652\times10^{3}\delta_Y = 0\,, \\
\ddot{\delta}_Y - 9.565\theta_X + 2.802\times10^{2}\delta_Y = 0\,,
\end{cases}
$$

$$
\begin{cases}
\ddot{\theta}_Y + 4.418\times10^{2}\theta_Y + 7.652\times10^{3}\delta_X = 0\,, \\
\ddot{\delta}_X + 9.565\theta_Y + 2.802\times10^{2}\delta_X = 0\,,
\end{cases}
$$

$$
\ddot{\theta}_Z + 9.163\times10^{2}\theta_Z = 0,
$$

$$
\ddot{\theta}_Z + 9.163\times10^{2}\theta_Z = 0;
$$

(b) If the kinematic chain $A_1B_1C_1$ consists of rigid elements, then it results in

$$[\mathbf{K}_{system}] = \begin{bmatrix} 0 & 3.188\times10^{1} & 0 & 1.698\times10^{3} & 0 & 6.377\times10^{2} \\ -9.565\times10^{1} & 0 & -7.636 & 0 & 2.038\times10^{3} & 0 \\ 0 & 3.682\times10^{1} & 0 & 6.377\times10^{2} & 0 & 7.363\times10^{2} \\ 0 & 0 & 0 & 0 & -9.565\times10^{1} & 0 \\ 0 & 1.841 & 0 & 3.188\times10^{1} & 0 & 3.682\times10^{1} \\ 0 & 0 & 1.527\times10^{1} & 0 & -7.636\times10^{1} & 0 \end{bmatrix}$$

and the matrix differential system

$$\begin{cases} \ddot{\theta}_x + 5.154\times10^{1}\theta_x + 1.488\times10^{2}\theta_z = 0\,, \\ \ddot{\theta}_y + 1.104\times10^{2}\theta_y - 2.952\times10^{2}\delta_x = 0\,, \\ \ddot{\theta}_z - 5.399\times10^{2}\theta_x + 7.977\times10^{2}\theta_z = 0\,, \\ \ddot{\delta}_x - 4.782\theta_y + 1.273\times10^{2}\delta_x = 0\,, \end{cases}$$

which separates into the systems

$$\begin{cases} \ddot{\theta}_x + 5.154\times10^{1}\theta_x + 1.488\times10^{2}\theta_z = 0\,, \\ \ddot{\theta}_z - 5.399\times10^{2}\theta_x + 7.977\times10^{2}\theta_z = 0\,, \end{cases}$$
$$\begin{cases} \ddot{\theta}_y + 1.104\times10^{2}\theta_y - 2.592\times10^{2}\delta_x = 0\,, \\ \ddot{\delta}_x - 4.782\theta_y + 1.273\times10^{2}\delta_x = 0\,. \end{cases}$$

For the second case (Section 6.2):

(a) if all kinematic chains consist of elastic elements, then the system of differential equations reads

$$\begin{cases} \ddot{\theta}_x + 2.827\times10^{1}\theta_x - 1.959\times10^{2}\delta_y = 0\,, \\ \ddot{\theta}_y + 2.827\times10^{1}\theta_y + 1.959\times10^{2}\delta_x = 0\,, \\ \ddot{\theta}_z + 5.864\times10^{1}\theta_z = 0\,, \\ \ddot{\delta}_x + 1.530\theta_y + 1.793\times10^{1}\delta_x = 0\,, \\ \ddot{\delta}_y - 1.530\theta_x + 1.793\times10^{1}\theta_y = 0\,, \\ \ddot{\delta}_z + 7.069\delta_z = 0, \end{cases}$$

which separates into the systems

$$\begin{cases} \ddot{\theta}_x + 2.827\times10^{1}\theta_x - 1.959\times10^{2}\delta_y = 0\,, \\ \ddot{\delta}_y - 1.530\theta_x + 1.793\times10^{1}\delta_y = 0\,, \end{cases}$$
$$\begin{cases} \ddot{\theta}_y + 2.827\times10^{1}\theta_y + 1.959\times10^{2}\delta_x = 0\,, \\ \ddot{\delta}_x + 1.530\theta_y + 1.793\times10^{1}\delta_x = 0\,, \end{cases}$$
$$\ddot{\theta}_z + 5.864\times10^{1}\theta_z = 0,$$
$$\ddot{\delta}_z + 7.069\delta_z = 0;$$

(b) if the kinematic chain $A_1B_1C_1$ consists of rigid elements, then it results in the following system of differential equations

$$\begin{cases} \ddot{\theta}_x + 3.299\theta_x + 9.522\theta_z = 0\,, \\ \ddot{\theta}_y + 7.069\theta_y - 7.557\delta_x = 0\,, \\ \ddot{\theta}_z - 3.145\times10^{1}\theta_x + 5.105\times10^{1}\theta_z = 0\,, \\ \ddot{\delta}_x - 0.765\theta_y + 8.149\delta_x = 0\,, \end{cases}$$

which separates into the systems

$$\begin{cases} \ddot{\theta}_x + 3.299\theta_x + 9.522\theta_z = 0\,, \\ \ddot{\theta}_z - 3.455 \times 10^1\theta_x + 5.105 \times 10^1\theta_z = 0\,, \end{cases}$$

$$\begin{cases} \ddot{\theta}_y + 7.069\theta_y - 7.557\delta_x = 0\,, \\ \ddot{\delta}_x - 0.765\theta_y + 8.149\delta_x = 0\,. \end{cases}$$

For the third case (Section 6.3):

(a) if all kinematic chains consist of elastic elements, then the system of differential equations takes the form

$$\begin{cases} \ddot{\theta}_x + 4.418 \times 10^2\theta_x - 7.652 \times 10^3\delta_y = 0\,, \\ \ddot{\theta}_y + 2.400 \times 10^4\theta_y + 4.157 \times 10^5\delta_x - 2.356 \times 10^5\delta_z = 0\,, \\ \ddot{\theta}_z + 2.535 \times 10^4\theta_z + 2.443 \times 10^5\delta_y = 0\,, \\ \ddot{\delta}_x + 5.196 \times 10^2\theta_y + 9.144 \times 10^3\delta_x - 5.101 \times 10^3\delta_z = 0\,, \\ \ddot{\delta}_y - 9.565\theta_x + 6.109 \times 10^2\theta_z + 6.389 \times 10^3\delta_y = 0\,, \\ \ddot{\delta}_z - 2.945 \times 10^2\theta_y - 5.101 \times 10^3\delta_x + 3.055 \times 10^3\delta_z = 0\,, \end{cases}$$

which separates into the systems

$$\begin{cases} \ddot{\theta}_x + 4.418 \times 10^2\theta_x - 7.652 \times 10^3\delta_y = 0\,, \\ \ddot{\theta}_z + 2.535 \times 10^4\theta_z + 2.443 \times 10^5\delta_y = 0\,, \\ \ddot{\delta}_y - 9.565\theta_x + 6.109 \times 10^2\theta_z + 6.389 \times 10^3\delta_y = 0\,, \end{cases} \quad \begin{cases} \ddot{\theta}_y + 2.400 \times 10^4\theta_y + 4.157 \times 10^5\delta_x - 2.356 \times 10^5\delta_z = 0\,, \\ \ddot{\delta}_x + 5.196 \times 10^2\theta_y + 9.114 \times 10^3\delta_x - 5.101 \times 10^3\delta_z = 0\,, \\ \ddot{\delta}_z - 2.945 \times 10^2\theta_y - 5.101 \times 10^3\delta_x + 3.055 \times 10^3\delta_z = 0\,; \end{cases}$$

(b) if the kinematic chain $A_1B_1C_1$ consists of rigid elements, then one obtains the following system of differential equations

$$\begin{cases} \ddot{\theta}_x + 5.154 \times 10^1\theta_x + 1.488 \times 10^2\theta_z = 0\,, \\ \ddot{\theta}_y + 1.104 \times 10^2\theta_y - 2.952 \times 10^2\delta_x = 0\,, \\ \ddot{\theta}_z - 5.399 \times 10^2\theta_x + 7.977 \times 10^2\theta_z = 0\,, \\ \ddot{\delta}_x - 4.782\theta_y + 1.273 \times 10^2\delta_x = 0\,, \end{cases}$$

which separates into the systems

$$\begin{cases} \ddot{\theta}_x + 5.154 \times 10^1\theta_x + 1.488 \times 10^2\theta_z = 0\,, \\ \ddot{\theta}_z - 5.399 \times 10^2\theta_x + 7.977 \times 10^2\theta_z = 0\,, \end{cases} \quad \begin{cases} \ddot{\theta}_y + 1.104 \times 10^2\theta_y - 2.952 \times 10^2\delta_x = 0\,, \\ \ddot{\delta}_x - 4.782\theta_y + 1.273 \times 10^2\delta_x = 0\,. \end{cases}$$

For the fourth case (Section 6.4):

(a) if all kinematic chains consist of elastic elements, then one obtains the system of differential equation

$$\begin{cases} \ddot{\theta}_x + 3.755 \times 10^3\theta_x - 1.913 \times 10^3\theta_y \\ \quad -3.313 \times 10^4\delta_x - 6.504 \times 10^4\delta_y - 3.826 \times 10^5\delta_z = 0, \\ \ddot{\theta}_y - 1.913 \times 10^3\theta_x + 2.511 \times 10^4\theta_y \\ \quad +4.348 \times 10^5\delta_x + 3.313 \times 10^4\delta_y - 2.135 \times 10^5\delta_z = 0, \\ \ddot{\theta}_z + 2.993 \times 10^4\theta_z + 3.967 \times 10^4\delta_x + 2.214 \times 10^5\delta_y = 0, \\ \ddot{\delta}_x - 4.142 \times 10^1\theta_x + 5.435 \times 10^2\theta_y + 3.919 \times 10^1\theta_z \\ \quad +1.039 \times 10^4\delta_x + 2.214 \times 10^2\delta_y - 4.622 \times 10^3\delta_z = 0 \\ \ddot{\delta}_y - 8.130 \times 10^1\theta_x + 4.142 \times 10^1\theta_y + 5.536 \times 10^2\theta_z \\ \quad +2.214 \times 10^2\delta_x + 7.918 \times 10^3\delta_y + 8.283 \times 10^2\delta_z = 0, \\ \ddot{\delta}_z - 4.782 \times 10^1\theta_x - 2.669 \times 10^2\theta_y \\ \quad -4.662 \times 10^3\delta_x + 8.283 \times 10^2\delta_y + 3.607 \times 10^3\delta_z = 0; \end{cases}$$

(b) if the kinematic chain $A_1B_1C_1$ consists of rigid elements, then one obtains the system of differential equations

$$\begin{cases} \ddot{\theta}_x + 4.382 \times 10^2\theta_x - 2.009 \times 10^3\theta_y + 1.265 \times 10^3\theta_z + 2.255 \times 10^4\delta_x = 0\,, \\ \ddot{\theta}_y + 1.966 \times 10^3\theta_x + 9.387 \times 10^2\theta_y - 1.687 \times 10^3\theta_z - 2.509 \times 10^3\delta_x = 0\,, \\ \ddot{\theta}_z - 4.589 \times 10^3\theta_x - 5.467 \times 10^3\theta_y + 6.780 \times 10^3\theta_z + 4.437 \times 10^4\delta_x = 0\,, \\ \ddot{\delta}_x + 1.726 \times 10^2\theta_x - 4.065 \times 10^1\theta_y - 7.572 \times 10^1\theta_z + 1.082 \times 10^3\delta_x = 0\,. \end{cases}$$

References

1. Gallardo-Alvarado, J.; Posadas-Garcia, J.-d.-D. Mobility analysis and kinematics of the semi-general 2 (3-RPS) series-parallel manipulator. *Robot. Comput.-Integr. Manuf.* **2013**, *29*, 463–472. [CrossRef]
2. Gallardo-Alvarado, J.; Camarillo-Gomez, K.A.; García-Murillo, M.A. A Gough/Stewart-type platform under a combined scheme of actuation. *Int. J. Adv. Manuf. Technol.* **2013**, *68*, 981–991. [CrossRef]
3. Gallardo-Alvarado, J.; Rodriguez-Castro, R.; Aguilar-Nájera, C.R.; Pérez-González, L. A novel six-degrees-of-freedom series-parallel manipulator. *J. Mech. Sci. Technol.* **2012**, *26*, 1901–1909. [CrossRef]
4. Gallardo-Alvarado, J.; García-Murillo, M.A.; Nazul Islam, M.; Abedinnasab, M.H. A simple approach to solving the kinematics of the 4-UPS/PS (3RIT) parallel manipulator. *J. Mech. Sci. Technol.* **2016**, *30*, 2303–2309. [CrossRef]
5. Yi, B.-J.; Kim, W.K. Task-oriented type synthesis of the lower-mobility parallel mechanisms with a common platform. *J. Mech. Sci. Technol.* **2018**, *32*, 5373–5387. [CrossRef]
6. Bu, W.; Yan, S.; Chen, J.; An, X. Mobility analysis for parallel manipulators based on intersection of screw manifolds. *J. Mech. Sci. Technol.* **2016**, *30*, 4345–4352. [CrossRef]
7. Nazari, A.A.; Hasani, A.; Beedel, M. Screw theory-based mobility analysis and projection-based kinematic modeling of a 3-CRRR parallel manipulator. *J. Braz. Soc. Mech. Sci. Eng.* **2018**, *40*, 357. [CrossRef]
8. Hu, B.; Lu, Y.; Tan, Q.; Yu, J.; Han, J. Analysis of stiffness and elastic deformation of a 2 (SP+SPR+SPU) serial-parallel manipulator. *Robot. Comput.-Integr. Manuf.* **2011**, *27*, 418–425. [CrossRef]
9. Kong, Y.; Cheng, G.; Guo, F.; Gu, W.; Zhang, L. Inertia matching analysis of a 5-DOF hybrid optical machining manipulator. *J. Mech. Sci. Technol.* **2019**, *33*, 4991–5002. [CrossRef]
10. Wang, Q.; Su, J.; Lv, Z.; Zhang, L.; Lin, H.; Xu, G. Efficient hybrid method for forward kinematics analysis of parallel robots based on signal decomposition and reconstruction. *Adv. Mech. Eng.* **2017**, *9*, 1–14. [CrossRef]
11. Zhao, J.-S.; Fen, Z.-J.; Zhou, K.; Gao, Y.-F. The design kinematic chains based on the principle of invariable terminal constraints. *Int. J. Adv. Manuf. Technol.* **2005**, *26*, 138–143. [CrossRef]
12. Afroun, M.; Dequidt, A.; Vermeiren, L. Revisiting the inverse dynamics of the Gough-Stewart platform manipulator with special emphasis on universal-prismatic-spherical leg and internal singularity. *Proc. Int. Inst. Mech. Eng. Part C J. Mech. Eng. Sci.* **2012**, *226*, 2422–2439. [CrossRef]
13. Hernández Martinez, E.E.; Valdez Peña, S.I.; Sánchez Soto, E. Towards a Robust Solution of the Non-linear Kinematics for the General Stewart Platform with Estimation of Distribution Algorithms. *Int. J. Adv. Robot. Syst.* **2013**, *10*, 1–11. [CrossRef]
14. Li, B.; Cao, Y.; Zhang, Q.; Wang, C. Singularity Representation and Workspace Determination of a Special Class of the Gough-Stewart Platforms. *Int. J. Adv. Robot. Syst.* **2013**, *10*, 1–13. [CrossRef]
15. Müller, A.; Shai, O. A systematic approach to the instantaneous duality of mechanisms and its application. *Proc. Int. Inst. Mech. Eng. Part C J. Mech. Eng. Sci.* **2016**, *230*, 437–444. [CrossRef]
16. Andrievskiy, B.R.; Arseniev, D.G.; Zegzhda, S.A.; Kazunin, D.V.; Kuznetsov, N.V.; Leonov, G.A.; Tovstik, P.E.; Tovstik, T.P.; Yushkov, M.P. Dynamics of a Stewart platform. *Vestn. St. Petersburg Univ. Math.* **2017**, *50*, 297–309. [CrossRef]
17. Şumnu, A.; Güzelbey, I.H.; Çakir, M.V. Simulation and PID control of a Stewart platform with linear motor. *J. Mech. Sci. Technol.* **2017**, *31*, 345–356. [CrossRef]
18. Meng, Q.; Zhang, T.; He, J.-F.; Song, J.-Y.; Han, J.-W. Dynamic modeling of a 6-degree-of-freedom Stewart platform driven by a permanent synchronous motor. *J. Zhanjiang Univ. Sci. C (Comput. Electron.)* **2010**, *11*, 751–761. [CrossRef]
19. Kalani, H.; Rezaei, A.; Akbarzadeh, A. Improved general solution for the dynamic modeling of Gough-Stewart platform based on principle of virtual work. *Nonlinear Dyn.* **2016**, *83*, 2393–2418. [CrossRef]
20. Leonov, G.A.; Zegzhda, S.A.; Zuev, S.M.; Ershov, B.A.; Kazunin, D.V.; Kostygova, D.M.; Kuznetsov, N.V.; Tovstik, P.E.; Tovstik, T.P.; Yushkov, M.P. Dynamics and Control of the Stewart platform. *Dokl. Phys.* **2014**, *59*, 405–410. [CrossRef]
21. Jakobovič, D.; Budin, L. Forward Kinematics of a Stewart Platform Mechanism. In Proceedings of the INES 2002, 6th International Conference on Intelligent Engineering Systems, Opatija, Croatia, 26–29 May 2002.
22. Gallardo-Alvarado, J. Jerk distribution of a 6-3 Gough-Stewart platform. *Proc. Inst. Mech. Eng. Part K J. Multi-Body Dyn.* **2003**, *217*, 77–84. [CrossRef]
23. Bai, X.; Junkins, J.L.; Turner, J.D. Dynamic Analysis and Adaptive Control of a Stewart Platform Using a Novel Automatic Differentiation Method. In Proceedings of the AIAA/AAS Astrodynamics Specialist Conference and Exhibit, Keystone, CO, USA, 21–24 August 2006.

24. Hajimirzaallan, H.; Ferraresi, C.; Moosavi, H.; Massah, M. An analytical method for the inverse dynamic analysis of the Stewart platform with asymmetric-adjustable payload. *Proc. Int. Inst. Mech. Eng. Part K J. Multi-Body Dyn.* **2013**, *227*, 162–171. [CrossRef]
25. Zhou, H.; Cao, Y.; Li, B.; Wu, M.; Yu, J.; Chen, H. Position-Singularity Analysis of a Class of the 3/6-Gough-Stewart Manipulators based on Singularity-Equivalent-Mechanism. *Int. J. Adv. Robot. Syst.* **2012**, *9*, 1–9. [CrossRef]
26. Zhao, Q.; Wang, N.; Spencer, B.F., Jr. Adaptive position tracking control of electro-hydraulic six-degree-of-freedom driving simulator subject to perturbation. *Simul. Trans. Soc. Modeling Simul. Int.* **2015**, *91*, 265–275. [CrossRef]
27. Pedrammehr, S.; Mahboubkhah, M.; Khani, N. Improved dynamic equations for the generally configured Stewart platform manipulator. *J. Mech. Sci. Technol.* **2012**, *26*, 711–721. [CrossRef]
28. Alyushin, Y.-A.; Elenev, S.-A. Mathematical Model of a Stewart Platform Motion. *J. Mach. Manuf. Reliab.* **2010**, *39*, 305–312. [CrossRef]
29. Lazard, D.; Merlet, J.-P. The (true) Stewart platform has 12 configurations. In Proceedings of the 1994 IEEE International Conference on Robotics and Automation, San Diego, CA, USA, 8–13 May 1994. [CrossRef]
30. Huang, C.-I.; Chang, C.-F.; Yu, M.-Y.; Fu, L.-C. Sliding-Mode Tracking Control of the Stewart Platform. In Proceedings of the 5th Asian Control Conference, Melbourne, Australia, 20–23 July 2004. [CrossRef]
31. Lee, S.-H.; Song, J.-B.; Choi, W.-C.; Hong, D. Position control of Stewart platform using inverse dynamics control with approximate dynamics. *Mechatronics* **2003**, *13*, 605–619. [CrossRef]
32. Gallardo-Alvarado, J. Enhancing the originality of the Stewart platform through its kinematic analyses. *Proc. Int. Inst. Mech. Eng. Part C J. Mech. Eng. Sci.* **2012**, *226*, 3013–3025. [CrossRef]
33. Ke, W.; Fuzhou, D.; Xianzhi, Z. Algorithm and experiments of six-dimensional force/torque dynamic measurements based on a Stewart platform. *Chin. J. Aeronaut.* **2016**, *29*, 1840–1851. [CrossRef]
34. Afzali-Far, B.; Lidström, P.; Nilsson, K. Parametric damped vibrations of Gough-Stewart platforms for symmetric configurations. *Mech. Mach. Theory* **2014**, *80*, 52–69. [CrossRef]
35. Tang, J.; Cao, D.; Yu, T. Decentralized vibration control of a voice coil motor-based Stewart parallel mechanism: Simulation and experiments. *Proc. Int. Inst. Mech. Eng. Part C J. Mech. Eng. Sci.* **2018**, *233*, 132–145. [CrossRef]
36. Meng, Q.; Zhang, T.; He, J.-F.; Song, J.-Y.; Yuan, C.-Y. Fault-tolerant control under uncertain Stewart platform under loss of the actuator effectiveness. *Proc. Int. Inst. Mech. Eng. Part C J. Mech. Eng. Sci.* **2014**, *228*, 1286–1298. [CrossRef]
37. Zhao, Q.; Gao, F. Bond graph modelling of hydraulic six-degree-of-freedom motion simulator. *Proc. Int. Inst. Mech. Eng. Part C J. Mech. Eng. Sci.* **2012**, *226*, 2887–2901. [CrossRef]
38. Damic, V.; Cohodar, M. Dynamic Analysis of Stewart Platform by Bond Graphs. *Proceedia Eng.* **2015**, *100*, 226–233. [CrossRef]
39. Halder, B.; Saha, R.; Sanyal, D. Semi-isotropic design of a Stewart platform through constrained optimization. *Proc. Int. Inst. Mech. Eng. Part C J. Mech. Eng. Sci.* **2015**, *231*, 1897–1906. [CrossRef]
40. Xie, Z.; Li, G.; Liu, G.; Zhao, J. Optimal design of a Stewart platform using the global transmission index under determinate constraint of workspace. *Adv. Mech. Eng.* **2017**, *9*, 1–14. [CrossRef]
41. Shao, Z.-F.; Tang, X.; Wang, L.-P. Optimum Design of 3-3 Stewart Platform Considering Inertia Property. *Adv. Mech. Eng.* **2013**, *5*, 249121. [CrossRef]
42. Tourajizadeh, H.; Yousefzadeh, M.; Tajik, A. Closed Loop Optimal Control of a Stewart Platform Using an Optimal Feedback Linearization Method. *Int. J. Adv. Robot. Syst.* **2016**, *13*, 134. [CrossRef]
43. Taghizadeh, M.; Yarmohammadi, M.J. Development of a Self-tuning PID Controller on Hydraulically Actuated Stewart Platform Stabilizer with Base Excitation. *Int. J. Control Autom. Syst.* **2018**, *16*, 2990–2999. [CrossRef]
44. Li, Y.; Yang, X.L.; Wu, H.T.; Chen, B. Optimal design of a six-axis vibration isolator via Stewart platform by using homogeneous Jacobian matrix formulation based on dual quaternions. *J. Mech. Sci. Technol.* **2018**, *32*, 11–19. [CrossRef]
45. Keshtkar, S.; Poznyak, A.S.; Hernandez, E.; Oropeza, A. Adaptive Sliding Mode Controller Based on the "Super-Twist" State Observer for Control of the Stewart Platform. *Autom. Remote Control* **2017**, *78*, 1218–1233. [CrossRef]
46. Yao, R.; Zhu, W.; Hunag, P. Accuracy Analysis of Stewart Platform Based on Interval Analysis Method. *Chin. J. Mech. Eng.* **2013**, *26*, 29–34. [CrossRef]
47. Sun, T.; Lian, B.; Song, Y. Stiffness analysis of a 2DoF over-constrained RPM with an articulated traveling platform. *Mech. Mach. Theory* **2016**, *96*, 165–178. [CrossRef]
48. Wu, M.; Mei, J.; Zhao, Y.; Niu, W. Vibration reduction of delta robot based on trajectory planning. *Mech. Mach. Theory* **2020**, *153*, 104004. [CrossRef]
49. Wang, G.; Wang, L. Dynamics investigation of spatial parallel mechanism considering rod flexibility and spherical joint clearance. *Mech. Mach. Theory* **2019**, *117*, 83–107. [CrossRef]
50. Liu, S.; Dai, J.; Sheng, G.; Li, A.; Cao, G.; Feng, S.; Meng, D. Dynamic analysis of spatial parallel manipulator with rigid and flexible couplings. *J. Cent. South Univ.* **2017**, *24*, 840–853. [CrossRef]
51. Li, Y.; Zheng, H.; Chen, B.; Sun, P.; Wang, Z.; Shuai, K.; Yue, Y. Dynamic Modeling and Analysis of 5-PSS/UPU Parallel Mechanism with Elastically Active Branched Chains. *Chin. J. Mech. Eng.* **2020**, *33*, 44. [CrossRef]
52. Jia, Y.-H.; Xu, S.-J.; Hu, Q. Dynamics of a spacecraft with large flexible appendage constrained by multi-strut passive damper. *Acta Mech. Sin.* **2013**, *29*, 294–308. [CrossRef]
53. Zhao, Y.; Jin, Y.; Zhang, J. Kinetostatic Modeling and Analysis of an Exechon Parallel Kinematic Machine (PKM) Module. *Chin. J. Mech. Eng.* **2016**, *29*, 33–44. [CrossRef]

54. Jiao, J.; Wu, Y.; Yu, K.; Zhao, R. Dynamic modeling and experimental analyses of Stewart platform with flexible hinges. *J. Vib. Control* **2018**, *25*, 151–171. [CrossRef]
55. Ebrahimi, S.; Eshaghiyeh-Firoozabadi, A. Dynamic Performance Evaluation of Serial and Parallel RPR Manipulators with Flexible Intermediate Links. *Iran. J. Sci. Technol. Trans. Mech. Eng.* **2016**, *40*, 160–180. [CrossRef]
56. Yun, Y.; Li, Y. Design and analysis of a novel 6-DOF redundant actuated parallel robot with compliant hinges for high precision positioning. *Nonlinear Dyn.* **2010**, *61*, 829–845. [CrossRef]
57. Ma, S.; Duan, W. Dynamic Coupled Analysis of the Floating Platform Using the Asynchronous Coupling Algorithm. *J. Mar. Sci. Appl.* **2014**, *13*, 85–91. [CrossRef]
58. Inner, B.; Kucuk, S. A novel kinematic design, analysis and simulation tool for general Stewart platforms. *Simul. Trans. Soc. Modeling Simul. Int.* **2013**, *89*, 876–897. [CrossRef]
59. Tabacu, S.; Negrea, R.F.; Negrea, D. Experimental, numerical and analytical investigation of 2D tetra-anti-chiral structure under compressive loads. *Thin-Walled Struct.* **2020**, *155*, 106929. [CrossRef]
60. Furqan, M.; Suhaib, M.; Ahmad, N. Studies on Stewart platform manipulator: A review. *J. Mech. Sci. Technol.* **2017**, *31*, 4459–4470. [CrossRef]
61. Pnevmatikos, N.G.; Thomos, G.C. Stochastic structural control under earthquake excitations. *J. Struct. Control Health Monit.* **2014**, *21*, 620–633. [CrossRef]